

Doctoral Thesis



For a doctoral degree
doctor rerum naturalium (Dr. rer. nat.)
at the Graduate School of Life Sciences (Section Biomedicine)

Development of an osteochondral cartilage defect model

Entwicklung eines osteochondralen
Knorpeldefektmodells

Submitted by
Andrea Schwab
born in Würzburg
Würzburg 2017

Submitted on

Members of the Committee:

Chairperson: Prof. Dr. Markus Engstler

Primary supervisor: Prof. Dr. Heike Walles

Supervisor (second): Prof. Dr. Jürgen Groll

Supervisor (third): Prof. Dr. Gerjo J.V.M.van Osch

Date of public defense:

Date of receipt of certificates:

Abstract

The limited intrinsic self-healing capability of articular cartilage requires treatment of cartilage defects. Material assisted and cell based therapies are in clinical practice but tend to result in formation of mechanical inferior fibro-cartilage in long term follow up. If a lesion has not been properly restored degenerative diseases are diagnosed as late sequela causing pain and loss in morbidity. Complex three dimensional tissue models mimicking physiological situation allow investigation of cartilage metabolism and mechanisms involved in repair. A standardized and reproducible model cultured under controllable conditions *ex vivo* to maintain tissue properties is of relevance for comparable studies.

Topic of this thesis was the establishment of an cartilage defect model that allows for testing novel biomaterials and investigate the effect of defined defect depths on formation of repair tissue.

In part I an *ex vivo* osteochondral defect model was established based on isolation of porcine osteochondral explants (OCE) from medial condyles, 8 mm in diameter and 5 mm in height. Full thickness cartilage defects with 1 mm to 4 mm in diameter were created to define *ex vivo* cartilage critical size after 28 days culture with custom developed static culture device. In part II of this thesis hydrogel materials, namely collagen I isolated from rat tail, commercially available fibrin glue, matrix-metalloproteinase cleavable poly(ethylene glycol) polymerized with heparin (starPEGh), methacrylated poly(N-(2-hydroxypropyl) methacrylamide mono-dilactate-poly(ethylene glycol) triblock copolymer/methacrylated hyaluronic acid (MP/HA), thiol functionalized HA/allyl functionalized poly(glycidol) (P(AGE/G)-HA-SH), were tested cell free and chondrocyte loaded (20 mio/ml) as implant in 4 mm cartilage defects to investigate cartilage regeneration. Reproducible chondral defects, 8 mm in diameter and 1 mm in height, were generated with an artificial tissue cutter (ARTcut[®]) to investigate effect of defect depth on defect regeneration in part III. In all approaches OCE were analyzed by Safranin-O staining to visualize proteoglycans in cartilage and/or hydrogels. Immuno-histological and -fluorescent stainings (aggrecan, collagen II, VI and X, proCollagen I, SOX9, RUNX2), gene expression analysis (aggrecan, collagen II and X, SOX9, RUNX2) of chondrocyte loaded hydrogels (part II) and proteoglycan and DNA content (Part I & II) were performed for detailed analysis of cartilage regeneration.

Part I: The development of custom made static culture device, consisting of inserts in

which OCE is fixed and deep well plate, allowed tissue specific media supply without supplementation of TGF β . Critical size diameter was defined to be 4 mm.

Part II: Biomaterials revealed differences in cartilage regeneration. Collagen I and fibrin glue showed presence of cells migrated from OCE into cell free hydrogels with indication of fibrous tissue formation by presence of proCollagen I. In chondrocyte loaded study cartilage matrix proteins aggrecan, collagen II and VI and transcription factor SOX9 were detected after *ex vivo* culture throughout the two natural hydrogels collagen I and fibrin glue whereas markers were localized in pericellular matrix in starPEGh. Weak stainings resulted for MP/HA and P(AGE/G)-HA-SH in some cell clusters. Gene expression data and proteoglycan quantification supported histological findings with tendency of hypertrophy indicated by upregulation of collagen X and RunX2 in MP/HA and P(AGE/G)-HA-SH. Part III: In life-dead stainings recruitment of cells from OCE into empty or cell free collagen I treated chondral defects was seen.

Separated and tissue specific media supply is critical to maintain ECM composition in cartilage. Presence of OCE stimulates cartilage matrix synthesis in chondrocyte loaded collagen I hydrogel and reduces hypertrophy compared to free swelling conditions and pellet cultures. Differences in cartilage repair tissue formation resulted in preference of natural derived polymers compared to synthetic based materials. The *ex vivo* cartilage defect model represents a platform for testing novel hydrogels as cartilage materials, but also to investigate the effect of cell seeding densities, cell gradients, cell co-cultures on defect regeneration dependent on defect depth. The separated media compartments allow for systematic analysis of pharmaceuticals, media components or inflammatory cytokines on bone and cartilage metabolism and matrix stability.

Zusammenfassung

Aufgrund der geringen Selbshheilungsfähigkeit von artikulären Knorpel erfordern Knorpeldefekte eine orthopädische Behandlung. Bislang konnte mit material- oder zellbasierenden Behandlungsstrategien keine funktionelle Regeneration von Knorpeldefekten erreicht werden. In Langzeitstudien zeigt sich vermehrt die Bildung von mechanisch instabilem fibrosen Knorpel. Als Spätfolge nicht vollständig verheilter Knorpeldefekte wird die degenerative Erkrankung Osteoarthritis diagnostiziert. 3-dimensionale Gewebemodelle, die die physiologischen Gegebenheiten nachahmen erlauben einen Einblick in die Mechanismen während der Defektheilung. Dem subchondralen Knochen kommt eine kritische Rolle in der Regeneration nach Mikrofrakturierung zu, weshalb ein Knorpelmodell auf osteochondralen Gewebe basieren sollte.

Thema der Arbeit war es ein standardisiertes Knorpeldefektmodell zu etablieren, das die Testung neuer Hydrogelformulierungen sowohl zellfrei als auch zellbeladen hinsichtlich deren Regenerationspotential ermöglicht und den Einfluss der Knorpeldefekttiefe auf die Regeneration zu analysieren.

Teil I der Arbeit umfasste die Etablierung des *ex vivo* osteochondralen Defektmodells, basierend auf der Isolation von porcinen osteochondralen Explantaten (OCE) mit einem Durchmesser von 8 mm und einer Höhe von 5 mm aus der medialen Kondyle. Full thickness Knorpeldefekte mit einem Durchmesser zwischen 1 mm und 4 mm wurden induziert, um den kritischen Defektdurchmesser nach 28 Tagen Kultur in einer neuartigen statischen Kulturplatte zu definieren. In Teil II stand die Testung von Hydrogelen aus Kollagen I isoliert aus Rattenschwänzen, kommerziell erhältlicher Firbrinkleber, Matrix-Metalloproteinase cleavable poly(Ethylen Glycol) polymerisiert mit Heparin (starPEGh), methacrylates poly(N-(2-hydroxypropyl) methacrylamid mono-dilactate-poly(Ethylene Glycol) triblock copolymer/methacrylated Hyaluronsäure (MP/HA), thiol functionalisiertes HA/allyl functionalisiertes poly(Glycidol) (P(AGE/G)-HA-SH) als zellfreies oder mit 20 Mio/ml Chondrozyten beladenes Implantat im Knorpeldefekt mit einem Durchmesser von 4 mm im Fokus. Ein automatisiertes Verfahren zur Wundsetzung (ARTcut[®]) erlaubte in Teil III der Thesis das Kreieren von reproduzierbaren chondralen Defekten mit 4 mm Durchmesser und 1 mm Tiefe in das OCE Modell, um den Einfluss der Defekttiefe auf die Knorpelregeneration zu analysieren.

Das Knorpelgewebe des OCE und/oder Hydrogele wurde in allen Experimenten mittels Safranin-O auf Proteoglykangehalt untersucht. Immunhistologische und -fluoreszenzfärbung

knorpelspezifischer Marker, Genexpressionsanalysen der Chondrozyten beladenen Hydrogele (Teil II) und Quantifizierung der Proteoglykane und des DNA Gehalts (Teil I & II) folgten nach *ex vivo* Kultur.

Teil I: Die neu entwickelten statischen Kulturkammern setzen sich aus Inserts, in denen das OCE fixiert ist, und einer 6 Well-Platte zusammen. Dadurch wird eine Gewebespezifische Medienversorgung mit Knorpelmedium ohne TGF β in den Inserts und Knochenmedium in der Vertiefung der Wellplatte ermöglicht. Die kritische Defektgröße im *ex vivo* Modell wurde mit 4 mm festgesetzt. Teil II: Biomaterialien als Implantate im Knorpeldefekt zeigten ein materialabhängiges Regenerationspotential. Die Einwanderung von Zellen aus dem OCE in zellfreie Hydrogele resultierte in der Lebend-Tot Färbung bei Kollagen I und Fibrinkleber mit der Tendenz der Synthese von fibrösem Knorpel. Die Chondrozyten beladenen Hydrogele aus Kollagen I und Fibrinkleber zeigten eine homogene Positivfärbung für die hyalinen Proteine Aggrecan, Collagen II und X und des Knorpeltranskriptionsfaktors SOX9, wohingegen die Färbung bei starPEGh lokal in der perizellulären Region lokalisiert war. Die weiteren Materialien MP/HA und P(AGE/G)-HA-SH wiesen eine schwache Positivfärbung an einzelnen Zellclustern auf. Die Genexpressionsanalyse und die Quantifizierung der Proteoglykane bestätigten die histologischen Ergebnisse mit der Tendenz der Hypertrophie, belegt durch Hochregulierung von Kollagen X und RunX2, bei Chondrozyten eingebettet in MP/HA und P(AGE/G)-HA-SH. Teil III: In der Lebend-Tot Färbung konnte die Einwanderung von Zellen aus dem Knorpel des OCE in den Leerdefekt und zellfreies Kollagen I Hydrogel nachgewiesen werden.

Separierte und Gewebe spezifische Medienversorgung erwies sich als kritischer Faktor zur Aufrechterhaltung der Knorpel ECM. Die Anwesenheit des OCE stimuliert Knorpelmatrixsynthese, die für das *in vitro* kultivierte Chondrozyten beladene Kollagen I nachweislich geringer vorhanden war. Außerdem war die Produktion des hypertrophen Markers Kollagen X im Implantat im OCE weniger stark ausgeprägt als in der *in vitro* Kultur. Die Unterschiede der Knorpelregeneration deutet auf die Bevorzugung von natürlichen Polymeren gegenüber den synthetisch basierten Hydrogelen hin. Das *ex vivo* Knorpeldefektmodell stellt eine Plattform zur Testung neuer Hydrogelmaterialien als Knorpelimplantate dar. Weiterhin kann das Modell zur Analyse von Zellbesiedlungsstrategien als auch für Zell-Ko-Kulturen im Hinblick auf die Defektregeneration herangezogen werden. Die getrennten Medienreservoirs ermöglichen weiterhin die systematische Analyse von Medienkomponenten oder entzündlichen Zytokinen auf die Vitalität und Stabilität von Knochen und Knorpelgewebe.

Contents

1	Introduction	1
1.1	Articular cartilage	2
1.1.1	Biology of articular cartilage tissue	2
1.1.2	Cartilage defects	4
1.2	Cartilage treatments	5
1.2.1	Marrow stimulating treatments	6
1.2.2	Material assisted treatments	6
1.2.3	Cell based treatments	7
1.2.4	Osteochondral grafts	8
1.2.5	Limitations of cartilage treatments	8
1.3	Cartilage implant development: From the material to an advanced therapy medicinal product	9
1.3.1	Advanced therapy medicinal products (ATMPs)	9
1.3.2	Marketing authorization of ATMPs	10
1.3.3	ATMPs for cartilage regeneration	11
1.4	TE of cartilage	11
1.4.1	Cell source	11
1.4.1.1	Chondrocytes (CZs)	11
1.4.1.2	Multipotent stromal cells (MSCs)	12
1.4.1.3	Cell co-cultures	12
1.4.2	Materials	13
1.4.2.1	Synthetic materials	13
1.4.2.2	Natural materials	14
1.4.3	Bioreactors	15
1.5	Test systems: an alternative to animal experiments	16
1.5.1	<i>In vitro</i> models	17
1.5.2	<i>Ex vivo</i> models	18
2	Aim	20
3	Materials	22
3.1	Biologic material	22
3.2	List of chemicals	22

3.3	List of enzymes	25
3.4	Cell culture techniques: Culture media and buffer	26
3.5	Hydrogel materials and peptides	28
3.6	Biochemical and protein analysis: Buffers and solutions	30
3.7	Histology: Antibodies and solutions	31
3.8	Gene expression analysis: Primers and solutions	33
3.9	Kits	34
3.10	Laboratory devices and software	35
3.11	Laboratory equipment	36
4	Methods	37
4.1	Establishment of <i>ex vivo</i> osteochondral defect model with critical size defects	37
4.1.1	Isolation of osteochondral tissue explants	37
4.1.2	Static culture	38
4.1.3	Dynamic culture under constant flow	39
4.2	Cartilage defect creation	40
4.2.1	Clinical standard: Biopsy punch	40
4.2.2	Automated, standardized method: Artificial tissue cutter	41
4.3	Cell culture methods: Cell isolation, expansion and characterization	42
4.3.1	Cell isolation	42
4.3.1.1	CZ isolation	42
4.3.1.2	Mesenchymal stromal cell (MSC) isolation	42
4.3.2	Cell counting	43
4.3.3	Freezing and thawing of cells	43
4.3.4	Embedding of cells into hydrogel material	44
4.3.5	CZ characterization	44
4.3.5.1	CZ population doubling	44
4.3.5.2	CZ pellet culture	44
4.4	Preparation of hydrogel biomaterials	45
4.4.1	Collagen I hydrogel	45
4.4.1.1	Isolation of collagen I from rat tails	45
4.4.1.2	Protein characterization of isolated collagen I from rat tail by western blot	46
4.4.1.3	Collagen I hydrogel preparation	47
4.4.1.4	Free swelling culture of pCZ loaded collagen I hydrogel	47
4.4.2	Fibrin glue	47
4.4.3	Four armed poly(ethylene glycol) polymerized with heparin (starPEGh)	48

4.4.3.1	Peptide augmented starPEGh	48
4.4.4	PEG and partially metacrylated poly[N-(2-hydroxypropyl) methacrylamide mono/dilactate (MP/HA)]	49
4.4.5	Thiol functionalized hyaluronic acid/allyl functionalized poly (glycidol) (P(AGE/G)-HA-SH)	50
4.5	Viability staining	51
4.5.1	Live-dead staining	51
4.5.2	3-(4,5-dimethyl-2-thiazol)-2,5-diphenyl-2H-tetrazolium bromide (MTT) staining	51
4.6	Biochemical characterization: Proteoglycan and DNA content	51
4.6.1	Papain digestion of cartilage tissue and hydrogels	52
4.6.1.1	Blyscan™ sulfated Glycosaminoglycan assay	52
4.6.1.2	Dimethylmethylene blue assay	52
4.6.2	DNA quantification	53
4.7	Histological, immuno-histological and immuno-fluorescent stainings	53
4.7.1	Sample preparation and embedding	53
4.7.1.1	Plastic embedding	54
4.7.1.2	Paraffin embedding and decalcification	54
4.7.2	Safranin-O staining	54
4.7.3	Immuno-histological stainings	55
4.7.4	Immuno-fluorescent stainings	55
4.8	Gene expression analysis	55
4.8.1	RNA isolation	56
4.8.2	cDNA synthesis	56
4.8.3	Qualitative realtime polymerase chain reaction (qRT PCR)	56
4.9	Migration of cells in hydrogels: time lapse experiments	58
4.9.0.1	Structural characterization by scanning electron microscopy	58
4.10	Statistics and data analysis	58
5	Results	59
5.1	Establishment of <i>ex vivo</i> osteochondral defect model with critical size defects	59
5.1.1	Influence of isolation, defect creation and <i>ex vivo</i> culture on explant viability	59
5.1.2	<i>Ex vivo</i> critical size defect: Viability, proteoglycan content and cell recruitment	61
5.1.3	Prototype bioreactor: Influence of dynamic culture on viability	65
5.2	Characterization of collagen I isolated from rat tail	67

5.3	Characterization of porcine articular cartilage and porcine chondrocytes . . .	68
5.3.1	Phenotypical characterization of pChondrocytes and articular cartilage	68
5.3.2	Chondrocyte pellet culture and free swelling culture of collagen I loaded hydrogel	69
5.4	<i>Ex vivo</i> evaluation of novel biomaterials	71
5.4.1	Cell free hydrogel material testing	71
5.4.2	Chondrocyte loaded hydrogel material testing	74
5.4.2.1	Characterization of hydrogel materials: histology and pro- teoglycan content	74
5.4.2.2	Gene expression analysis	80
5.4.2.3	Influence of peptide augmented starPEGh material on ECM synthesis	83
5.4.3	Migration of cells in hydrogels: time lapse experiments	83
5.5	Influence of defect depth on cartilage regeneration	85
5.5.1	Viability and cell migration in chondral defects	85
6	Discussion	87
6.1	Osteochondral explant model: Relevance of subchondral bone and tissue specific media supply	87
6.1.1	Role of subchondral bone in cartilage regeneration	88
6.1.2	Tissue specific media is critical to maintain cartilage ECM during <i>ex vivo</i> culture	89
6.1.3	Bioreactor for dynamic culture of explants	91
6.2	<i>Ex vivo</i> evaluation of cartilage regeneration in the osteochondral defect model	92
6.2.1	Definition of <i>ex vivo</i> critical size diameter in osteochondral defect model	92
6.2.2	Stimulative effect of osteochondral explant on cartilage matrix pro- duction	94
6.2.3	Hydrogel materials revealed differences in repair of full thickness cartilage defects	96
6.2.4	Partial thickness defects: Repair and cell recruitment	102
6.2.5	Conclusion	103
7	Outlook	105
7.1	Clinical relevance: cartilage therapies and simulated OA	105
7.1.1	Defect geometry and treatment approaches	105
7.1.2	Inflammatory conditions	106

- 7.2 Influence of culture conditions: Low oxygen tension and cartilage biomechanics 107
 - 7.2.1 Oxygen tension 107
 - 7.2.2 Cartilage biomechanics 107

- 8 Appendix A-1**

List of Figures

1	Prevalence and distribution of arthrosis in Germany in 2015.	1
2	Zonal structure of articular cartilage.	3
3	Cartilage treatment techniques	5
4	Guide for cartilage treatment of lesions located in femoral condyle.	6
5	Schematic representation of the experimental approaches in this thesis. . .	21
6	Isolation of osteochondral explants (OCE) from porcine femoral medial condyle.	38
7	Osteochondral platform for static <i>ex vivo</i> culture.	38
8	Prototype bioreactor for dynamic culture of osteochondral explants (OCE). .	39
9	Creation of full thickness cartilage defects.	40
10	Artificial tissue cutter (ARTcut [®]).	41
11	Collagen I isolation from rat tail.	45
12	Macroscopic illustration for preparation of three hydrogel materials in specific molds and depiction of fabricated materials after polymerization. .	49
13	Live–dead staining of osteochondral explants (OCE) at day 0 and after 28 days <i>ex vivo</i> culture.	60
14	Safranin-O staining of osteochondral explant (diameter 8 mm) without defect cultured for 56 days <i>ex vivo</i> with tissue specific media.	60
15	MTT viability staining of osteochondral explants (OCE) with full thickness cartilage defects at day 0 and after 28 days <i>ex vivo</i> culture.	61
16	Definition of <i>ex vivo</i> critical size cartilage defect.	62
17	Scanning electron microscopy (SEM) images of osteochondral explant (OCE) with 4 mm defect after 28 days <i>ex vivo</i> culture.	63
18	Quantification of proteoglycans (GAG) in superficial (SZ), middle (MZ) and deep zone (DZ) and GAG release during static <i>ex vivo</i> culture.	64
19	Characterization of subchondral bone of porcine osteochondral explant. . .	66
20	Experimental set up to measure pressure of media through subchondral bone of osteochondral explant (OCE).	66
21	Characterization of collagen I isolated form rat tails.	67
22	Microscopical images of porcine chondrocytes (passage 1) during <i>in vitro</i> expansion.	68

23	Macroscopic images and live–dead staining of cell free hydrogel (collagen I, fibrin glue) cultured 28 days in <i>ex vivo</i> defect model.	71
24	Histological stainings of cell free hydrogel (collagen I, fibrin glue) cultured 28 days in <i>ex vivo</i> defect model.	72
25	Histological stainings of cell free tested HydroZONES materials in osteochondral model after 28 ays.	73
26	MTT staining and macroscopic images of porcine chondrocyte loaded hydrogels (20 mio/ml).	74
27	Heat map to qualitatively summarize the immuno–histological and –fluorescent stainings of pChondrocyte loaded hydrogel materials cultured for 28 days <i>ex vivo</i> in osteochondral defect model.	75
28	Immuno–histological (IHC) stainings of collagen I, fibrin glue, starPEGh, MP/HA and P(AGE/G)–HA–SH materials at day 0 and after 28 days <i>ex vivo</i> culture.	77
29	Immune–fluorescent (IF) stainings of collagen I, fibrin glue, starPEGh, MP/HA and P(AGE/G)–HA–SH materials.	78
30	Quantification of proteoglycans (GAG) in chondrocyte loaded hydrogels at day 0 and after 28 days <i>ex vivo</i> culture.	79
31	Gene expression analysis of chondrocyte loaded hydrogels cultured 28 days in <i>ex vivo</i> system.	82
32	Cell migration in hydrogel materials displaying maximum migration distance and velocity as bar chart with mean values including standard deviation.	84
33	Creation of 1 mm chondral defects in osteochondral explant with ARTcut®.	85
34	Live–dead images of osteochondral explants (OCE) with chondral defects (4 mm x 1 mm) either left untreated or with cell free collagen I hydrogel. (A–B) Top view focusing on the cartilage ring or (A’–B’) on the bottom of chondral defects at day 0. (C–C’) OCE with untreated chondral defect or (D–D’) implanted cell free collagen I hydrogel after 28 days static culture. Migration of cells with elongated shape from cartilage into defects was seen. (Scale bar (A’, B’, C–D) 500 µm, (A, B, D’) 100 µm)	86
35	Calcein labeling of subchondral bone of osteochondral explant (diameter 8 mm) cultured for 56 days <i>ex vivo</i> with tissue specific media.	A-1
36	Isotype controls for histological stainings on pocine articular cartilage.	A-2

-
- 37 Immuno-fluorescent and -histological stainings of pChondrocyte pellet, pChondrocytes embedded in collagen I hydrogel cultured for 28 days under free swelling conditions or in osteochondral defect model and native porcine articular cartilage. A-3
- 38 Safranin-O staining of chondral defects at day 0 and after 28 days *ex vivo* culture A-4

List of Tables

1	ICRS classification of articular cartilage defects.	4
2	Components and media supplements for preparation of cell culture media and solutions.	22
3	List of all chemicals used for preparation of buffers and staining solutions.	23
4	List of enzymes.	25
5	Composition of cell culture media.	26
6	Overview of buffers for cell culture techniques.	27
7	List of materials for fabrication of collagen I, fibrin glue, 50 % matrix-metalloproteinase (MMP) cleavable four armed poly(ethylene glycol) polymerized with heparin (starPEGh), PEG and partially metacrylated poly[N-(2-hydroxypropyl) methacrylamide mono/dilactate] (MP/HA) and allyl- and thiol-functional linear poly(glycidol) (P(AGE/G)-HA-SH) hydrogel.	28
8	List of peptides for augmentation with starPEGh hydrogel.	29
9	Overview of composition of all buffers used for histology or biochemical analysis.	30
10	List and composition of solutions for T9100 plastic embedding.	31
11	Composition of solutions for histological stainings.	31
12	List of primary and secondary antibodies for immuno-histological (IHC) and -fluorescent (IF) stainings.	32
13	Porcine primer pairs for quantitative qRT PCR (s: sense, a: antisense).	33
14	List of commercially available kits for analysis.	34
15	List of devices.	35
16	List of software for data recording.	35
17	List of (single use) laboratory equipment and plastic ware.	36
18	Protocol for quantitative reverse transcriptase gene expression analysis with CFX-cycler.	57
19	Summary of accumulated (acc.) GAG release from osteochondral explant culture without, 1 mm, 2 mm and 4 mm full thickness defect in cartilage media after 28 days <i>ex vivo</i> culture. Statistical significance was determined by student's T-Test between day 0 and day 28, (n=3-5).	65

20	Calculation of cell number of 2D expanded pChondrocytes in terms of cell numbers and DNA content at day 3, day 7 and day 9 including standard deviation.	69
21	Calculation of target stability value referred as M-value of selected combinations of housekeeping genes combinations.	80

List of Abbreviation

Abbreviation	meaning
ACI	autologous chondrocyte implantation
ACIC	autologous cartilage induced chondrogenesis
ACT3D-CS	autologous chondrocyte transplantation of 3D chondrocyte spheroids
AMIC	autologous matrix induced chondrogenesis
ARTcut	artificial tissue cutter
ATMP	advanced medicinal therapy product
BSA	bovine serum albumin
CZ	chondrocyte
col I	collagen type I
col II	collagen type II
col VI	collagen type VI
col X	collagen type X
DAB	3,3'-diaminobencidine
DAPI	4',6-diamidino-2-phenylindole
DMMB	dimethylmethylene blue
DZ	deep zone
ECM	extracellular matrix
EDTA	ethylenediaminetetraacetic acid
EF1	elongation factor 1 alpha
EMA	European medical agency
EtOH	ethanol
EU	European Union
FCS	fetal calve serum
FDA	food and drug administration
GAG	glycosaminoglycan / proteoglycan
GAPDH	glyceraldehyde-3-phosphate dehydrogenase
GNL	gel neutralizing solution
hbFGF	human basic fibroblast growht factor
HMBS	hydroxymethylbilane synthase
HPRT	hypoxanthine-guanine phosphoribosyltransferase
HRS	horse radish peroxidase
IF	immuno-fluorescent

IHC	immuno-histology
ITS	insulin, transferrin and selenic acid
KLER	peptide (decorin-moiety) with collagen II affinity
MACI	matrix-assisted autologous chondrocyte implantation
mmHG	mm mercury
MMP	matrix metalloproteinase
MP/HA	poly(ethylene glycol) and partially metacrylated poly[N-(2-hydroxy prolyl)methacrylamide mono/dilactate
MSC	multipotent stromal cells
MTT	3-(4,5-dimethyl-2-thiazol)-2,5-diphenyl-2H-tetrazolium bromide
MZ	middle zone
OA	osteoarthritis
OATS	osteocondral autograft transplantation
OCA	osteocondral allograft
OCE	osteocondral explant
P(AGE/G)-HA-SH	thiol functionalized hyaluronic acid/allyl functionalized poly(glycidol)
pCZ	porcine chondrocytes
PBS	phosphate buffered saline (without magnesium chloride and calcium chloride)
PBST	PBS tween
PCR	polymerase chain reaction
PEG	poly(ethylene glycol)
PenStrep	penicillin-streptomycin
PG	polyglycidol
qRT PCR	qualitative reverse transcriptase polymerase chain reaction
RGD	peptide (GCWGGRGDSP) mediating cell adhesion
rpm	rounds per minute
RUNX2	runt-related transcription factor 2
SDHA	succinate dehydrogenase subunit A
SOX9	SRY (sex related Y chromosom)-gene related (high mobility group) box 9
starPEGh	four armed poly(ethylene glycol) polymerized with heparin
SZ	superficial zone
SZP	superficial zone protein
TbSp	trabecula spacing
TBST	tris buffered saline supplemented with 0.05% (v/v) tween
TbTh	trabecula thickness

TE	tissue engineering
TGF	transforming growth factor
U	units
WYRGL	peptide with collagen II binding site
YWHAZ	housekeeping gene, uncharacterized protein

1. Introduction

The musculoskeletal system comprising bones, joints, muscles, tendons and cartilage provides human body with support and stability. In 2015, arthroscopic procedures of articular cartilage and the menisci were the fourth most prevalent surgery in Germany accounted with more than 261 000 cases [1]. Musculoskeletal diseases cause chronic pain and lead to loss in morbidity to patients. The largest group of patients are the aged population with a mean age above 60 years suffering from chronic or inflammatory diseases like osteoporosis, osteoarthritis (OA) or sclerosis. In Germany, 50 % of women and 33 % of men between 70 and 79 years of age suffer from arthrosis [2,3]. Among arthrosis patients, knee arthrosis is diagnosed in 45 % followed by hip arthrosis (42 %) [4]. In contrast, 67 % of men and only 33 % women develop cartilage rupture [5]. Addressing people undergoing

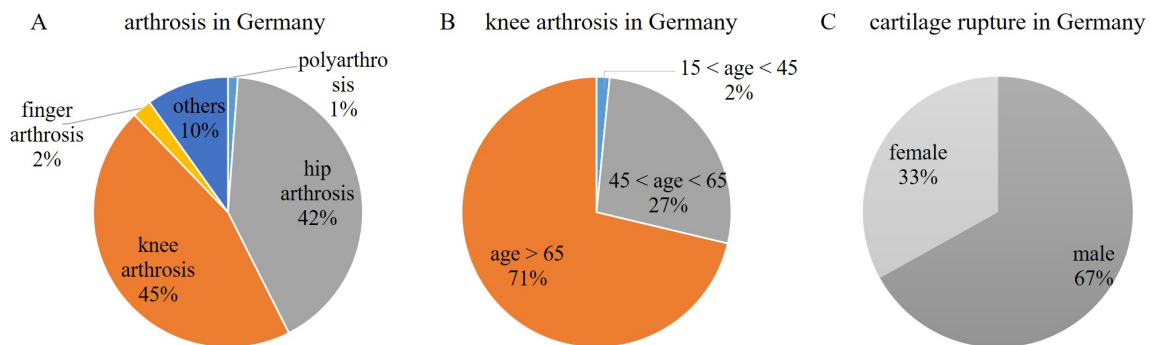


Figure 1 Prevalence and distribution of arthrosis in Germany in 2015. (A) Knee arthrosis accounts majority of cases (188 000) followed by hip arthrosis (172 000). Polyarthrosis (4 900) and finger arthrosis (9 600) are only minor cases. (B) Patients suffering from knee arthrosis increases with age. Percentage of patients diagnosed with arthrosis is highest in for people above 65 years of age (71 %). (C) Cartilage rupture in Germany occurs more frequently in men (67 %) than women (33 %) [1, 4, 5].

knee arthroscopy, chondral lesions are identified in around 60 % of the procedures with a prevalence of OA in one third of the patients [6].

The complex joint physiology in the knee is the result of the interplay of bones like tibia, femur, patella and fibula, tendons, ligaments including anterior cruciate, posterior cruciate, medial collateral, lateral collateral, menisci and muscles. The ends of the long bones of femur and tibia are protected by articular cartilage to reduce friction between the joint surfaces and absorbs and distributes forces across the knee during movement. At every movement the knee has to withstand approximately 3.5 times of the person's bodyweight [7].

1.1 Articular cartilage

In the human body there are three types of cartilage: articular cartilage at the end of long bones and nose, elastic cartilage at the external ear and fibrous cartilage present in menisci and intervertebral discs. These types of cartilage are characterized by their extracellular matrix (ECM) composition and structure including cartilage fiber thickness. Regarding the objective of this thesis, the following paragraphs focus on the biology and properties of articular (hyaline) cartilage.

1.1.1 Biology of articular cartilage tissue

Articular cartilage is an avascular visco-elastic and anisotropic tissue composed of 70 % to 80 % by weight of water [8,9]. The solid components of the slightly translucent white ECM contains collagens, proteoglycans and non collagenous proteins [10]. Collagen type II fibers are the predominant component of the articular cartilage ECM forming the collagenous network. Besides, collagen type VI, IX, X and XI are found in articular cartilage [11,12]. In normal articular cartilage collagen VI is localized in pericellular matrix and plays a role in anchoring chondrocytes to the ECM by interaction with chondrocyte receptors [13]. One representative of non-collagenous proteins is superficial zone protein (SZP), that has shown to play a role in lubrication since it is a hyaluronan binding protein [14].

Within the collagen II network large macromolecules, the proteoglycans, are encapsulated to the ECM. Proteoglycans consist of a core protein to which polysaccharide unions, termed glycosaminoglycans (GAGs), are attached. Most abundant GAGs in articular cartilage are chondroitin sulfate, keratan sulfate or dermatan sulfate which are negatively charged in an aqueous environment. The proteoglycan monomer (core protein with GAG) is attached via a link protein to a hyaluronan backbone summarized as aggrecan the major proteoglycan in articular cartilage. The transcription factor SRY (sex related Y chromosom)-gene related (high mobility group) box 9 (SOX9) regulates aggrecan synthesis [8, 15–18].

The ability of GAGs to absorb water results in high swelling pressure due to the dense concentration of negative charges. The pressure resisted in cartilage ECM by tensile forces of the collagen network. Cartilage ECM represents combination of a fluid and solid phase of cartilage resulting in visco-elastic properties. During mechanical compression e.g. by loading water is forced out of the knee joint. After unloading the repulsion of negatively charged GAGs lead to reformation to initial shape with simultaneous water attraction into the ECM [8, 19].

Cartilage ECM is maintained by the single cell type in cartilage, the chondrocytes. With a high matrix to cell ratio the chondrocytes make up less than 2 % of the tissue volume [20]. Chondrocytes reside isolated in the ECM with a limited cellular crosstalk being reduced to cell-matrix interaction. They are attached to the cartilage ECM surface through the surface hyaluronic acid binding receptor cluster of differentiation receptor 44 (CD44) that binds to the hyaluronan backbone of proteoglycans [17, 21].

In contrast to most other tissues, articular cartilage is avascular and aneural. Following, chondrocyte nutrient supply takes place by diffusion from the synovial fluid. As a consequence, chondrocytes in the cartilage ECM are exposed to a gradient in nutrients and oxygen that decreases from the joint surface (6 % O₂) to the deep zone (2 % O₂) at the interface to subchondral bone [22–24].

From a micro structural and biochemical point of view articular cartilage is characterized by its unique zonal interplay of chondrocytes and ECM shown in figure 2. Articular cartilage is structured into four distinct regions: the superficial, middle, deep zone and calcified layer. Left image in figure 2 focuses on cells whereas collagen fiber orientation is shown in the right image [25, 26]. Within these zones the chondrocyte morphology, cell

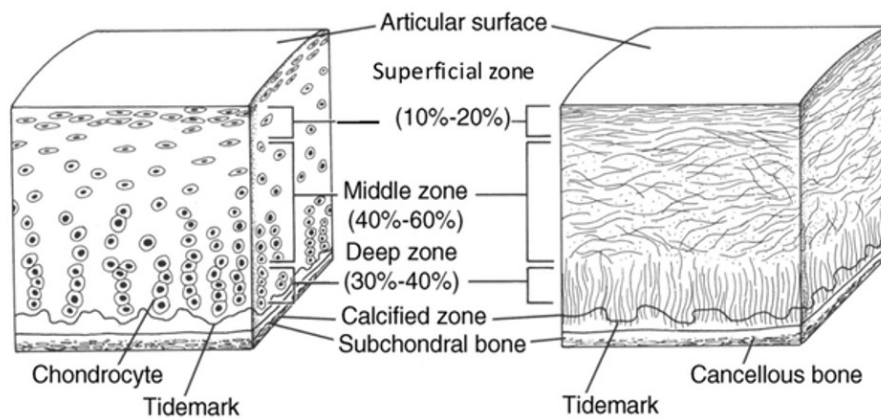


Figure 2 Zonal structure of articular cartilage. Chondrocytes and extracellular matrix are hierarchical organized in three zones: superficial zone, middle zone and deep zone. Subchondral (cancellous) bone is connected to deep zone of cartilage via the calcified zone and tidemark. Chondrocyte morphology and arrangement varies in the three zones from elongated shape in superficial zone to round morphology in deep zone. Parallel collagen fiber alignment to cartilage surface in superficial zone and perpendicular orientation in deep zone. Reproduced from Buckwalter *et al.* 1994 [26] with permission, copyright (1994) Wolters Kluwer Health, Inc.

alignment, biochemical composition of ECM and collagen fiber alignment varies. The calcified zone represents the interface between cartilage and subchondral (cancellous) bone. In the superficial zone chondrocytes are flattened and form a dense layer on the surface

expressing SZP also known as proteoglycan 4 (PRG4) [14]. The collagen type II fibers are aligned parallel to the surface along the direction of shear to resist shear stress and compression forces [27, 28]. The proteoglycan content shows in the superficial zone the lowest amount compared to middle and deep zone [25].

In the middle and deep zone chondrocytes appear more ellipsoidal compared to superficial zone. Chondrocytes in the middle zone are aligned along the randomly orientated collagen fibers [28]. Collagen II, aggrecan and cartilage intermediate layer protein are expressed in this zone with the maximum amount of proteoglycan present in articular cartilage [29].

In the deep zone chondrocytes display the lowest cell concentration of all zones and are arranged in columns along the collagen fibers that are perpendicular orientated to the surface [25, 30, 31]. Chondrocytes in the calcified zone undergo terminal differentiation marked by presence of hypertrophic marker collagen type X [32, 33]. The hypertrophic maturation of chondrocytes is induced by runt-related transcription factor 2 (RunX2), also known as Cbfa1 [34, 35]. The interface between cartilage and subchondral bone where collagen fibers of articular ECM anchor to the underlying bone is termed calcified zone (tidemark) [29, 36].

1.1.2 Cartilage defects

Cartilage defects are caused either by trauma, occurring in aged people above 60 years or being late sequela of concomitant knee injuries e.g. meniscal surgery, anterior crucial ligament reconstruction [37]. Trauma patients include sports related and accidental injuries of the knee joint in all age groups. Risk factors that initiate but also lead to progression of cartilage defects are trauma, inflammatory diseases in the knee joint, obesity and/or chronic overload [37–40]. After an initial event cartilage ECM changes and degenerates marked e.g. by joint swelling, fibrillation, softening, cartilage thinning and loss of proteoglycans.

Table 1 ICRS classification of articular cartilage defects. Cartilage defects are classified depending on lesion severity. Modified from international cartilage repair society (ICRS) and [41].

ICRS classification	Description and severeness of cartilage defects
ICRS 0	no defect
ICRS 1	intact surface / slight softening
ICRS 2	cartilage defect depth <50 % cartilage thickness
ICRS 3	cartilage defect depth >50 % cartilage thickness
ICRS 4	cartilage defect reaches subchondral bone

This causes reduction in mechanical properties accompanied by increased damage even under normal loading during every day life. The degeneration events may be a silent progress without pain. Lately, when subchondral bone is exposed during degeneration

progress, this causes severe pain and can progress to OA [42, 43].

Cartilage defects are classified by the international cartilage repair society (ICRS) based on the outerbridge classification that is dependent on the defect depth and severity into five groups summarized in table 1 [41]. ICRS 1 refers to cartilage defects with an intact surface while defects reaching subchondral bone are summarized in ICRS 4. ICRS 1 and ICRS 3 are further subdivided which are not mentioned here for reasons of clarity.

1.2 Cartilage treatments

Non surgical procedures like the application of anti-inflammatory drugs can help to reduce pain but is not an effective method to restore severe cartilage defects. Dependent on the anatomical location, lesion size, depth and severity various treatment options, either cell free or marrow stimulating techniques, cell based (autologous chondrocyte implantation (ACI), osteochondral allograft / autograft transplantation) or material assisted approaches like cell seeded bio-materials, are performed in clinical practice [44]. The procedure of these treatments including defect debridement and characteristics of ACI, matrix assisted autologous chondrocyte implantation (MACI) and microfracture, is shown in figure 3. The

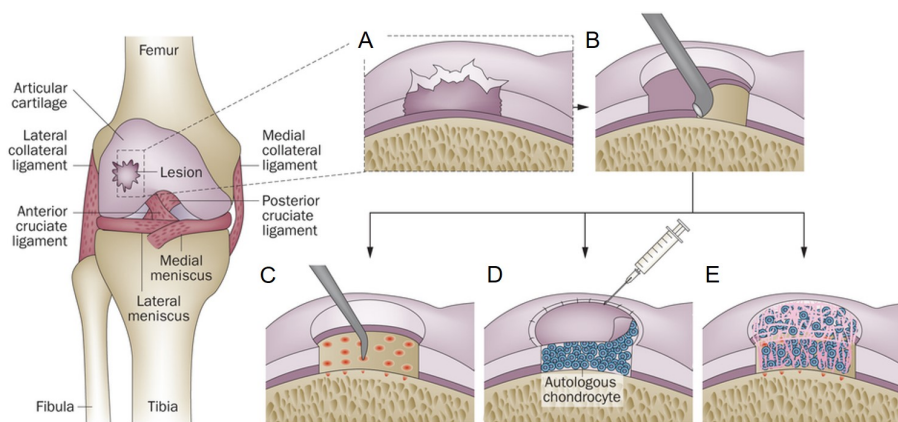


Figure 3 Cartilage treatment techniques. (A) Full thickness cartilage defect in the condyle (B) being debrided to cylindrical defect geometry. Three different treatment approaches are depicted in C-E): (C) microfracture, (D) autologous chondrocyte implantation (ACI), (E) matrix assisted autologous chondrocyte implantation (MACI). Reprinted by permission from Macmillan Publishers Ltd: Nature Reviews Rheumatology, Makris *et al.* 2014 [45], copyright (2014).

decision for one treatment option is supported by a treatment guide based on lesion size, lesion localization and patient's demand summarized in figure 4 [46]. This theoretical guide supports orthopedic surgeons in decision making for the suggested treatment approach according to ICRS standards. The choice for one treatment strategy assesses the severity of lesion, location but also the patients lifestyle (level of activity) and if the patient underwent

a previous cartilage treatment. These factors also influence the regeneration process and thus the outcome after surgical intervention [37, 47].

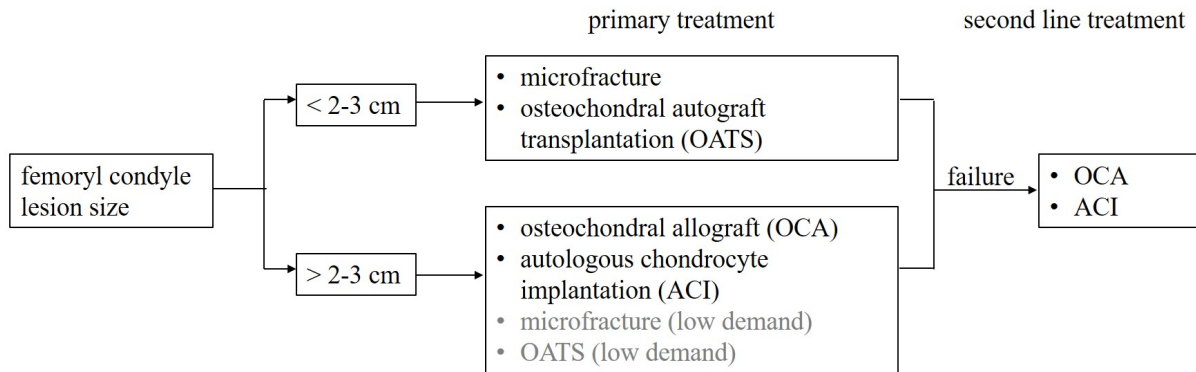


Figure 4 Guide for cartilage treatment of lesions located in femoral condyle. Dependent on lesion size and patient activity level orthopedic surgeons decide for treatment technique following the scheme. Small lesions (2–3 cm) are treated with microfracture or osteochondral autograft transplantation (OATS). Large defects (2–3 cm) are recommended to treat with osteochondral allograft (OCA) or autologous chondrocyte implantation (ACI). Patients with low demand can also be treated with microfracture or OATS. If the first operation does not lead to success ACI or OCA are recommended options for second treatment line. Modified from Coole *et al.* and Makris *et al.* [45, 46].

1.2.1 Marrow stimulating treatments

Addressing cartilage injury lesions in femoral condyle smaller than 2–3 cm², they are treated with marrow stimulation technique or osteochondral allografts (OCA) further described in section 1.2.4 [46]. Marrow stimulation technique also known as microfracture is a single step surgery. Hereby, the surgeon penetrates the subchondral bone by drilling several small diameter holes (4 mm in depth) into the lesion side to induce a bleeding and subsequent clot formation [48, 49]. Microfracture reduces pain and swelling and improves patient’s satisfaction characterized in terms of function and level of activity and quality of life but shows indication of deterioration from 18 months post-operatively [50]. Long-term failure of cartilage restoration is due to the formation of fibrous tissue that outweighs presence of hyaline repair tissue [47, 51]. One possibility to improve outcome after microfracture is to cover the defect with periosteal flap, natural collagen based membrane or synthetic membrane further described in chapter 1.2.2.

1.2.2 Material assisted treatments

Covering defects after microfracture technique with a bio-material is termed autologous matrix-induced chondrogenesis (AMIC) or autologous collagen-induced chondrogenesis

(ACIC) when a collagen membrane is used [52]. This novel cell free approaches (ACIC, AMIC) emerged to treat full thickness cartilage defects in single step surgeries. In detail, a collagen I-III membrane (Chondro-Gide[®], Geistlich Pharma AG) is fabricated in a way to prevent ingrowth of cells from synovial capsule into defect and represent a barrier to stabilize and keep the forming blood clot in the defect. Further clinical used materials are among others Bioseed C (BioTissue Technologies GmbH, Germany), NovoCart[®] 3D (TETEC Tissue Engineering Technologies AG, Germany), Cartipatch (Tissue Bank of France, France) and CaReS (Arthro Kinetics AG, Austria).

In patients where microfracture does not lead to clinical improvement and successful cartilage repair or in severe (osteocondral) defects ACI and osteochondral transplants (autologous or allogenic) are two further options.

1.2.3 Cell based treatments

In contrast to microfracture, ACI is a two step surgery performed in osteochondral lesions localized in load bearing regions. After harvesting chondrocytes by enzymatic digestion from autologous cartilage biopsy of non load bearing region in the joint they are expanded *in vitro* to increase number of cells for transplantation. In a second surgery the expanded chondrocytes are injected into the defect and covered with periosteal flap to keep cells in the defect [53]. Major drawback of the periosteal flap is the formation of hypertrophic tissue. To keep cells localized in defect and provide 3D environment fibrin glue has been widely used on top of chondrocyte layer. In order to overcome the hypertrophic tissue formation and graft failure of the periosteal flap alternative materials (e.g. Chondro-Gide[®], Geistlich Pharma AG) are used to replace the periosteal flap. A randomized study covering full thickness defects of ACI procedure with collagen or periosteal flap did not show significant differences 2 years post-operatively [54]. In contrast, McCarthy *et al.* reported significant higher collagen II presence in immunohistological stainings of the repair tissue at mean time point of 16 to 19 months postoperatively [55].

The second generation of ACI represents the MACI. MACI is characterized by combining a scaffold material with ACI procedure. Chondrocytes are seeded on a scaffold material providing a 3D environment to guide matrix synthesis and cultured for three days *in vitro* prior to implantation [56,57]. In a comparable study of ACI covered with collagen membrane or periosteal flap and MACI procedure comparable outcomes were reported [57,58].

The third generation of ACI describes an advanced approach of a matrix assisted autologous chondrocyte transplant (ACT3D-CS) developed and patented by co.don AG (Tetlow). The ACT3D-CS differs from ACI by the fact that 3D chondrocyte spheroids are generated *in vitro* over 8–10 weeks prior to implantation. This procedure is on the way to enter the

European market. Two clinical studies (phase II and III) are ongoing in which ACT3D-CS products are implanted in cartilage defects, either in different doses or compared to microfracture technique, to assess efficacy and safety (ClinicalTrials.gov Identifier: NCT01225575, NCT01222559). An internal report of the co.don AG comments on a significant improvement of patients 3 years postoperative compared to pre-operative situation [59].

1.2.4 Osteochondral grafts

Osteochondral allograft (OCA) is performed in patients to repair large full thickness cartilage defects (ICRS grade 3–4). In contrast, osteochondral autologous transplantation (OATS) is performed predominantly for smaller defects. Since this procedure requires isolation of tissue from a healthy region in the knee joint of the patient the size of the grafts is limited. OATS also represents a good option for second line treatment of defects that failed in first surgical intervention [46]. The term mosaicplasty refers to procedure in which multiple small diameter osteochondral grafts are transplanted. In both methods, cylinders are harvested from low load bearing side of the patella femoral joint and transplanted into the lesion with high survival rate and clinical success in more than 79 %–94 % of treatments depending on localization of lesions with OCA and OATS are limited by the availability of sufficient amount of donor tissue in low weight bearing areas from which osteochondral cylinders or cartilage tissue is harvested. Additionally, the surface shape for tissue isolation is a further issue for autologous transplant isolation. However, survival rate of osteochondral autografts in mid- to long term (10–14 years) counts with more than 60 % [60].

1.2.5 Limitations of cartilage treatments

Cartilage treatments aim to reduce pain and thus increase patients well-being in everyday life. Clinical results of all methods introduced above show satisfactory outcome from patient point of view in short-term follow ups up to 5 years. Several studies compare ACI with microfracture, MACI against ACI with controversial discussed results with a tendency for improvement in outcome for ACI or MACI compared to microfracture [61]. The outcome is dependent on a broad variety of factors like patient health, defect characteristic, cell number and age which will not be further addressed in this section. Another critical factor that has been addressed after microfracture is the mobilization and rehabilitation program e.g. weight-bearing restrictions, controlled application of motion, restoration of muscle function that needs to be designed patient specific to improve regeneration and quality of diseased tissue and prevent cartilage degeneration [62, 63].

One finding stated in most clinical studies independently of treatment strategy, is the formation of fibrous tissue. Fibrous tissue or fibrocartilage characterized by inferior mechanical properties and formation of collagen I compared to hyaline articular cartilage [64].

However, there is no treatment option known leading to long-term restoration of defects with articular cartilage tissue. An alternative to implant autologous or allogenic harvested tissue or cells is Tissue Engineering (TE) representing a method to produce mature cartilage tissue for implantation which is discussed in section 1.4.

1.3 Cartilage implant development: From the material to an advanced therapy medicinal product

All treatments which are performed in clinics have to be regulatory approved by local authority to ensure accuracy, safety, security to patients. In the European Union products are approved by the European Medicines Agency (EMA). In order to prevent misinterpretations referring categorization of human cells and tissue products in different countries the regulatory issues described here focus on the European market.

1.3.1 Advanced therapy medicinal products (ATMPs)

The way to commercialize a product or treatment approach for clinical application is dependent on different factors of the biological products, drugs and medical devices. In 2001 the EMA released a regulation (2001/83/EG) to create a community code for medical products for human use. 2001/83/EG defines the admission requirements for pharmaceuticals, classified as gene therapeutics and somatic cell therapies, in the European market.

With the emerging field of TE the EMA modified in 2007 the regulation from 2001 to define requirements from a technical and scientific point of view for novel gene therapeutics, medical devices, combined therapies (Regulation (EC) No 1394/2007). Regulation (EC) No 1394/2007 extended the classification of pharmaceuticals defined in 2001/83/EG by tissue engineered products (TEP) and combined products. Together with gene therapeutics and somatic cell therapy they are summarized as ATMPs and defined as follows (2001/83/EG, 2003/63EC, Regulation (EC) No 1394/2007, 2009/120/EC):

- A gene therapeutic describes an active agent that contain or consist of a recombinant nucleic acid to regulate, repair, replace, remove or add a genetic sequence in human and its therapeutic, prophylactic or diagnostic impact is in direct relation to the

product (e.g DNA-plasmid encoding growth factor).

- Somatic cell therapy medical product is based on substantially modified cells or tissues or does not serve for same function in donor and recipient. Additionally, the treatment, prevention and diagnosis of disease is attributed by pharmacological, immunological or metabolic impact (e.g. donated allogenic postmortem liver cells).
- TEPs are defined as biological pharmaceuticals if it contains biotechnological processed cells or tissue and is characterized by its potential to regenerate, recover or replace human tissue (e.g. autologous chondrocyte implantation).
- A combined ATMP is a medical device including either viable cells or tissue parts or in case of non living cells/ tissue parts the primary mode of action affects human body as chief impact (e.g. autologous expanded chondrocytes seeded on a scaffold).

A detailed description and further information about ATMPs is available in the above mentioned regulations. If a product fabricated from non living material and by physical process it is not classified as ATMPs.

1.3.2 Marketing authorization of ATMPs

ATMPs have to fulfill same requirements as pharmaceuticals for marketing approval and have to provide information for application specified in the Commission Directive 2009/120/EC. Basis for marketing approval are the results from clinical trials. Clinical trials demand good clinical and manufacturing practice and are categorized in three phases addressing different issues concerning safety (phase I), protocol testing (phase II), safety and efficacy (phase III) to compare the outcome with existing treatments. Before receiving the permission for clinical trials data from non- or pre-clinical trials and validation of manufacturing process are required. Pre-clinical data includes animal studies in large animals (e.g. goats) as proof of principle testing in a relevant set up but also toxicological studies (ectopic mouse model or orthotopic model in e.g. sheep or goat). Validation of manufacturing process includes functional tests regarding cell characterization (gene expression) in cell culture and also animal models.

1.3.3 ATMPs for cartilage regeneration

The introduction of ATMPs and regulation for marketing authorization protects patients to be treated with products that fulfill best standard, quality and ensure safety. From the introduction of ATMP regulations two marketing authorization applications for cartilage treatments have completed the procedure: ChondroCelect, a tissue engineering product, is approved for treatment of single symptomatic cartilage defects in adults. MACI procedure is classified as combined ATMP for repair of symptomatic, full thickness cartilage defects (3 – 20 cm²) in the knee of adult patients.

1.4 TE of cartilage

In order to overcome some limitations of cell based cartilage treatments concerning sufficient amount of healthy tissue for cell isolation or tissue transplantation TE approaches gained increasing interest. TE describes a method to combine cells, scaffold material and external stimuli like bioactive molecules or (bio)mechanics resulting in 3D constructs. These 3D constructs are matured *in vitro* under controlled physiological conditions (37°C, 5 % CO₂, 95 % humidity) in culture devices under static or dynamic conditions to generate an artificial biomimetic cartilage tissue for transplantation in patients. Alternatively, cartilage TE products can be used as *in vitro* models. In general, cells for TE approaches are autologous or allogenic harvested, expanded *in vitro*, seeded on a biomaterial to serve as 3D structural support for the cells during tissue maturation.

1.4.1 Cell source

From clinical point of view the cells should be harvested from tissue in a sufficient amount and easy way. In cartilage TE chondrocytes and multipotent stromal cells (MSC) are the two most widely used cell types and discussed in the following paragraphs.

1.4.1.1 Chondrocytes (CZs)

For cartilage TE chondrocytes (CZ) are the first choice. However, they are limited due to diseased tissue in patients suffering from OA or other degenerative processes in cartilage and have shown changes in proliferation and chondrogenic capacity [65]. Before CZs are injected into defect side, cells have to be expanded *in vitro* which is a long process during which the cells undergo phenotypically changes and de-differentiate [66,67]. When expanded CZ are seeded on biomaterials they need to be re-differentiated to stimulate articular cartilage ECM synthesis. The re-differentiation potential decreases with the

number of passages marked by a reduced gene expression level [66,67].

During the last years there is an increasing interest in CZs isolated from nasal biopsies. Nasal cartilage has articular character and the isolation of nasal CZs is similar to CZs derived from articular joint tissue. In contrast to joint derived cartilage, nasal cartilage can be harvested minimal invasively and does not show changes in OA patients. After *in vitro* expansion of nasal CZs these cells have shown superior results concerning proliferation and cartilage matrix synthesis compared to articular CZs [68,69]. In a first human trial the feasibility and safety of autologous nasal CZs for AMIC procedure with comparable magnetic resonance scores to ACI and microfracture was demonstrated [70].

1.4.1.2 Multipotent stromal cells (MSCs)

An alternative cell type to CZs are MSCs. They can be isolated from various tissues including bone marrow, adipose tissue, umbilical cord or synovial membrane and show high proliferation potential [71–73]. The multipotent character of MSC is characterized according minimal criteria for specific surface proteins by presence of CD 73, CD 90 and CD 105 and absence of CD 14, CD 34 and CD 45 as well as differentiation potential towards adipogenic chondrogenic and osteogenic lineage [74]. Chondrogenesis is induced by addition of dexamethasone, TGF- β 1 or 3 into pellet culture for 21 days [75]. Drawback of MSC *in vitro* chondrogenic differentiation is the risk of hypertrophic differentiation and subsequent progress to undergo endochondral ossification marked by expression of collagen I and X. Furthermore, during long term *in vitro* culture of MSC seeded on an alginate or hyaluronic acid scaffold the proteoglycan production and mechanical properties of the construct decreased from day 56 on [76]. This phenotypic instability of chondrogenic differentiated MSC limits application of MSC for cartilage repair.

MSC isolated from synovial membrane have shown promising results to differentiate more likely to articular cartilage producing cells that can overcome instability in chondrogenic phenotype of differentiated bone marrow derived MSC [72,77]. Functionality and *in vivo* phenotype of synovial and bone marrow derived MSC revealed differences dependent on origin. Synovia MSCs resulted in a more fibrous tissue formation (collagen I) while bone marrow MSC underwent endochondral differentiation [72,78].

1.4.1.3 Cell co-cultures

Combinations of bone marrow derived MSC and articular or nasal CZs (ratio 80:20) have shown improvement in cartilage matrix production, CZ proliferation and MSC chondrogenesis [79–81]. The combination of CZs and MSC are a promising approach. Due to the reduced amount of CZs (20 %) in co-culture compared to mono-culture the amount

of isolated CZs is sufficient for treatments without expansion *in vitro*. Following, primary CZs (passage 0) without expansion overcome limitations during *in vitro* expansion and being injected together with MSCs in a single-step knee arthroscopy. Nevertheless, further investigations are needed to analyze whether articular cartilage matrix production can be maintained or become hypertrophic in later stages.

TE cartilage products can be either used as *in vitro* test systems (high throughput, controllability) to replace animal models e.g. for cytotoxic testings or investigate addition of growth factors or other biomolecules on viability and maturation of the constructs. In a second row, TE constructs can be implanted into animals for pre-clinical studies or as transplant in humans for cartilage treatments.

1.4.2 Materials

Materials, either synthetic, natural or a combination of both, provide a 3D environment to cells. For application in patients materials have to be bio-compatible and bio-resorbable and do not degrade with cytotoxic side products. Pore size, porosity and degree of inter-connectivity are important properties to allow cell infiltration, cell migration, matrix deposition, delivery of nutrients and removal of waste products via diffusion [82]. The degradation time should match with the rate cells synthesize new ECM. Coupling materials with bio-active molecules (e.g. growth factors) are not necessary but can stimulate matrix synthesis, cell attachment and cell proliferation. Focusing on materials for cartilage TE, the material has to provide mechanical stability to withstand shear and compressive forces in the knee joint.

A broad variety of synthetic (e.g. poly(glycolic acid), poly(ethylene glycol), poly(caprolactone)), natural (e.g. alginate, collagen, fibrin) or composites (e.g. collagen I-hyaluronic acid-fibrinogen) are used for cartilage TE which are not discussed in detail in this thesis. Different groups have shown the stimulative effect of material composition on cell phenotype, cell differentiation and ECM synthesis being summarized elsewhere [83]. Due to the injectability to fill defects of any shape and the advantage of homogenous cell distribution, hydrogels are one material class suitable for cartilage TE. Hydrogels are characterized by their high water contents comparable to cartilage ECM. Moreover, hydrogel materials have shown to support round phenotype of CZs or stimulate chondrogenic differentiation [84].

1.4.2.1 Synthetic materials

Main advantage of synthetic polymers is the tunability of mechanical and chemical properties dependent on molecular weight and the possibility to fabricate scaffolds in different structures and shape. Moreover, synthetic materials are fabricated under high

standardized conditions that minimizes large batch to batch differences. Poly(ethylene glycol) (PEG) gained increasing interest for application in drug delivery, food and more recently in TE [85]. The mechanical properties of PEG are comparable to cartilage and the hydrophilic character allowing the adsorption of proteins, growth factors and other biomolecules [86].

PEG is a bio-inert material that does not degrade. Modification with bioactive molecules by co-polymerization with peptides or natural polymers results in partially degradable PEG [87]. Due to the hydrophilic character PEGs are swelling under aqueous conditions and form hydrogels with viscoelastic properties when cross-linked [88]. The degradation rate of a four armed star-shaped PEG polymerized with heparin can be adjusted by incorporation of matrix-metalloproteinase (MMP) cleaving sites [89,90]. Degradable PEG materials (e.g. by MMP modification) have shown their ability to enhance cartilage matrix production of embedded CZs or stimulate MSC chondrogenesis [91–93]. First results of cartilage formation of a cell loaded PEG-hyaluronic acid hydrogel for intervertebral disk regeneration [94]. Combination of PEG and chondroitin sulfate indicated to reduce terminal differentiation of MSC under dynamic loading conditions [95].

Another method to increase cell-material interaction represents the cell adhesion motif RGD [96]. RGD is characterized to increase cell proliferation, cell morphology and showed a positive effect on cell vitality [97,98].

1.4.2.2 Natural materials

Natural materials simulate native ECM in terms of composition and can be fabricated as hydrogel materials. Natural hydrogels like fibrin and collagen are highlighted by their fibrous structure and biodegradability. *In vitro* cultured hydrogels like alginate, fibrin or collagen being embedded with CZs resulted in cartilage matrix formation characterized by increase in GAG content over time and even showed ability to re-differentiate expanded CZs [99–101].

A commercially available collagen hydrogel is CaReS-1S[®] (Arthro Kinetics AG, Germany), a ready to use collagen I (3 mg/ml) implant. CaReS-1S is used cell free and recommended to treat focal, full layer defects (ICRS class 3 and 4). The collagen hydrogel is described to support a reparative response and thus stimulating defect regeneration [102]. Pre-clinical studies in minipigs showed the colonization of the implant in the defect zone forming a hyaline like regenerated tissue with comparable outcome as in MACI treatment [103,104]. In a clinical study significant improvement in functional score was reported when 6 cm² defects were treated with autologous CZ loaded CaReS-1S at 2 year follow up [105]. In a case study treatment of a young patient showed collagen II synthesis in histological

stainings in repair tissue [106].

Major disadvantage of some natural derived hydrogels like collagen I and fibrin is the shrinkage due to low mechanical strength as result of cell remodeling of the bio-material [99]. To overcome this issue synthetic hydrogel materials can be combined with natural materials to increase mechanical properties with a certain degree for controllability of material properties. With the emerging technology of novel material fabrication methods as the emerging field of bio-printing there is a growing interest in fabricating cartilage scaffolds mimicking the native tissue in composition and anatomic complexity. First attempts are published on printing patient specific zonal structured cartilage implants [107].

1.4.3 Bioreactors

In vitro maturation of complex 3D TE constructs is accompanied by limited diffusion of nutrients under static *in vitro* conditions [108]. To ensure sufficient supply of nutrients to cells embedded throughout the scaffolds and removal of waste products bioreactors are a culture method that allows for control and monitoring of *in vitro* conditions in a dynamic environment. Bioreactors open the opportunity to study cellular mechanisms under defined and standardized culture conditions with the option to control, monitor or record oxygen tension or other metabolic activities *in situ* [109].

Articular cartilage is a non vascularized tissue and gets nutrients via diffusional mass transfer from synovial fluid. Therefore, cartilage TE constructs do not necessary be perfused. More sophisticated are the use of bioreactors for application of physical stimuli by dynamic culture conditions that has been shown to have advantageous effect on biochemical ECM composition, bio-mechanics and morphology compared to static conditions [110]. Cartilage in the knee joint experiences a complex interplay of compressive, tensile and shear forces which maintain tissue functionality and prevents degenerative processes. *In vitro* culture under mechanical loading like compression force, shear stress or tensile fore can stimulate cartilage matrix synthesis, gene expression levels, structural organization, increase in bio-mechanical properties and cell fate [111,112].

The results on how cell loaded scaffolds or cartilage explants respond to mechanical stimuli revealed differences due to the variety of loading protocols, differing in duration ranging between hours and days, frequency from 0.01 – 1.0 Hz, magnitude of loading differing percentage of strain (1 – 10 %) and/or tension (5 – 20 %) and also choice of scaffold materials and cell species. To simulate the mechanical conditions in the knee joint more closely complex bioreactors have been developed so stimulate physical foreces like compression, hydrostatic pressure, tension and shear [113,114]. Till now there is only one multi-axial bioreactor system published that is able to apply physiological loading in

terms of interface shear motion and unconfined dynamic compression [114, 115]. Schaetti *et al.* showed that chondrogenic induction of MSC seeded polyurethane scaffold without exogenous TGF- β media supplementation was present only in the multiaxial loading regime (compression and shear) and not in the single mode [114]. Cochis *et al.* reported that chondrogenic gene expression ratios of collagen II : collagen I, collagen II : collagen 10 and aggrecan : collagen I were significantly upregulated in MSC seeded methylcellulose-based hydrogel stimulated for 1 h a day with the multi-axial bioreactor compared to non-loading group [116]. From a technical point of view multi-axial bioreactor systems are challenging in terms of complying with good manufacturing practice and the development of sophisticated technical efforts allowing for convenient handling [109, 117].

Once the mechanical loading exceed physiological range the cellular response can induce disadvantageous effects or remain unchanged to non loading conditions. It is obvious that a cartilage explant need a different loading protocol compared to a TE cartilage product to stimulate tissue functionality. In summary, TE is a promising approach but for cartilage transplants the right choice of cell type(s), cell number, material and culture protocol has not been found to result in a functional and mechanical articular cartilage transplant.

1.5 Test systems: an alternative to animal experiments

In 2003 the EU released a regulation for animal experiments (2003/15/EG) that has forbidden animal experiments for cosmetic products in the EU since 2004. From then on there was an ascending interest in the development of alternative models like test systems to reduce, refine and replace animal experiments for other applications. The controllability of physiological parameters and the repeatability of experiments with a high throughput to set up experiments in a statistical relevant amount are a general demand on test systems. In animal studies, all these parameters cannot be addressed since animal experiments in large animals in goat, horse or sheep that are clinically relevant raise high costs for animal caring and pose ethical issues [118, 119]. Drawback of small animal studies (e.g. mice, rats) is the joint size that is not comparable to human joint. Additionally, the articular surface in small animals is made up of few cell layers that does not reflect human articular cartilage in thickness with mean value of 2.35 mm [120].

Test systems, regardless for which application, can be built following the bottom up or the drop down principle. The bottom up principle describes the way of growing TE products based on biomaterials which are seeded with primary cells or cell lines and cultured *in vitro* under physiological conditions (37°C, 5 % CO₂) to generate artificial tissues. On the

contrary, the top down principle means the isolation of native tissue explants which are subsequently cultured under sterile conditions. Test systems based on tissue explants from animal or human source are defined in this thesis as *ex vivo* cultures.

1.5.1 *In vitro* models

High controllability and standardization of culture conditions and parameters are given for *in vitro* cultures of CZ or MSC seeded bio-materials that are cultured under free swelling conditions in well plates [121–123]. Drawback of these modes is the *in vitro* culture of an isolated cell type in a cell specific media. Especially MSC seeded materials need the supplementation of culture media with TGF- β 1, 2 or 3 up to 10 ng/ml to induce chondrogenic differentiation, to elevate cartilage matrix synthesis or to re-differentiate monolayer expanded CZs [75, 124]. However, it is obvious that these *in vitro* cultures to engineer cartilage like tissue miss the complexity of native cues in terms of interplay with other cell types and surrounding and/ or interfering tissues in the synovial capsule. Bio-compatibility testings, cell-material interactions and effect of material properties like porosity, pore size, cross linking, stiffness on cellular behavior and ECM matrix production in a controlled environment with high throughput are major application of these models. A more complex *in vitro* model is the combination of two scaffold materials to generate a composite or biphasic scaffold. Combination of CZs seeded collagen I/III membrane (Chondro-Gide[®], Geistlich Pharma AG) and a commercially available devitalized cancellous bone scaffold (Tutobone[®], Tutogen Medical GmbH) with fibrin glue resulted in a TE osteochondral *in vitro* model [68]. The generation of this more complex *in vitro* model opens the possibility to study cartilage and bone interactions on cellular level, the influence on matrix production and tissue integration at the cartilage-bone interface. Barandun *et al.* showed with this osteochondral model that nasal CZs seeded on collagen membrane resulted in better integration and matrix production compared to articular cartilage even when the osteochondral construct was cultured in media without TGF- β 1 [68]. Bone is a tissue that is permanently remodeled by osteoblast, osteoclast and osteocyte activity [125, 126]. CZs in cartilage exhibit stimuli not only from presence of bone like material but also from cellular signaling between the two tissues. In a different set-up CZs and or MSC seeded in agarose hydrogel (chondral part) and bone marrow derived MSC encapsulated in alginate hydrogel (bone part) were cultured separately (2 weeks), combined for co-culture (4 weeks) *in vitro* and then implanted in nude mice (6 weeks) showed endochondral bone formation in bone phase [127].

To further study the stimulative effect of bone cells on cartilage phenotype, matrix production and chondrogenesis this model would be suitable with a high degree of controllability,

repeatability and low donor variation if cells from selected donors are used. When different cell types included in one construct the cell or tissue specific media supply pose a further burden that has to be dealt with by specific culture chambers.

1.5.2 *Ex vivo* models

In contrast to *in vitro* models *ex vivo* models are characterized by culture of a tissue explants from human or animal source. The presence of native tissue represents a higher degree of complexity compared to *in vitro* models with the issue of biological variations dependent on localization in the joint and donor variability. Main advantage of *ex vivo* cultures is the presence of native tissue that can have a stimulative effect on cells and secretes soluble factors into culture media during matrix remodeling.

Cartilage tissue isolated from (knee) joints can be cultured *ex vivo* to address influence of cytokines, growth factors, nutrients on CZ viability and cartilage matrix properties under defined conditions. After creation of a defect in the cartilage center interaction of cell free or cell loaded cartilage scaffolds or TE cartilage constructs with articular cartilage can be studied in these cartilage only explants.

Ex vivo chondral models that address regeneration of cartilage defects with scaffold based treatments have shown their applicability to investigate scaffold material-cartilage integration [128–130]. One application of cartilage only explants is to analyze different glueing methods on scaffold material-cartilage or cartilage-cartilage integration. This integration studies are of relevance to investigate optimal fixation between scaffold and cartilage for *in vivo* studies.

Similar to one tissue *in vitro* models the cartilage only discs are lacking the presence of subchondral bone. Articular cartilage in the knee environment is attached to subchondral bone via calcified layer that transfers mechanical forces to cartilage [131]. From clinical practice it is demonstrated that subchondral bone is a key factor for successes in cartilage regeneration after microfracture [132, 133]. Therefore, osteochondral explants represent the physiology in the joint more closely in terms of gradients in nutrient supply and oxygen tension. In previous studies it was shown that subchondral bone promotes cartilage homeostasis and chondrogenesis of MSC seeded in cartilage defects compared to cartilage only model [134, 135]. Additionally, the subchondral bone including bone marrow located in the inter trabecular space hosts bone cells including osteoblasts, osteoclasts and osteocytes and blood cells like hematopoietic MSC, fibroblasts or monocytes that provides a natural cell source in case of defect regeneration [131, 136–138]. Limitation of this first described osteochondral model is the decrease in bone viability and cartilage matrix degradation in terms of decrease in collagen II and aggrecan gene expression over time but less reduction

compared to cartilage only explants [134]. Regardless of the limitations, the group showed the applicability of the model for studying cartilage treatments.

In contrast to animal models, *ex vivo* cartilage and osteochondral models allow testing of various materials in parallel under same conditions to investigate the stimulative effect of material composition, scaffold structure on ECM synthesis, material remodeling, cell phenotype, material-tissue integration and cell infiltration at multiple time points. Major requirement to a test system for cartilage regeneration are beside standardized and reproducible culture conditions the preservation of metabolic activity and ECM composition.

2. Aim

Current cartilage treatment strategies focus on symptom and pain relief that often results in formation of fibrous tissue which is different in ECM and has superior mechanical properties compared articular cartilage. From the scientific point of view cartilage treatments should aim to achieve formation of regenerated tissue in structure, function and bio-mechanical properties of native articular cartilage.

Commercially available implant material used for trauma patients result in higher success rates compared to the aged population (patients over 60 years of age) suffer from OA. The differences in outcome of cartilage regeneration therapies in patients is caused by the defect depth, age, patients health and diseased state of the articular cartilage tissue [47,50]. Chondrocytes of OA patient and patients over 60 years are less metabolic active and respond less to external stimuli compared to chondrocytes from healthy and young patients resulting in less matrix synthesis [139–141]. Therefore, chondrocytes of diseased and older patients need additional structural and / or biochemical stimuli and support by cell seeding of cartilage implants to enhance tissue regeneration. In order to improve preclinical evaluation of novel materials and treatment strategies test systems are necessary to evaluate and characterize the regenerative potential *ex vivo*. One advantage of test systems are the controllability of *ex vivo* cultures and the possibility to simulate different defect scenarios *in vitro* in a reproducible way.

The overall aim of this thesis was the establishment of an *ex vivo* osteochondral cartilage defect model that allows preclinical testing and development of new cartilage treatment strategies. This doctoral thesis is structured into the following three parts (figure 5):

1. Establishment of an *ex vivo* cartilage defect model with critical sized defects.
2. *Ex vivo* evaluation of novel bio-materials as scaffold based cartilage treatment strategies in osteochondral defects.
3. Modification of defect geometry. Influence of defect depth on cartilage regeneration.

The first part of the thesis describes the isolation of porcine osteochondral explants, the development of a custom made static culture platform and the modification of explants with cartilage defects. In order to define the critical size diameter in the *ex vivo* defect model cartilage defects ranging from 1 mm to 6 mm were created and cultured *ex vivo* without any treatment with tissue specific media.

The second part of this thesis focuses on the *ex vivo* evaluation of novel bio-materials as scaffold based cartilage treatment strategies in osteochondral defects. Within the

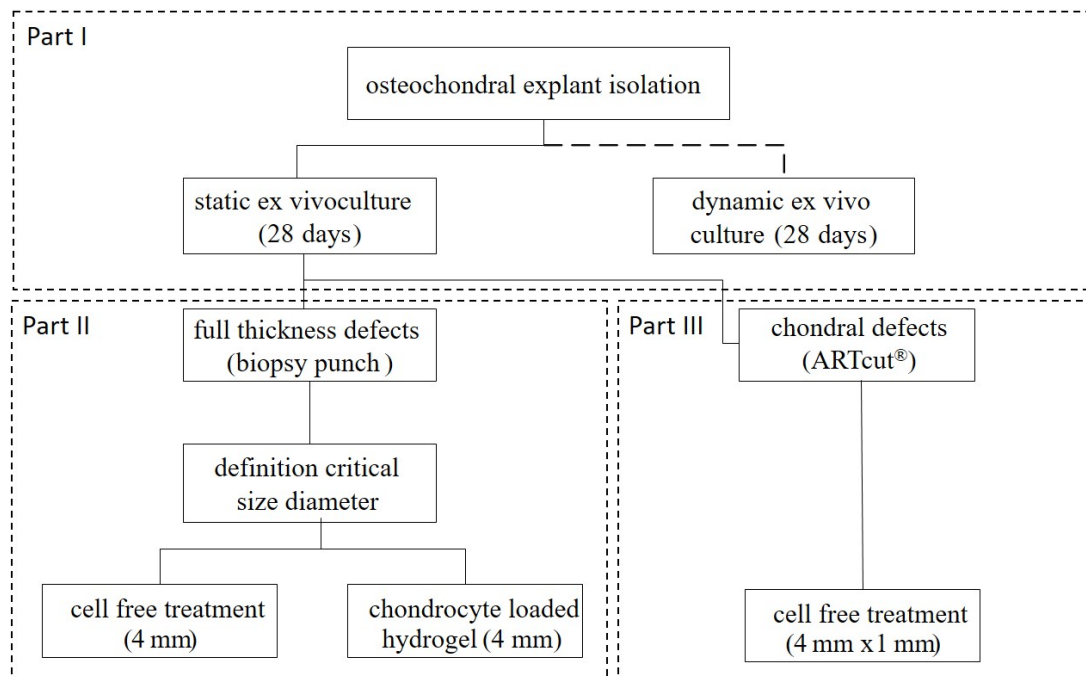


Figure 5 Schematic representation of the experimental approaches in this thesis. Establishment of osteochondral defect model (part I), bio-material testing in full thickness defects (part II) and implementation of artificial tissue cutter as standardized method to create chondral defects (part III).

European project HydroZONES (2007-2013, grant agreement no. 309962) three novel hydrogel materials were developed. Commercially available fibrin glue and collagen I hydrogel, isolated from rat tails, served as clinical and internal control materials. All hydrogel materials were screened on their regenerative potential in the *ex vivo* osteochondral defect model in a cell free and chondrocyte loaded approach.

In the third part of this thesis, we modified the osteochondral defect model in terms of cartilage defect depth. With the help of the custom made wounding machine artificial tissue cutter (ARTcut[®]) we realized standardized partial thickness defects to mimic chondral fissures in early stage OA.

Freshly isolated, *ex vivo* cultured OCE and hydrogel materials were analyzed by viability staining (MTT, live-dead-staining). Evaluation of cartilage regeneration and matrix deposition in the hydrogels followed after 28 days *ex vivo* by (immuno-) histological stainings, biochemical analysis (GAG, DNA) and gene expression analysis was only included for chondrocyte loaded hydrogel screening.

3. Materials

In this chapter biologic material, chemicals, media supplements, buffers, enzymes, antibodies, primer pairs, commercially available kits, equipment and plastic disposables are described and listed which are used to perform the methods described in section 4 of this thesis. If nothing else is stated PBS was used without calcium- and magnesium chloride.

3.1 Biologic material

In this thesis osteochondral cartilage bone explants were isolated from porcine femoral condyles which were retrieved from a local slaughter house (butcher Kirchner, Würzburg, Germany or The Netherlands). The domestic pigs were aged between 6–8 months. Primary porcine CZs were isolated from the lateral condyles of the slaughter house material according to the procedure described in the methods chapter. Primary porcine mesenchymal stromal cells were isolated from bone marrow aspirate of 6–8 weeks young domestic pigs (pig farm Niedermeyer, Dettelbach, Germany). Bone marrow was aspirated after animal death.

3.2 List of chemicals

Single components and basic media for preparation of explant and cell culture media as well as chemicals for cell culture techniques and analytical procession are summarized in table 2 and table 3.

Table 2 Components and media supplements for preparation of cell culture media and solutions.

chemical	supplier
3-isobutyl-1-methylxanthine (IBMX)	VWR, A0695
antibiotic-antimycotic (100x)	Gibco, 15240
10 000 U/ml Penicillin, 10 000 µg/ml Streptomycin, 25 µg/ml Fungizone	
ascorbic acid 2-phosphate Magnesium salt	Wako chemicals, 013-19641
β -glycerophosphate	Sigma-Aldrich, G9422
chondroitin sodium salt	Sigma-Aldrich, C4384
dexamethasone	Sigma-Aldrich, D4902
dimethylsulfoxide (DMSO)	Sigma-Aldrich, D2438

Table 2

chemical	supplier
DMEM HG	Gibco, 32430-027
EDTA	Sigma-Aldrich, 5134
FCS	Gibco, 10270106
ficoll-Paque PREMIUM (1.077 g/ml)	GE healthcare, 17-5442-03
ITS ⁺ premix	BD, 354352
l-proline	Sigma-Aldrich, P5607-25G
PBS ⁻ (without CaCl ₂ and MgCl ₂)	Sigma, D8537
recombinant human basic FGF	R&D Systems, 233-FB-025
recombinant human TGF- β 1	R&D Systems, 240-B
sodium pyruvate (100x, 100 mM)	Gibco, 11360

Table 3 List of all chemicals used for preparation of buffers and staining solutions.

chemical	supplier
2-Methoxyethylacetat	Merck, S7222461616
2-Propanol	Carl Roth, 6752
acetic acid, glacial	Sigma-Aldrich,
acetone	Carl Roth, 5025
antibody Diluent, Background Reducing	Dako, S302283
CaCl ₂	VWR, 1.02391.1000
chloroform	Sigma-Aldrich, 288306
DAB+Chromogen	Dako, K3468
dako pen	Dako, S002
DMMB	Sigma-Aldrich, 34108
EDTA-Na ₂ Salt x 2H ₂ O	Sigma-Aldrich, E5134
entellan	Merck, 1079610500
ethanol 96 %	Carl Roth, T171.3
ethanol absolute	Carl Roth, 9065.2
fast green	Sigma-Aldrich, F-7258
fluomount DAPI	Biozol, SBA-0100-20
glycine	Sigma-Aldrich, G8898
hardener 1	Heraeus Kulzer, 64715444
hardener 2	Heraeus Kulzer, 66039185
HCl 37 %	Roth, 4625

Table 3

chemical	supplier
hematoxylin (mayer)	Morphisto, 10231
hematoxylin (weigert)	Morphisto, 10225
heparin Natrium 25 000	Ratiopharm, 03029843
HEPES	Sigma-Aldrich, H3375
histofix (4 % v/v paraformaldehyde)	Carl Roth, P087.3
hydrogen peroxide	Carl Roth, 8070
L-Cystein hydrochloride	Carl Roth, 3468.1
MTT (3-(4,5-Dimethyl-2-thiazolyl)-2,5-diphenyl-2H-tetrazolium bromide)	Serva, 20359
Na ₂ HPO ₄	AppliChem, A1046
NaCl	Sigma-Aldrich, S7653
NaH ₂ PO ₄	Sigma-Aldrich, S3139
NaOH 1 N	Merck, HC60683537
PMMA	Heraeus Kulzer, 66010251
QIAzol	Quiagen, 79306
regler	Heraeus Kulzer, 66039184
safranin-O	Sigma-Aldrich, 84120
serum donkey	Sigma-Aldrich, G9023
T9100 neu	Heraeus Kulzer, 66006735
TissueTek®	Sakura, 4583
trizma base	Sigma-Aldrich, T6066
trizol reagent	Life Technologies, 15596
trypan blue	Sigma-Aldrich, T8154-100ml
tween-20	VWR, 8221840500
xylene	Roth, 9713

3.3 List of enzymes

This section summarizes enzymes used for cell culture techniques or antigen retrieval in immuno-histological or immuno-fluorescent stainings.

Table 4 List of enzymes.

enzyme	activity	description	supplier
collagenase (CLS-2)	230 U/mg	Prepared to contain higher clostridial activity. Suggested for bone, heart, liver and salivary primary cell isolation.	Cell Systems, LS004176
collagenase NB-4	≥ 10 U/mg	Collagenase NB-4 contains class I and class II collagenase and a balanced ratio of proteolytic side activities	Serva, 1745401
collagenase P		Collagenase from <i>C. histolyticum</i> is used for the dissociation of tissues.	Roche, 11213865001
trypsin	≥ 40 μ kat/g	Trypsin is a protease used for protein digestion that cleaves peptide bonds preferably at the carboxyl side of the amino acids lysine or arginine.	Serva, 37289.02
trypsin EDTA (10x)	0,5 % / 0,2 % in PBS	trypsin EDTA is used to release adherent cells from tissue culture plates for passaging	PAA, L11-003
pepsin	$\geq 2\ 500$ U/mg	Pepsin is a peptidase used to digest proteins.	Sigma-Aldrich P7012
hyaluronidase from bovine testes	3 000 U/mg	Hyaluronidase degrades hyaluronan and cleaves glycosidic bonds in hyaluronic acid, chondroitin, and chondroitin sulfate.	Sigma-Aldrich H4272
pronase		Pronase is a mixture of several non-specific proteases that digest proteins down to single amino acids.	Roche, 11459643001
papain	≥ 10 U/mg	Papain papaya latex is a cysteine protease that cleaves peptide bonds of basic amino acids.	Sigma- Aldrich, P4762

3.4 Cell culture techniques: Culture media and buffer

Composition of cell culture media and buffer used for cell culture techniques are described in this section.

Table 5 Composition of cell culture media.

media	composition	volume
pMSC expansion media	DMEM HG	89 % (v/v)
	FCS	10 % (v/v)
	antibiotic-antimycotic	1 % (v/v)
	hbFGF	10 ng/ml
ITS ⁺ premix	insulin	0.625 mg/ml
	transferrin	0.625 mg/ml
	selenious acid	0.625 mg/ml
	bovine serum albumin	125 mg/ml
	linoleic acid	0.535 mg/ml
antibiotic-antimycotic (100x)	penicillin	10 000 U/ml
	streptomycin	10 000 µg/ml
	amphotericin B	25 µg/ml
chondrogenic (cartilage) media	DMEM HG	97 % (v/v)
	antibiotic-antimycotic	1 % (v/v)
	ITS ⁺ premix	1 % (v/v)
	sodium pyruvate	1 % (v/v) (1 mM)
	ascorbic-acid-2-phosphate	50 µg/ml (0.17 mM)
	l-proline	40 µg/ml (0.35 mM)
	dexamethasone	100 nM
bone media	DMEM HG	89 % (v/v)
	FCS	10 % (v/v)
	antibiotic-antimycotic	1 % (v/v)
	ascorbic-acid-2-phosphate	50 µg/ml (0.17 mM)
	β -glycerophosphate	216 µg/ml (10 mM)
	dexamethasone	100 nM

Table 6 Overview of buffers for cell culture techniques.

buffer (application)	composition	final concentration
PBS/EDTA (cell culture)	PBS	
	EDTA	0.54 mM
trypsin-EDTA 1x (cell culture)	PBS/EDTA	90 % (v/v)
	Trypsin-EDTA (10x)	10 % (v/v)
FACS buffer	PBS	
	EDTA 2mM	2 mM
	BSA	0.5 % (v/v)
collagenase digestion (chondrocyte isolation)	DMEM HG	
	FCS	10 % (v/v)
	collagenase 2 CLS-2	0.5 % (m/v)
	antibiotic-antimycotic	2 % (v/v)
Gel neutralizing solution (pH 8.5)	DMEM (2x)	
	chondroitin sulfate	0.05 mg/ml
	HEPES (3 M)	0.9 M
	FCS	3 % (v/v)
live-dead-staining solution (viability staining)	DMEM HG	
	Calcein AM	2 μ M
	Ethidium homodimer-1	4 μ M
MTT solution (viability staining)	DMEM HG	
	MTT	1 mg/ml

3.5 Hydrogel materials and peptides

Polymers, solutions and proteins used to fabricate hydrogel materials are listed in this section.

Table 7 List of materials for fabrication of collagen I, fibrin glue, 50 % matrix-metalloproteinase (MMP) cleavable four armed poly(ethylene glycol) polymerized with heparin (starPEGh), PEG and partially metacrylated poly[N-(2-hydroxypropyl) methacrylamide mono/dilactate] (MP/HA) and allyl- and thiol-functional linear poly(glycidol) (P(AGE/G)-HA-SH) hydrogel.

material	component	final concentration	supplier
collagen I	collagen I from rat tail	3 mg/ml	(TERM, Wuerzburg)
fibrin glue (Tissu- col Duo S)	Fibrinogen	4.7-7.3 mg	Baxxter B133052
	Thrombin	0.43 mg	
starPEGh	starPEG-MMP-SH	1.21 % (m/v)	Felix Schrön
	starPEG-SH	1.77 % (m/v)	(IPF, Dresden)
	heparin HM6	2.285 % (m/v)	
MP/HA	HAMA	1.1 % (w/v)	Anna Abbadessa
cell free	pHPMA-lac-PEG	22 % (w/v)	(UMC, Utercht)
	Irgacure	0.044 % (w/v)	Sigma Aldrich, I2959
MP/HA	HAMA	1 % (w/v)	Anna Abbadessa
cell loaded	pHPMA-lac-PEG	25 % (w/v)	(UMC, Utercht)
	Irgacure	0.05 % (w/v)	Sigma Aldrich, I2959
P(AGE/G)- HA-SH	P(AGE/G)	5 % (w/v)	Simone Stichler (FMZ, University of Würzburg)
	HA-SH	5 % (w/v)	
	Irgacure	0.05 % (w/v)	Sigma-Aldrich, I2959

Peptides (RGD, WYRGL and KLER) were custom fabricated at the Leibniz institue for polymer Research (IPF) in Dresden and kindly provided for preparation of peptide modified starPEGh material.

Table 8 List of peptides for augmentation with starPEGh hydrogel.

peptide	molecular weight [g/mol]	amino acid sequence	function	supplier
WYRGL	952.15	CWYRGL	ligand with collagen II α -1 binding site [142]	IPF, Dresden
RGD	990.06	GCWGGRGDSP	RGD mediates adhesion between cells and the ECM [143, 144]	IPF, Dresden
scrambled RGD	1022.00	(Acetyl)C Doa1Doa1 GR D G SP (NH ₂)	Control experiments to determine the specificity of cell adhesion caused by a genuine RGD peptide	Cellendes GmbH, 09-P-003
KLER	646.81	CKLER	Decorin-moiety with affinity to collagen II. [144, 145]	IPF, Dresden

3.6 Biochemical and protein analysis: Buffers and solutions

Composition of buffers for biochemical analysis and buffers for western blot analysis are described in the following tables.

Table 9 Overview of composition of all buffers used for histology or biochemical analysis.

buffer (application)	composition	final concentration
phosphate buffer (digestion buffer, pH 6.5)	S1 NaH_2PO_4 in milliQ water	500 mM
	S2 Na_2HPO_4 in milliQ water mix 5 parts S1 and 4 parts S2	5000 mM
papain digestion buffer	L-Cystein	5 mM
	EDTA	500 mM
	phosphate buffer	100 mM
	papain	140 µg/ml
	ultra pure water	
BSA (blocking buffer histology)	BSA	5 % (m/v)
	PBS 1x	
PBST (washing buffer histology)	Tween	0.05 % (v/v)
	PBS 10x	1 l
	deionized water	fill up to 10 l
TBS (10x)	Tris base	25 mM
	NaCl	150 mM
	in deionized water	
TBST (washing buffer western blot)	TBS 10x	1 l
	Tween	0.05 % (v/v)
	deionized water	fill up to 10 l

3.7 Histology: Antibodies and solutions

Table 10 List and composition of solutions for T9100 plastic embedding.

buffer	composition	volume
pre-infiltration solution I	basis solution T9100neu	200 ml
	xylene	200 ml
pre-infiltration solution II	basis solution T9100neu	200 ml
	hardener 1	1 g
pre-infiltration solution III	basis solution T9100neu (destabilized)	200 ml
	hardener 1	1 g
infiltration solution	basis solution T9100neu (destabilized)	250 ml
	PMMA	20 g
	hardener 1	2 g
solution A	basis solution T9100neu (destabilized)	500 ml
	PMMA	80 g
	hardener 1	4 g
solution B	basis solution T9100neu (destabilized)	50 ml
	hardener 2	4 ml
	regler	2 ml

Table 11 Composition of solutions for histological stainings.

buffer	composition	concentration
acid alcohol	Hydrochloric acid (37 %)	1 % (v/v)
	ethanol (70 %)	
acetic acid	acetic acid, glacial	1 % (v/v)
	distilled water	
safranin-O	Safranin-O	0.1 % (m/v)
	distilled water	
fast green	Fast green	0.01 % (m/v)
	distilled water	
iron hematoxylin (weigert)	Solution A	mix equal volumes
	Solution B	

Table 12 List of primary and secondary antibodies for immuno-histological (IHC) and -fluorescent (IF) stainings.

antibody	clone	host	isotype	conc.	dilution	demasking	supplier
aggrecan	EPR7785	mouse	IgG1	1 mg/ml	1:2000 (IHC) 1:100 (IF)	1 mg/ml pronase in PBS	Invitrogen, AHP0012
collagen I	EPR7785	rabbit	IgG	875 µg/ml	1:1000 (IHC)	4 mg/ml pepsin in 0.01 N HCl & 2 mg/ml hyaluronidase in PBS	abcam, ab138492
collagen II	II-4C11	mouse	IgG1	1 mg/ml	1:1000 (IHC) 1:100 (IF)	4 mg/ml pepsin in 0.01 N HCl & 2 mg/ml hyaluronidase	MP Bio, 63171
collagen VI	NKI-GoH3	rat	IgG2a	1 mg/ml	1:400 (IHC) 1:100 (IF)	1 mg/ml pronase in PBS	Biomol, 600-401- 108
collagen X	COL-10	mouse	IgM	1 mg/ml	1:100 (IHC) 1:100 (IF)	1 mg/ml pronase in PBS	Sigma-Aldrich, C7974
proCollagen I	M-58	rat	IgG1		1:100 (IHC)	5mg/ml trypsin in deionized water	Merck Millipore, MAB1912
RunX2	-	mouse	IgG2a	0.1 mg/ml	1:100 (IF)	1 mg/ml pronase in PBS	abcam, ab76956
SOX9	3C10	mouse	IgG2a	1 mg/ml	1:100 (IF)	2 mg/ml hyaluronidase in PBS	abcam, ab76997
antibody			conc.	dilution	conjugation	supplier	
donkey	anti rat		454 mg/ml	1:200	Alexa fluor 647	Invitrogen, A18744	
donkey	anti mouse		1 mg/ml	1:400	Alexa fluor 647	Invitrogen, A31571	
donkey	anti rabbit		1 mg/ml	1:400	Alexa fluor 555	Invitrogen, A31572	

3.8 Gene expression analysis: Primers and solutions

Table 13 Porcine primer pairs for quantitative qRT PCR (s: sense, a: antisense).

primer	annealing temperature	sequence	supplier
aggrecan	58°C	s AGCCTTTCAGGAAGGCACC as GCCTCTGATTCATCTGTCTG	Eurofins
collagen II α 1	58°C	s AGGTCTTCCTGGCAAAGATG as CAACATCGCCCCGGTCTC	Eurofins
collagen X	58°C	sCTTTGTAAAGGAAGGACAGAG as ACGTACTCAGAGGAGTACAG	Eurofins
SOX9	58°C	s ACCACCCGGATTACAAGTAC as GTTGGAGATGACGTCGCTG	Eurofins
RunX2	58°C	s ACCCTACCCGGGCTCTTC as TTGTCAACGCCATCGTTCTG	Eurofins
HPRT	58°C	s TGGACTAATTATGGACAGGAC as TTTCAAATCCAACAAAGTCTGG	Eurofins
EF1 α	58°C	s GCTTTAATGTCAAAAACGTGTC as ACTGTCTGTCTCATGTCACG	Eurofins
primer	annealing temperature	Assay ID	supplier
β -actin	60°C	qSscCED0011147 10042976	Bio-Rad Laboratories GmbH
GAPDH	60°C	qSscCED0017494 10042976	Bio-Rad Laboratories GmbH
HMBS	60°C	qSscCED0012281 10042976	Bio-Rad Laboratories GmbH
SDHA	60°C	qSscCED0006997 10042976	Bio-Rad Laboratories GmbH

3.9 Kits

Summary of all commercially available kits for sample analysis are listed in table 14 including the single components contained in the respective kit.

Table 14 List of commercially available kits for analysis.

Kit (application)	components	supplier
Live/Dead Viability/ Cytotoxicity Kit (for mammalian cells)	Calcein AM Ethidium homodimer-1	Molecular Probes, MP03224
Quant-iT™ PicoGreen dsDNA Assay Kit	20x TE buffer (200 mM Tris-HCl, 20 mM EDTA, pH 7,5) λ DNA standard 100 µg/ml Quant-iT™ PicoGreen dsDNA reagent	Invitrogen, P7589
Blyscan™ sulfated Glycosaminoglycan assay (GAG quantification)	chondroitin sulfate 100 µg/ml Dye Dye reagent Dye dissociation reagent	Biocolor, B1000
DCS Super Vision 2 HRP-Polymer-Kit (immune histology)	DCS Polymer-Enhancer DCS HRP-Polymer reagent (label) DAB substrate buffer	DCS Innovative, PD000KIT
iScript™ cDNA Synthesis kit (cDNA synthesis)	5x Mango-Taq reaction buffer for reverse transcriptase iScript reverse transcriptase, nuclease free water	Bio-Rad Laboratories GmbH, 170-8891
Amersham ECL Prime Western Blotting Detection Reagent (Western Blot)	Lumino Enhancer Solution Peroxide Solution	Biozym, 541015

3.10 Laboratory devices and software

Laboratory equipment, devices and software for sample processing are listed in this section.

Table 15 List of devices.

device	company
Artificial tissue cutter (ICP3020)	Isel Germany AG
AxioVision 40C	Carl Zeiss
bench saw KS 230	Proxxon
Bio-Rad CFX 96	Bio-Rad
Biorevo BZ-9000	Keyence Deutschland
centrifuge MultifugeX3R	Thermo Fisher-Scientific
Confocal laser scanning microscope TCD SP8	Leica
cordless drill driver	Makita
cryostat CN1859 UV cryostat	Leica
cyto-centrifuge	Leica
Infinite 200 PRO NanoQuant	Tecan Deutschland
JEOL JSM 7500F	JEOL GmbH
microtome SM 2010R	Leica
microcentrifuge 5417R	Eppendorf
Neubauer improved cell counting chamber	Hartenstein
plate reader	Tecan Deutschland
rotation microtome RM 2255	Leica
thermocycler SensQuest	BioRad

Table 16 List of software for data recording.

application	software	company
microscope / brightfield, fluorescence)	BLZ viewer BLZ analyzer	Keyence Deutschland
confocal microscope (time lapse)	Leica Application Suite X	Leica
SEM images	JEOL	JEOL GmbH
plate reader	Tecan i-control V 2.11	Tecan Deutschland
recording PCR data	CFX manager 3.1	Bio-Rad
Artificial tissue cutter	Pal-PC	Isel Germany AG
statistics	IBM SPSS 23.0	IBM Corporation

3.11 Laboratory equipment

Further laboratory (single) use equipment, especially equipment for culture platform, drilling tools, and plastic embedding are listed in the next table.

Table 17 List of (single use) laboratory equipment and plastic ware.

equipment	application	supplier
bioreactor	dynamic culture device	LifeTec BV
biopsy punch	defect creation	pfm medical, 81242
cradle insert for embedding form	plastic embedding	Heraeus Kulzer, 66009903
custom 6-wells deep plate	static culture device	LifeTec BV
embedding form 25 mm	plastic embedding	Heraeus Kulzer, 64708955
inserts for 6-wells plate	static culture device	LifeTec BV
microseal adhesive film	PCR	Biorad, MSC1001
μ -Slide Chemotaxis	Time lapse	IBIDI, 80326
O-ring MVQ70	sealing for inserts	arcus, 0081-16
polyethylene films	Cover T9100 slices	Heraeus Kulzer, 64712818
pumping tube	bioreactor set-up	Ismatec, SC0746
silicon tube	bioreactor set-up	arcus, 0081-16
trepan mill	OCE isolation	MF dental, F229L080

4. Methods

This chapter describes all cell culture methods and the analytics, characterization and assays which were performed in this thesis. If nothing else is stated PBS was used without calcium- and magnesium chloride.

4.1 Establishment of *ex vivo* osteochondral defect model with critical size defects

The establishment of the *ex vivo* osteochondral cartilage defect model is based on porcine material due to the similarities in joint size and anatomy [146–149]. Beside CZ loaded study, pigs were retrieved from a slaughter house (Kirchner in Würzburg). The screening of CZ loaded materials was performed with slaughter house material from the Netherlands. All pigs were mean aged between six to eight months.

Domestic pigs are characterized skeletally mature at around 12 months [150]. Since we are bound to the slaughter house material the pigs used for the models in this thesis are not skeletally mature [151]. The medial condyle is the area in the knee joint with the highest load bearing and thus this region represents a higher probability for cartilage defects compared to lateral condyle [6].

4.1.1 Isolation of osteochondral tissue explants

Cylindrically osteochondral explants (OCE), 8 mm in diameter and 5 mm in total height, were isolated from medial femoral condyles of six to eight month old landrace pigs as detailed described elsewhere [152]. Figure 6 shows a collection of photographs depicting the single steps for OCE isolation and cutting of subchondral bone.

OCE were incubated over night in chondrogenic medium (DMEM HG, L-ascorbic-acid-2-phosphate (50 mg/ml), dexamethasone (100 nM), L-proline (40 µg/ml), ITS⁺ premix (1 % (v/v)), sodium pyruvate (1 mM)) supplemented with 2 % (v/v) antibiotic-antimycotic (200 U/ml penicillin, 200 µg/ml streptomycin, 0.5 µg/ml Amphotericin B) to test sterility. Static culture was performed in a custom made culture platform which was developed and owned by LifeTec Group BV. Culture device is characterized by its separated media compartments for tissue specific media supply to cartilage and bone during *ex vivo* culture that is realized with 6 well plates and inserts shown in figure 7.

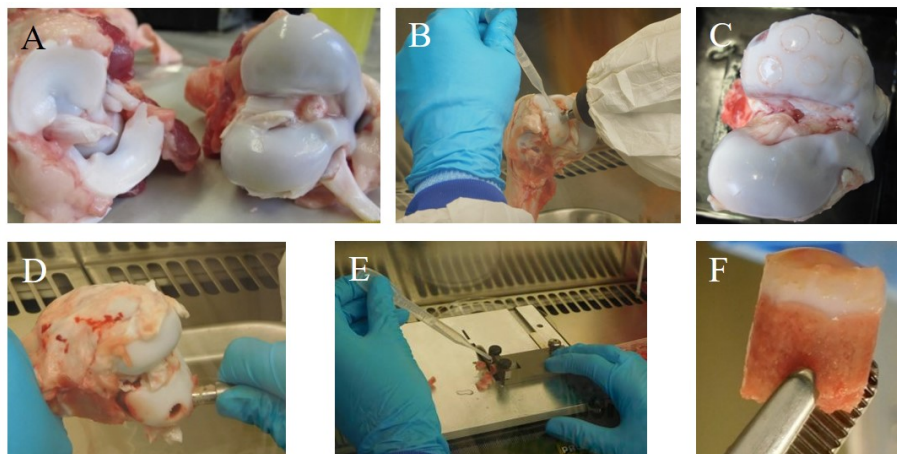


Figure 6 Isolation of osteochondral explants (OCE) from porcine femoral medial condyle. (A) opening knee capsule, (B–C) drilling, (D) break out of OCE from condyle, (E) adjusting OCE height by sawing subchondral bone and (F) explant ready for culture.

4.1.2 Static culture

OCE were fixed in transwell and placed in custom made *ex vivo* osteochondral culture system as previously described [152].

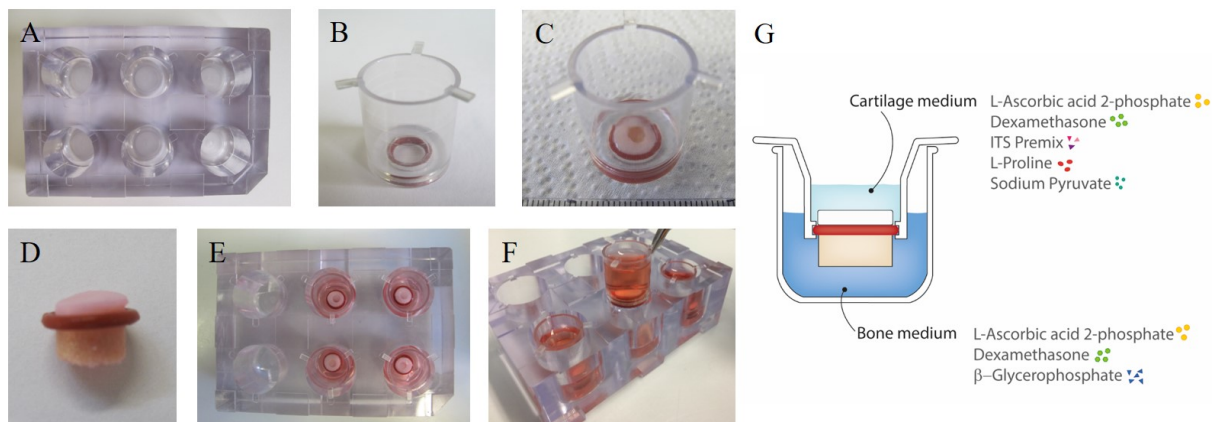


Figure 7 Osteochondral platform for static *ex vivo* culture. (A) 6 well plate, (B–C) insert to fix osteochondral explant. (D) O-ring at calcified layer ensures media separation during culture. (E) Inserts were transferred in 6 well-plates filled with bone media in cavities and (F) cartilage media into insert. (G) Schematic drawing of media and plug in static culture device. Modified from Schwab *et al.* [152].

The unique feature of this static culture platform is the separated media compartments that allows tissue specific nutrient supply during *ex vivo* culture. Separation of cartilage media in the insert and bone media in each cavity of 6 well plate is achieved by an O-ring at the bone–cartilage interface of the OCE. To mimic physiological conditions no TGF- β was added to the 3 ml chondrogenic media. Transwell with OCE was placed in

custom made 6 well plates filled with 3 ml bone media (DMEM HG, FCS (10 % (v/v)), L-ascorbic-acid-2-phosphate (50 mg/ml), β -glycerophosphate (10 mM), dexamethasone (100 nM) with 1 % (v/v) antibiotics (100 U/ml penicillin, 100 μ g/ml streptomycin, 0.25 /ml Amphotericin B) in each cavity. Media was changed every 3–4 days and supernatant was stored at -80°C for further analysis.

4.1.3 Dynamic culture under constant flow

Diffusion of nutrients and waste removal in *ex vivo* culture of tissue explants or TE products can be enhanced under direct perfusion [153]. Therefore, a prototype bioreactor for dynamic culture of OCE (6.5 mm in diameter) was designed in collaboration with LifeTec Group BV. From theoretical point of view the bioreactor was designed to allow for perfusion of OCE subchondral bone and thus increase bone viability during *ex vivo* culture. A schematic drawing is illustrated in figure 8 A illustrating bone media in red and cartilage media in blue. The bioreactor consists of a two-piece housing that is hold together with

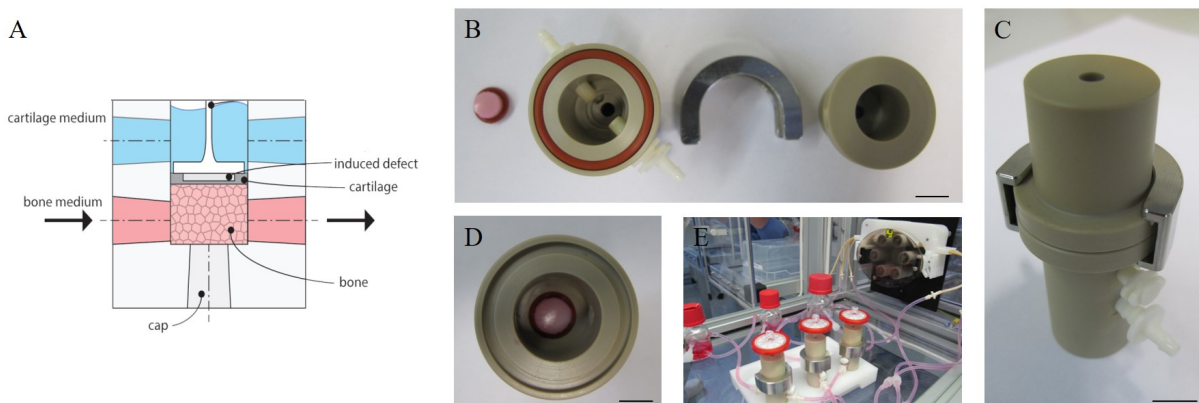


Figure 8 Prototype bioreactor for dynamic culture of osteochondral explants (OCE). (A) Schematic drawing of prototype bioreactor design allowing for bone perfusion (red: bone media, blue: cartilage media). (B) Bioreactor consists of an upper part, bottom part and a metal ring to clamp both part during culture. (C) Outer view of bioreactor with connectors in white. (D) Top view of bottom part containing OCE fixed with an O-ring. (E) Three bioreactors are placed on a tray and the lower inlet and outlet of subchondral bone compartment were connected to roller pump in incubator (37°C). Bone media is filled in media reservoirs that are connected via silicon tubes to the bioreactor. (Scale bar 1 mm)

a metal ring shown in figure 8 B–C. The upper compartment provides the possibility to connect air filter for gas exchange with cartilage part (figure 8 E). Similar to static culture device, OCE is fixed with an O-ring in the bottom part of the housing. Additionally, two inlets and two outlets are located at the cartilage and the bone compartment. Inlet and outlet at bone compartment were connected with silicon tubes to bone media reservoir and fixed on roller pump in incubator system (37°C). A constant flow (4 rpm, 1 ml/min,

7–10 mmHg) was applied during dynamic *ex vivo* culture for 28 days. Viability staining was performed in a first trial to evaluate advantage of bone perfusion during culture.

4.2 Cartilage defect creation

The modification of the OCE samples with cartilage defects was achieved with two methods, either manually following clinical standard with a biopsy punch or fully automated, that resulted in the realization of different defect geometries which are described in the following paragraphs.

4.2.1 Clinical standard: Biopsy punch

Full thickness cartilage defects were created in OCE with a commercially available biopsy punch. To investigate critical size defects in *ex vivo* cultured OCE we created full thickness cartilage defects with 1 mm, 2 mm, 4 mm and 6 mm in diameter (figure 9). A critical size defect is defined as a defect that does not repair by itself. This experimental set-up aimed to investigate minimal diameter that does not heal spontaneously in the OCE of immature pigs. According to clinical performance as illustrated in figure 3 the residual

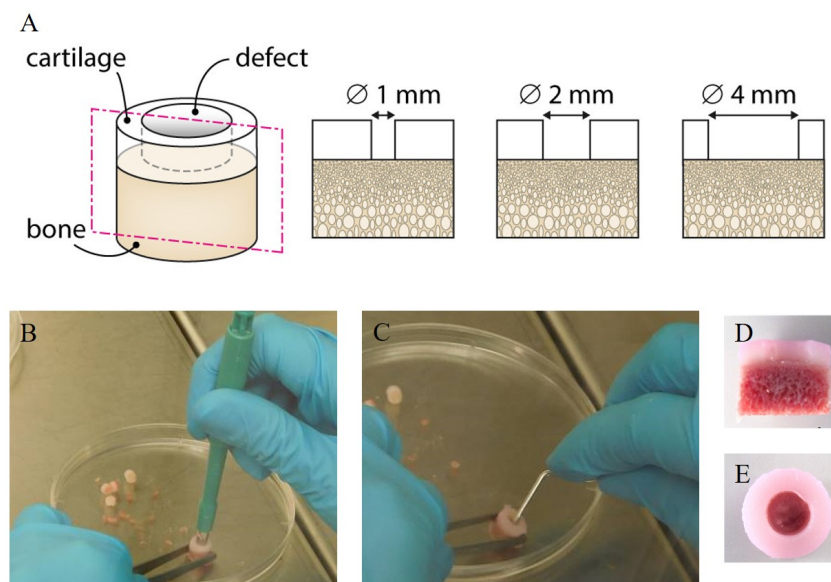


Figure 9 Creation of full thickness cartilage defects. (A). (B) 4 mm biopsy punch and subsequent (c) removal of cartilage from subchondral bone with sharp spoon. (D–E) Top view and cross section of explant with 4 mm defect. Adapted from Schwab *et al.* [152].

cartilage at calcified layer was removed with a sharp spoon (figure 9 C). Following, the underlying subchondral bone plate was opened to allow cell migration into defect side.

4.2.2 Automated, standardized method: Artificial tissue cutter

An *ex vivo* test system for systematic evaluation of chondral defect treatments requires standardized defects. With the automated tissue cutter (ARTcut[®]) we had a device that has been established for wounding of tissue engineered three dimensional skin equivalents [154]. ARTcut[®] is a prototype that was developed in the SkinHeal project (within the Markets Beyond Tomorrow program) in collaboration between department Tissue Engineering and Regenerative Medicine (Szymon Kurdyn) and Fraunhofer ISC, Center of Device Development Bronnbach (Andreas Diegeler, Philipp Maleska). The ARTcut[®] prototype consists of a computerized numerical controlled (ICP3020, Isel Germany AG) machine with three axes of driving, laser-beam for sensor control of drilling device, video control for documentation, bottom panel to fix supporting plate and UV light (VL-206.G, 254 nm, 6 W, LTF Labortechnik GmbH & Co KG) for sterilization and a plastic housing for protection (Fig. 10 A).

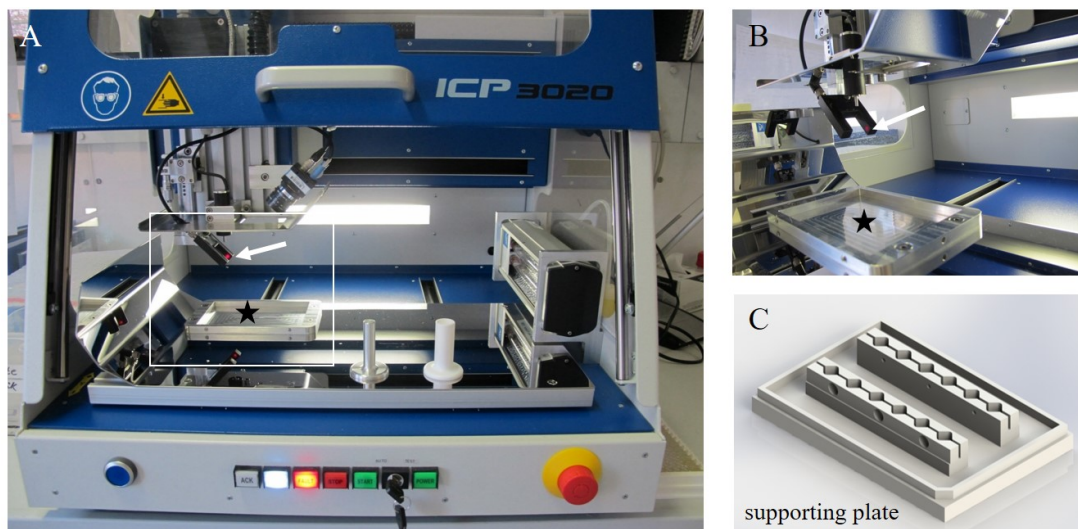


Figure 10 Artificial tissue cutter (ARTcut[®]). (A) Computerized numerical controlled device for automated wounding of samples. (B) Optical barrier (white arrow in (A)) detects surface of samples that allows creation of defects with standardized geometry. Miller or drill is placed in between this barrier without interfering the laser beam. (C) All samples are fixed in sample specific supporting plate placed on the bottom of the machine (marked by black star in (A)).

Main advantage of this prototype is the reproducible defect creation with standardized geometry realized by detection of sample surface with the laser-beam of the optical barrier shown in figure 10 B. The sensor controlled drilling depth is calculated for every single sample from the sample surface. The translation of this technology to create cartilage defects required design of supporting plate for fixation and to prevent rotation of samples during drilling (figure 10 C) which was placed in the machine on a metal holder marked by

black star in figure 10 A. The maximum number of OCE for parallel wounding is limited by the supporting plate to 12 OCE. Different milling speeds up to 20 000 rpm were tested for drilling cartilage defects with decision to proceed at 6 300 rpm to prevent heating of OCE at higher speeds. Chondral defects, 4 mm in diameter and 1 mm in depth, were created with a HVM mini miller.

4.3 Cell culture methods: Cell isolation, expansion and characterization

Standard cell culture techniques including isolation of primary porcine cells, freeze–thawing, 2D *in vitro* culture and embedding into hydrogel material are described in this chapter.

4.3.1 Cell isolation

4.3.1.1 CZ isolation

Porcine CZs (pCZs) were isolated from lateral condyles under aseptic conditions before OCE isolation from same joints. Minced cartilage pieces of n=4 joints were pooled and digested in digestion solution containing 1575 U/ml collagenase CLS–2 (230 U/ml) overnight on a roller bank at 37°C. Digested cartilage chips were passed through 70 µm cell strainer, washed with DMEM HG supplemented with 10 % (v/v) FCS and centrifuged at 425 g for 10 min with deceleration 7. After one washing step cells were resuspended in chondrogenic media and counted with Neubauer counting chamber. Till further use pCZs were incubated in 50 ml reagent tube filled with DMEM HG supplemented with 10 % (v/v) FCS in incubator.

4.3.1.2 Mesenchymal stromal cell (MSC) isolation

MSC were isolated from porcine bone marrow aspirate from the iliac crest of 4–6 weeks old german landrace pigs (pig farm Niedermeyer, Dettelbach, Germany). To prevent coagulation bone marrow aspirate was supplemented with heparin 1 ml (5 000 U/ml) and stored at 4°C till starting the cell isolation. Bone marrow aspirate, 1 : 1 diluted with PBS/EDTA, was pipetted on top of 15 ml Ficoll paque in 50 ml reagent tube without creating turbulence or mixture of the blood and ficoll phase. For phase separation of bone marrow samples the tubes were centrifuged at 1 300 g, 20 min, room temperature (20°C) with deceleration rate of 3 to prevent remixing after phase separation. Red blood cells and other molecules and cells with a higher density than Ficoll are collected on the bottom of the tube whereas mono–nucleated cells like MSCs are collected on top of the Ficoll

below the blood plasma. This phase in between the Ficoll and the blood plasma was aspirated and washed twice with 15 ml PBS and centrifuged at 500 g for 5 min at 20°C to remove residual Ficoll. For cell counting MSCs were resuspended with 3–5 ml DMEM HG supplemented with 10 % (v/v) FCS and 1 % (v/v) PenStrep. After MSC isolation cells were either expanded in T150 flask (200 000 cells/cm²) or frozen. For subsequent MSC expansion cells were cultured with 40 ml MSC expansion media consisting of DMEM HG supplemented with 1 ng/ml human basic FGF (hbFGF), 10 % (v/v) FCS and 1 % (v/v) PenStrep. After 3–4 days cells were washed with PBS/EDTA to remove residual blood and (peripheral) blood cells which had not attached to the culture flask to increase homogeneity of MSC expansion.

4.3.2 Cell counting

Counting of cells followed according the Neubauer method. *In vitro* cultured adherent cells had to be detached prior to cell counting. Therefore, cells were trypsinized with trypsin/EDTA (1x) for 5 min at 37°C. Enzymatic activity of trypsin was stopped with 1 ml FCS and cells were resuspended. After washing with PBS/EDTA washing buffer and centrifugation (425 g, 10 min, room temperature) CZs were resuspended in chondrogenic media (table 5). Cell suspension (after cell detachment or primary isolated cells) and trypan blue were mixed 1:1 (dilution factor 2) and pipetted onto the chamber of a neubauer improved chamber device. Cells in all four quadrants were manually counted. Calculation of the total cell number included the mean number of cells in the four large quadrants, dilution factor, volume in which cells were resuspended and the chamber volume factor (10 000).

4.3.3 Freezing and thawing of cells

Freezing of either primary isolated or *in vitro* expanded cells was performed by resuspending 1 mio cells in 800 µl expansion media. Reagent tubes for cryo-conservation were filled with 100 µl FCS and 800 µl of cell suspension added. In order to prevent crystal growth during freezing of cells 100 µl (10 % (v/v)) dexamethasone was pipetted on top of each vial for cryo-conservation. Reagent tubes were put in special freezing box called Mr. frosty and stored at –80°C for 24 h before transferring into liquid nitrogen for long term storage. The Mr. frosty ensured the freezing of cells at a constant conditions by lowering the temperature 1 °C within one hour. In preparation for thawing of cells expansion media was preheated in 37°C water bath. Cryo tubes containing 1 mio cells was thawed in the water bath till only a small ice crystal was left and completely transferred into a T150 flask containing 40 ml of expansion media. After 24 h media was changed including a washing

step with 40 ml PBS to remove dexamethasone and dead cells from cell population. During both procedures, thawing and freezing of cells, it was important to work fast to prevent unnecessary stress to the cells.

4.3.4 Embedding of cells into hydrogel material

During 2D *in vitro* culture pCZs undergo morphological changes accompanied by loss of chondrogenic gene expression profile [67]. In order to prevent dedifferentiation, pCZs were encapsulated into hydrogel systems direct after isolation without cell expansion in passage 0. For all hydrogel systems cell number was adjusted to a final concentration of 20 mio/ml hydrogel volume.

4.3.5 CZ characterization

Prior to pCZ embedding into hydrogel materials the growth behavior and phenotype of the cells were analyzed.

4.3.5.1 CZ population doubling

Primary pCZs de-differentiate during *in vitro* expansion under 2D conditions. In order to investigate the population doubling time of pCZs freshly isolated cells were seeded in 6 well plate (9200 cells/cm²), expanded with DMEM HG supplemented with 10 % (v/v) FCS and 1 % (v/v) antibiotics, and harvested at different time points (day 3, day 7, day 9). Cell numbers of pCZs were calculated in triplicate for each of n=3 wells. For cell counting cells were trypsinized with 2 ml trypsin/EDTA (1x) as described before, washed with 2 ml PBS/EDTA and centrifuged (425 g, 10 min, deceleration: 7). Cells were resuspended in DMEM HG and counted with neubauer improved chamber. After counting cells were pelleted in 1.5 ml reagent tube to aspirate media and stored at -20 °C for processing with DNA quantification.

4.3.5.2 CZ pellet culture

In order to investigate CZ phenotype and maturation during 3D *in vitro* culture 0.5 mio pCZs (passage 0) were centrifuged at 425 g for 10 min at 20°C in 15 ml reagent tube containing 0.5 ml cartilage media without growth factor supplementation to form a pellet. The next day, cell pellet was transferred into 24 well plate and cultured for 28 days with media change twice a week. After 28 days culture pellets were fixed with formalin (20 min, room temperature), washed with distilled water and rehydrated in increasing alcohol row including paraffin infiltration over night.

4.4 Preparation of hydrogel biomaterials

Cartilage defects in OCE were treated with three innovative hydrogel systems that have been developed within the European project HydroZONES (FP7/2007–2013, grant agreement no. 309962). All project partners kindly provided us with their material (table 7) including teaching of material handling and preparation. The hydrogel components are based on poly(ethylene glycol) or polyglycidol (PG), a structural analog of PEG, and compared to fibrin glue and 3 mg/ml collagen I hydrogel as clinical reference materials. Fibrin glue was polymerized directly into defects whereas all other materials were pipetted into custom made molds (4 mm diameter, 1.8 mm height) for polymerization (shown in figure 12) and transferred with forceps into cartilage defects. No hydrogel materials was fixed in the defect of OCE neither by glueing nor by suturing. Equipment needed for hydrogel preparation (molds, glass slides, spatula) were autoclaved for sterilization.

4.4.1 Collagen I hydrogel

4.4.1.1 Isolation of collagen I from rat tails

Collagen I was isolated from rat tails (Charles River) depicted in figure 11. After thawing in sterile PBS and washing with 70 % (v/v) EtOH for sterilization reasons, the tails were cut to two thirds to peel off the skin (figure 11 A). The white appearing tendons could drawn out with the help of forceps and collected in a petri dish filled with PBS (figure 11 B–C). Two washing steps with 70 % (v/v) EtOH for 10 min at room temperature followed to minimize the risk of infections. Subsequent washing with PBS followed to remove EtOH

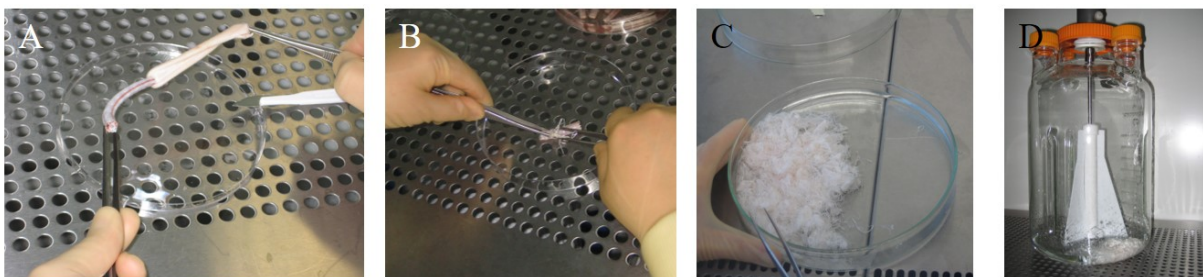


Figure 11 Collagen I isolation from rat tail. (A) Skin or rat tails was peeled off before (B) tendons could be drawn out and (C) collected in a petri dish. (D) Tendonds were transferred into spinner flask with 0.1 % acetic acid for dissolving under constant agitation.

access. Wet weighed was determined and tendons were transferred into spinner flask filled with 0.1 % (v/v) acetic acid (figure 11 D). During 10–14 days of incubation under constant agitation at 4°C the collagen dissolved in acetic acid. Solid residues of tendon leavings were removed from dissolved collagen solution by centrifugation (17 700 g, 1 h, 4°C). To

determine final collagen concentration 2–3 ml collagen solution was dried for at least 48 h at 60 °C and dry weighed. The final concentration of 10 mg/ml was adjusted by adding 0.1 % (v/v) acetic acid. Collagen I solution was aliquoted into 50 ml reagent tubes and stored at –20 °C.

4.4.1.2 Protein characterization of isolated collagen I from rat tail by western blot

After isolation of collagen I from rat tails a western blot analysis followed to specifically characterize the collagen I protein. The separation of proteins dependent on their molecular weight required a poly acrylamide gel loaded with sodium–dodecyl–sulfate (SDS). For denaturation of proteins in 4.5 mg/ml collagen I, the solution was 1:1 diluted with water, mixed with 5x loading buffer (Laemmli) and heated for 10 min at 90°C before loaded on SDS gel (6 % (w/v)) for electrophoresis at 25 mA for ap. 60 min in 1x SDS running buffer to separate collagen I protein bands. A protein marker (ProSieve QuadColor, 4.6–300 kDa) served as reference to determine molecular weight of protein bands on separation gel.

Preparation of the immune blot included stacking of SDS separation gel between Whatman paper and nitrocellulose membrane (poly(vinylidene) difluoride) and transfer on a plate electrode of the semi–dry–blotter. Application of an electric voltage (150 mA, 80 min) perpendicular to movement direction of the protein samples during electrophoresis induces transfer of the protein bands from the gel on the nitrocellulose membrane. Incubation of the membrane with blocking buffer for 1 h at room temperature containing milk powder (5 % (w/v)) in Tris Buffered Saline (TBS) supplemented with 0.05 % (v/v) Tween (TBST) in a 50 ml tube placed on a roller bank reduced unspecific bonding of primary antibody. Subsequently, membrane was washed three times with TBST washing buffer before primary antibody against collagen I diluted 1:1000 with blocking buffer was incubated over night at 4°C on a roller bank. Before incubated with secondary HRP linked mouse anti goat antibody (20°C, 1 h) 1:1000 diluted with blocking buffer, membrane was washed three times with washing buffer. After two washing steps immune blot was ready for development with amersham ECL prime Western Blotting detection reagent (reagent 1: peroxide solution, reagent 2: luminol enhancer solution). In presence of collagen I proteins on the membrane the HRP coupled secondary antibody develops the luminol of the western blotting detection kit to a chemiluminescent signal which is detected by the FluorChem Q (Cell Biosciences) imaging device.

4.4.1.3 Collagen I hydrogel preparation

For preparation of collagen hydrogels 2 volumes of collagen I solution (4.5 mg/ml) were mixed with 1 volume of gel neutralizing solution (GNL) to achieve 3 mg/ml end concentration. 26 μ l of collagen I hydrogel was pipetted into full thickness cartilage defects and polymerized for 20 min at 37°C. For cell loaded collagen I hydrogels pCZs (60 mio/ml) were resuspended in GNL, mixed with collagen solution and polymerized as described before.

4.4.1.4 Free swelling culture of pCZ loaded collagen I hydrogel

To investigate the stimulative effect of osteochondral explant on pCZ phenotype and matrix production one control group (20 mio cells/ml collagen I hydrogel) of collagen I implant was cultured under free swelling conditions in 24 well plate with cartilage media. Media change was performed according to explant cultures. After 28 days *in vitro* culture construct was fixed for 20 min in 4 % formalin (room temperature), washed in distilled water, rehydrated and paraffin embedded.

4.4.2 Fibrin glue

Fibrin glue is used for wound closure or as sealant in clinical practice. In cartilage defect treatment scaffolds are often fixed with fibrin glue to stay in place or in combination with ACI to inject and localize cells in the defect. Therefore, fibrin glue was included as fifth material group (reference material for clinical ACI procedure) in the OCE model. Moreover, the fibrin glue group allows comparison of the *ex vivo* results with pre-clinical and clinical data. For cell free hydrogel preparation fibrinogen (1 : 15 diluted in PBS) was mixed with thrombin (1 : 50 diluted with PBS) in equal volumes and 26 μ l were pipetted into each cartilage defect for polymerization (25 min, 37 °C, self assembly). For cell loaded fibrin gels pCZs were resuspended in fibrinogen with a concentration of 40 mio cells/ml and mixed with equal volume of thrombin and polymerized as described above. Due to rapid polymerization pCZs containing fibrinogen was pipetted directly into cartilage defects of OCE and mixed with thrombin.

4.4.3 Four armed poly(ethylene glycol) polymerized with heparin (starPEGh)

This hydrogel is based on star-shaped and four armed poly(ethylene glycol) (starPEG) combined with heparin (HM6), from now on referred as starPEGh, with a total solid content of 5 % (w/v) [89, 90]. The material was modified by Felix Schrön, Institute of polymer research (IPF) Dresden, Dresden, Germany. A more detailed description of polymer chemistry is published elsewhere [155].

Each component of starPEGh, namely PEG-SH, PEG-MMP and Heparin (HM6), were dissolved in PBS according to table 7. Equal volumes of thiol functionalized PEG (starPEG-SH; 48.4 mg/ml) and matrix metalloproteinase (MMP) functionalized PEG (starPEG-MMP-SH; 70.8 mg/ml) were mixed to achieve 50 % MMP cleavable PEG. The MMP functionalization of the inert PEG allows material remodeling by cells [155].

The degree of cross-linking is given by γ that represents the quotient of starPEG to heparin molecules. This means that a maximum of three PEG molecules can bind with two HM6 molecules resulting in $\gamma = 1.5$. HM6 was reconstituted with PBS (45.7 mg/ml), mixed in equal volumes with starPEG-MMP-SH and pipetted 24 μ l into each mold (Figure 12) for polymerization. Polymerization time was adjusted by adding 10 mM HCl to HM6 which lowered the pH value and thus resulted in a slower polymerization time within 30 seconds at room temperature.

For preparation of cell loaded starPEGh pCZs (40 mio/ml) were resuspended in HM6 solution before mixing equal volumes of HM6 with PEG-MMP-SH and polymerized as described before.

4.4.3.1 Peptide augmented starPEGh

To investigate the stimulative effect of chondrogenic related peptides (KLER, WYRGL, RGD, scrambled RGD) on cartilage matrix synthesis, viability and morphology the peptide augmented hydrogels were loaded with CZs and cultured for 4 weeks in OCE model as described above. RGD is described to mediate adhesion between cells and the ECM and thus promotes survival of encapsulated cells [143, 144]. The two peptides WYRGL and KLER (decorin-moiety) represent both high affinity to bind to collagen II α -1 binding sites, major collagen component in articular cartilage ECM [142, 144, 145, 156]. Scrambled RGD sequence served as negative control in this set-up to determine the specificity of cell adhesion caused by RGD peptide. Detailed information about peptides are summarized in table 8.

Preparation of peptide modified starPEGh required the adjustment of the γ value to $\gamma = 1.2$

in order to maintain mechanical properties of starPEGh without peptide augmentation. Four different peptides (WYRGL, KLER, RGD and scrambled RGD) were mixed with the HM6 component, each 2 M. Peptides are prepared with an amide at the C-terminal and NH_2 group at the N-terminal side to bind covalently to the hydrogel. 26 μl of peptide augmented and CZ loaded with 20 mio cells per ml starPEGh material was pipetted into each full thickness cartilage defect. The four peptide modifications were compared in $n=3$ independent experimental set-ups with starPEGh material.

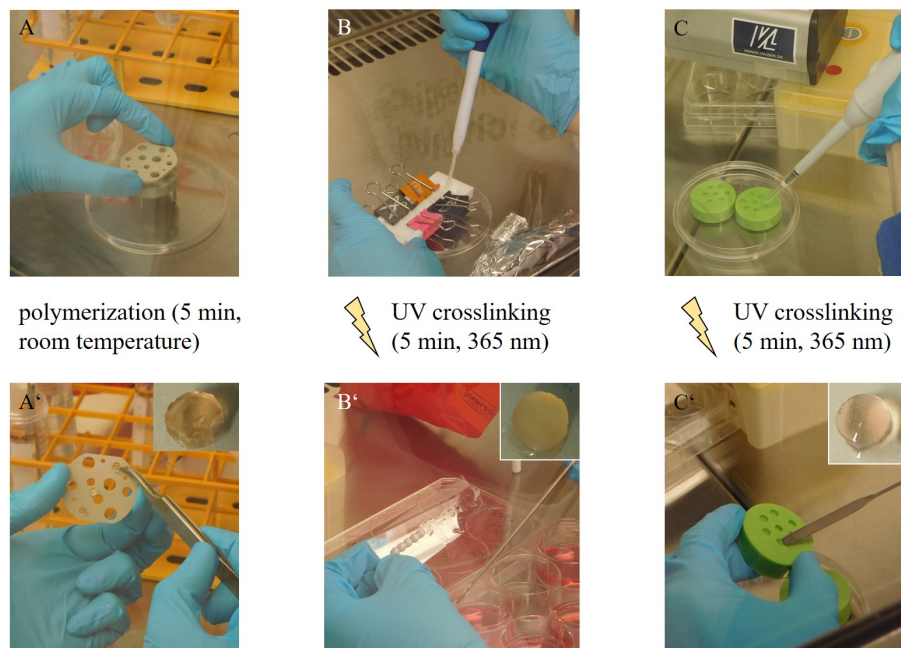


Figure 12 Macroscopic illustration for preparation of three hydrogel materials in specific molds and depiction of fabricated materials after polymerization. (A–A') Four armed poly(ethylene glycol) polymerized with heparin, (B–B') PEG and partially methacrylated poly[N-(2-hydroxypropyl) methacrylamide mono/dilactate], (C–C') Thiol functionalized hyaluronic acid/allyl functionalized poly(glycidol). starPEGh polymerized at room temperature after mixing heparin and PEG component, MP/HA and P(AGE/G)–HA–SH polymerized under UV irradiation (365 nm, 5 min).

4.4.4 PEG and partially methacrylated poly[N-(2-hydroxypropyl) methacrylamide mono/dilactate (MP/HA)]

The thermosensitive and biocompatible polymer is composed of partially methacrylated poly(N-2-hydroxypropyl) methacrylamide–mono–di–lactate–PEG–triblock copolymer (pHPMA–lac–PEG) in combination with methacrylated hyaluronic acid (HAMA). This material was developed by Anna Abbadessa, University Utrecht Medical Center (UMC), Department of Pharmaceutics, Utrecht Institute for Pharmaceutical Sciences, Utrecht, The Netherlands. Material properties and biological analysis of this material, from now

on referred as MP/HA, is detailed described elsewhere [157].

Cell free and cell loaded hydrogels differed in the end concentration of the photo initiator and the HAMA concentration. Polymers HAMA and M10P10 were dissolved with PBS according to table 7 in a sterile glass vial. Reconstitution of material had to be performed over night under constant stirring at 4°C to keep viscosity of hydrogel at lower level that can be pipetted.

Irgacure, a photo initiator, was added and vial was gently and constantly stirred overnight at 4°C in dark covered with an aluminum foil. Polymer solution was injected via the side channel into the injection mold body covered with glass slides and clamps to create oxygen free conditions during polymerization (figure 12 B). MP–HA solution is an oxidative unstable polymer and only gels in absence of oxygen. Hydrogel solution was injected into molds to complete fill the scaffolds cavities, incubated for 5 min at 37°C and cross-linked under UV irradiation (5 min, 365 nm, 3 cm distance) at room temperature. MP–HA scaffolds were removed from teflon mold and transferred into defects of OCE. For cell loaded hydrogels 20 mio cells/ml were resuspended in polymer solution on ice to prevent that the polymer solution became more viscous and proceeded with molding as described above.

4.4.5 Thiol functionalized hyaluronic acid/allyl functionalized poly (glycidol) (P(AGE/G)–HA–SH)

In contrast to the previous described materials this hydrogel is based on poly(glycidol) (PG) a structural analog of PEG that has recently been investigated for use as bioink [158]. PG was functionalized with allyl- and thiol groups as cartilage implant material from now on referred as (P(AGE/G)–HA–SH) . This material was developed by Simone Stichler, University Hospital Würzburg, Department of functional materials in medicine and dentistry, Würzburg, Germany. P(AGE/G)–HA–SH hydrogel was prepared by dissolving P(AGE/G) and sterile filtration through 0.2 µm sterile filter. After sterilization of HA–SH by UV irradiation (10 min at 254 nm) the polymer was mixed with P(AGE/G) and mixed with the photo initiator (Irgacure). pH value of hydrogel solution was adjusted by adding 5 M NaOH resulting in a neutral pH of pH7. P(AGE/G)–HA–SH hydrogel was pipetted into custom made molds (4 mm diameter, 1.8 mm height, V=24 µl), crosslinked by UV irradiation (365 nm, 5 min, distance 3 cm, room temperature) and transferred into cartilage defects (figure 12 C).

For preparation of pCZ loaded P(AGE/G)–HA–SH hydrogels, cells were resuspended in neutralized polymer solution with a density of 20 mio/ml prior to polymerization.

4.5 Viability staining

Viability and metabolic activity of OCE and pCZ loaded hydrogels were visualized either by live–dead–staining or MTT staining.

4.5.1 Live–dead staining

Viability of OCE and visualization of cells that may have been migrated into cell free hydrogels explants were analyzed by live–dead staining. OCE were incubated for 20 min in Calcein–AM (4 μ M) and ethidium–homodimer (2 μ M), washed with PBS and visualized microscopically (Keyence BZ–9000). Cytoplasm of living cells is stained by Calcein–AM in green (ex: 495 nm, em: 515 nm). In contrast, Ethidium homodimer–1 can penetrate the damaged cell membrane of dead cells and intercalate into the DNA. Red fluorescent staining (ex: 495 nm, em: 635 nm) results from binding of Ethidium homodimer–1 to nucleic acid in the cell nuclei.

4.5.2 3–(4,5–dimethyl–2–thiazol)–2,5–diphenyl–2H–tetrazolium bromide (MTT) staining

Metabolic activity of CZ loaded hydrogels (Fibrin, collagen, starPEG) was proven by (3–(4,5–dimethyl–2–thiazol)–2,5–diphenyl–tetrazolium bromide (MTT) staining at day 1 and day 28. Hydrogels were incubated with 1 mg/ml MTT solution (1:3 dilution of 3 mg/ml MTT stock solution with DMEM HG) for 90 minutes at 37°C, washed with PBS and macroscopic images were taken. Metabolic active cells reduce the yellow MTT reagent to a blue formazan product.

4.6 Biochemical characterization: Proteoglycan and DNA content

To characterize ECM proteins and amount of cells in cell free and cell loaded hydrogels as well as in cartilage tissue of OCE after *ex vivo* culture molecular analysis was performed. Proteoglycan (Blyscan[™] sulfated Glycosaminoglycan assay or dimethylmethylene blue (DMMB) assay) content and DNA (Quant–i[™] PicoGreen[®] dsDNA Assay) content were quantified at day 0 and 28 (n=3/material). The quantification of GAGs in the tissue or hydrogels is based on binding of the dye to negative charged molecules.

4.6.1 Papain digestion of cartilage tissue and hydrogels

For biochemical characterization of GAG and DNA content in OCE the cartilage was sliced into zonal layers of 50 μm with a cryotome to separate superficial (200 μm), middle (800 μm) and deep (400 μm) zone. Cartilage slices were collected in 2 ml reagent tubes and wet weighed before enzymatically digested with digestion buffer (table 9) containing 100 $\mu\text{g}/\text{ml}$ papain over night at 60 $^{\circ}\text{C}$. Culture medium samples were assayed without further dilution as described above. Cell loaded hydrogels were removed from OCE, wet weighed, freeze dried overnight, dry weighed and digested in papain digestion buffer containing 125 $\mu\text{g}/\text{ml}$ papain over night at 60 $^{\circ}\text{C}$.

4.6.1.1 Blyscan[™] sulfated Glycosaminoglycan assay

Papain digested samples of sliced cartilage and culture media supernatant were assayed with Blyscan[™] Glycosaminoglycan assay. GAG standards (0 to 50 $\mu\text{g}/\text{ml}$), tissue digests and supernatant was mixed with 500 μl dye reagent in reagent tube to bind negative charged proteins. After 30 min incubation on horizontal shaker the precipitate was centrifuged (1 200 g, 10 min). Dissociation reagent (500 $\mu\text{l}/\text{sample}$) allowed the dissolving of precipitate after discarding supernatant with dye reagent. From each sample duplicates of the dissociated solution (200 μl) were pipetted on clear 96 well plate and absorbance measured at 620 nm with a reference wavelength of 405 nm with a spectrometer (TECAN infinite). GAG content in samples was calculated based on standard curve.

4.6.1.2 Dimethylmethylen blue assay

DMMB based assay was performed according to the protocol of Farndale *et al.* [159]. Chondroitin–sulfate salt from shark cartilage served as standard which was diluted with ultrapure water to achieve an end concentration of 1 mg/ml. Standards (range between 0 $\mu\text{g}/\text{ml}$ to 50 $\mu\text{g}/\text{ml}$) and digested samples were centrifuged for 10 min at 12 000 g. 40 μl of each sample was pipetted in duplicates on a clear 96 well plate and filled up with 50 μl of DMMB substrate buffer with the help of a multichannel pipet. Absorbance was measured at 540 nm with reference wavelength at 595 nm with a spectrometer (TECAN infinite). GAG content in hydrogels (n=3 hydrogels for each material group) was calculated based on chondroitin standard curve. Internal testings to compare results of DMMB based assay and Blyscan Glycosaminoglycan assay did not reveal differences in GAG content. Following, all results are comparable.

4.6.2 DNA quantification

DNA content was assayed with Quant-iT[™] PicoGreen[®] dsDNA Assay according to manufacturer's instruction. Before starting the DNA assay 20x TE buffer and Quant-iT[™] PicoGreen[®] dsDNA reagent were diluted according to the manual with ultrapure water or 1xTE buffer. DNA content of cartilage digests was performed with standards in range between 1 ng/ml to 1 µg/ml. Due to low DNA content in CZ loaded hydrogels low range standard curve in range between 25 pg/ml to 25 ng/ml was selected. Standards and samples were pipetted (100 µl/well) in duplicates on black 96 well plate. Samples were mixed with PicoGreen[®] dsDNA reagent (100 µl/well) and fluorescence was spectroscopically measured at 520 nm with a reference wavelength of 480 nm (Tecan infinite). dsDNA content was calculated based on dsDNA standard curve.

4.7 Histological, immuno-histological and immuno-fluorescent stainings

The principle of histological stainings is the binding of cationic dyes (e.g. Safranin-O) or anionic dyes (e.g. hematoxylin) to negative or positive charged proteins on sliced samples. On the other hand, immuno-histochemical (IHC) and immuno-fluorescent (IF) stainings are based on specific binding of primary antibodies to the corresponding antigen of choice. A secondary antibody originating from a different species than the primary antibody is labeled with a dye, either horse radish peroxidase linked 3,3'-diaminobenzidine (DAB) for IHC or a fluorescent dye for IF.

For IHC a positive binding of the primary antibody in IHC is marked by a brown color at the side where the antigen corresponding to the primary antibody is localized visualized by light microscopy (Keyence BZ-9000). The localization of the antigen for IF is detected by fluorescence microscopy (Keyence BZ-9000) for excitation of the fluorescent dye at the respective wavelength [160].

4.7.1 Sample preparation and embedding

Samples for histological processing were either embedded in plastic (T9100) or in paraffin as described in the next paragraphs.

4.7.1.1 Plastic embedding

For histological stainings of cell free hydrogels, peptide augmented starPEGh and collagen I treated OCE under hypoxic conditions as well as in 1 mm defects, samples were fixed in 4 % paraformaldehyde (Roti-Histofix) for at least 24 h, dehydrated with increasing alcohol row (70 % EtOH, 80 % EtOH, isopropanol, xylenes) for 3 h each at room temperature and further tissue processed for plastic embedding (T9100) according manufacturer's instruction. In brief, samples were incubated with pre-infiltration solution I, III and III (24 h each, 4°C) and infiltration solution for at least 48 h at 4°C to allow complete infiltration of solutions in samples. From pre-infiltration solutions II on the T9100 basic solution was used after destabilization with an aluminum oxide filled column to allow immuno-histological stainings. After polymerization at -6°C over night in Teflon molds, plastic embedded samples were grind (Struers-Knuth-Rotor-3) with silicon-carbide sand paper (240 and 800 grade sand paper, Struers) to remove sample till reaching the defect area of the embedded OCE.

Samples were cut with rotation microtome (Leica RM 2255) to 4 µm slices, mounted on glass slides with 70 % EtOH, covered with PE foil to keep slices on glass slides and dried overnight at 60°C. Prior to (immuno-) histological and -fluorecent stainings, slides were deplastified (2x20 min xylene, 2x20 min 100 % 2-MEA, 2x10 min acetone, 2x5 min dH₂O).

4.7.1.2 Paraffin embedding and decalcification

In CZ loaded approach, OCE at day 13 and day 28 (n=2 of each hydrogel material) were fixed in 4 % formalin, decalcified with EDTA (14 % (w/v), pH 7.4) and tissue processed for paraffin embedding. Hydrogels only from day 0 and day 28 (both n=2 for each material) were directly embedded in paraffin. Samples were cut with microtome (Leica SM 2010R) to 0.5 µm slices, mounted on glass slides and dried for 25 min at 75°C. Prior to (immuno-) histological and immuno-fluorescent stainings, slides were deparaffinized in increasing alcohol row for 2x5 min xylene, 2x2 min 100 % EtOH, 2x2 min 96 % EtOH, 2x2 min 70 % EtOH and 2x2 min dH₂O.

4.7.2 Safranin-O staining

Safranin-O staining was performed to specifically detect proteoglycans in cartilage tissue. Nuclei were stained with Weigert's iron hematoxylin working solution for 8 min. After dipping in 1 % (v/v) acid alcohol and washing with tap water samples were incubated with 0.01 % (w/v) Fast Green for 2 min to stain cytoplasm. During incubation in 1 % (v/v) acetic acid for 1 min tissue was protonated before proteoglycans were stained with 0.1 %

(w/v) Safranin–O solution for 8 min that binds to negatively charged carboxyl groups and sulfonic acid esters on samples [160]. Excess and not bound dye was removed by washing with 70 % (v/v) EtOH. Slides were dehydrated as mentioned above and mounted with xylene based mounting media entellan. Cell nuclei are stained by iron hematoxylin in black, cytoplasm in green/blue and proteoglycans in red.

4.7.3 Immuno–histological stainings

For IHC stainings, antigens were enzymatically retrieved depending on antibody (table 12). Before incubation with antibody (antigens and dilutions see table 12) over night at 4°C, slides were blocked first with 3 % (v/v) H₂O₂ for 20 min and then with 5 % (w/v) bovine serum albumin for 30 min. All stainings were visualized with Horseradish–peroxidase kit following manufacturer’s instructions. 3,3’–diaminobenzidine peroxidase substrate was incubated for 90 sec. Cell nuclei were counter stained with mayers hematoxylin, rehydrated and mounted with entellan. All washing steps between blocking or chemical incubation were performed with PBS supplemented with 0.5 % (v/v) Tween. After drying at room temperature samples were microscopically visualized (Keyence BZ-9000).

4.7.4 Immuno–fluorescent stainings

For IF stainings, antigens were enzymatically retrieved as described above, blocked with 5 % (v/v) donkey serum for 20 min at room temperature and incubated with primary antibody diluted 1:100 in antibody diluent over night at 4°C. After washing to remove not bound primary antibody fluorescent labeled secondary antibody was incubated for 1 h at room temperature. All washing steps between blocking or chemical incubation were performed with PBS supplemented with 0.5 % (v/v) Tween. Slides were mounted with DAPI (4’,6–diamidino–2–phenylindole)–fluoromount–G to stain cell nuclei and visualized with fluorescence microscopy (Keyence BZ-9000) with respective excitation wavelength.

4.8 Gene expression analysis

In order to characterize pCZ phenotype seeded in hydrogels before and after *ex vivo* culture in osteochondral defect model, gene expression analysis for cartilage specific transcription factor SOX9 and matrix proteins collagen II and aggrecan was performed. Osteogenic transcription factor RUNX2 and matrix protein collagen type X were included to evaluate hypertrophic differentiation of cells.

4.8.1 RNA isolation

CZ seeded hydrogels (n=3 of each material) at three time points (day 0, day 13, day 28) were stored at -80°C for RNA isolation. RNA isolation of hydrogels (fibrin glue, collagen I, MP/HA, P(AGE/G)-HA-SH) was performed with TRIZOL according to manufacturer's instruction. starPEGh hydrogels were digested in 2 mg/ml collagenase (SERVA) for 30 min at 37°C prior to RNA isolation using InviTrap Spin Cell RNA Mini Kit. RNA quality and yield was spectrophotometrically measured using NanoDrop at 260 nm and 280 nm (Tecan infinite M200) and stored at -80°C till subsequent analysis to prevent RNA degradation.

4.8.2 cDNA synthesis

mRNA was processed for cDNA synthesis with the iScript[™] cDNA Synthesis kit according to manufacturer's instructions. A total amount of 500 ng mRNA (calculated from NanoDrop measurement) of each sample was mixed with 5x iScript[™] Reaction Mix (4 μl), iScript[™] Reverse Transcriptase (1 μl) and RNA free water to an end volume of 20 μl and transferred into thermocycler (SensQuest, BioRad). Transcription of mRNA started with accumulation of primer (5 min, 25°C), followed by elongation of cDNA (30 min, 42°C), separation of cDNA double strands (5 min, 85°C) and subsequent cooling to 4°C . cDNA was diluted 1:2 with PCR grade water to a final concentration of 12.5 ng/ μl and stored at -20°C .

4.8.3 Qualitative realtime polymerase chain reaction (qRT PCR)

Qualitative realtime PCR was performed with standard protocol including melt curve (Bio-Rad CFX Manager). For detailed information about primer sequence and annealing temperature see table 13. All samples were analyzed in duplicates containing 25 ng cDNA in each cavity of PCR 96 well plate. PCR mastermix composed of SsoFast[™] Eva Green[®] Supermix and primer pairs (4 pmol/ μl) from each gene of interest.

The PCR plate was sealed with transparent Microseal[®]-adhesive foil to prevent evaporation of samples during PCR following protocol summarized in table 18. An additional amplification step of 72°C was included in the protocol to control if the completion of primer coupling at annealing temperature was sufficient. The melt curve as last step in the protocol aimed to check the specificity of primer coupling to samples.

Ct values (number of cycle at which a specific threshold of fluorescence intensity was reached) were used to calculate gene expression levels. Ct values of pCZs were used to calculate the relative quantity (RQ) for each gene of interest by subtracting the Ct value of pCZs from Ct value of each sample. With the assumption of 100 % efficiency of the

Table 18 Protocol for qualitative realtime gene expression analysis with CFX-cycler.

step	temperature (°C)	duration (s)	comment
1	95	180	initial denaturation
2	95	10	denaturation
3	58–60	5	annealing temperature
4	72	20	elongation
			repeat steps 2–4 for total of 40 cycles
5	95	10	
6	65–95	10	melt curve (increase temperature in increments of 0.5)

primer pairs the RQ was calculated with the following formula:

$$RQ = 2^{(Ct_{(pCZs)} - Ct_{(sample)})}$$

Additionally, to gene of interest seven porcine house keeping (HK) genes β -actin, HMBS, GAPDH, SDHA, YWHAZ, EF1 α and HPRT were analyzed with all samples to find a stable combination of at least two housekeeping genes. For calculation of normalized gene expression values from RQ following the Ct method housekeeping genes are needed [161]. Target stability values (M-value) of five selected porcine housekeeping genes β -actin, HMBS, GAPDH, SDHA and YWHAZ over all material groups and freshly isolated pCZs were calculated with CFX-Software (BioRad) shown in table 18. For normalization of gene expression with normalization factor (NF) was calculated as follows [161]:

$$NF = \sqrt{RQ_{sample-HK1} \cdot RQ_{sample-HK2}}$$

The quotient of RQ and NF for each sample results in normalized gene expression expressed as $\Delta\Delta Ct$ [161]:

$$\Delta\Delta Ct = \frac{RQ_{sample}}{NF_{sample}}$$

4.9 Migration of cells in hydrogels: time lapse experiments

In order to investigate cell migration behavior of pCZs embedded in hydrogel materials in cartilage media, time lapse experiments were performed (AxioVision 40C, Carl Zeiss). Collagen I and starPEGh were chosen as representative natural and synthetic material. Porcine MSC embedded in 3 mg/ml collagen I hydrogel stimulated with TGF β 1 (10 ng/ml) and FCS (10 % (v/v)) served as positive control. Cells encapsulated in hydrogels (3 mio/ml) were observed in commercially available 1 μ slide Chemotaxis under physiological conditions in a humidity chamber. Images were taken in the observation chamber containing 7 μ l hydrogel over a period of 9 h. Cell movements were analyzed by manual tracking of at least 10 cells in the observation area (cell tracking tool, Image J). Migration speed (μ m/min) of tracked pCZs in different hydrogels and was calculated and compared to velocity of pMSCs in collagen I hydrogel.

4.9.0.1 Structural characterization by scanning electron microscopy

To visualize cell migration into defect of biopsies scanning electron microscopy (SEM) was performed in collaboration with Prof. Krohne at the Biocenter of University of Würzburg. After 4 weeks culture samples were washed with PBS and fixed over night with 6.25 % (v/v) glutaraldehyde in 50 mM phosphate buffer (pH 7.2) at 4 °C. Subsequently, samples were washed, dehydrated in series of acetone, critical point dried and sputtered with gold–palladium. SEM imaging was performed with JEOL JSM 7500F.

4.10 Statistics and data analysis

Quantitative data is presented as mean values including standard deviation. Statistical analysis of data was performed with IBM SPSS Statistics for Windows (Version 23.0, IBM Corporation). Results of biochemical quantification in OCE and GAG release in cartilage media (figure 18), pCZ loaded hydrogels (figure 30) and cell migration velocity (figure 32) were tested for significances with student's T-test (variances were assumed to be equal) because less than three groups were compared to each other.

Relative gene expression results (figure 31) were tested for statistical significance with one-way analysis of variances (ANOVA) over time with Bonferroni post-hoc test.

Significant differences was assumed in both cases for p-values <0.05.

5. Results

5.1 Establishment of *ex vivo* osteochondral defect model with critical size defects

In the first part of this thesis the osteochondral defect model including static culture device was developed and characterized. In order to establish a standardized and reproducible osteochondral explant culture model mimicking clinically relevant cartilage defects in humans the model established in this thesis is based on porcine material. Since healthy human material in an amount being sufficient to establish and characterize the model was not possible to get from the clinics we decided for porcine material from a local slaughter house. From literature we know that porcine material is comparable to humans when addressing joint size and weight-bearing [133].

In collaboration with LifeTec Group BV we developed a custom made culture culture platform that allows osteochondral explant culture with separated and thus tissue specific media supply. Details about the static culture system, including schematic drawings and evaluation of sealing and influence of media separation of ECM composition are described elsewhere [152].

5.1.1 Influence of isolation, defect creation and *ex vivo* culture on explant viability

The geometry of OCE was limited to the joint size and native surface concavity of domestic pigs. Maximum of 4–6 explants with a diameter of 8 mm were isolated from each medial condyle displaying a flat surface.

After 28 days *ex vivo* culture in static 6 well plate culture system with tissue specific media no macroscopic changes of OCE were observed. The O-ring to fix OCE in the inserts sealed the cartilage and bone media compartment. Following, communication of bone and cartilage tissue and diffusion of soluble factors are restricted to the calcified layer. Due to the creation of full thickness defects natural barrier of calcified layer was interrupted marked by an elevated media diffusion through subchondral bone into bone media indicated by decrease of cartilage media volume and parallel increase in bone media volume. The mixing of media from both compartments was negligible and did not influence explant culture. Creation of full thickness defects were classified to ICRS grade 4 displaying

defects reaching the subchondral bone and represent severe defects in clinical practice [37]. Harvest of OCE including drilling and defect creation did not influence cell viability at wounding sides (day 0).

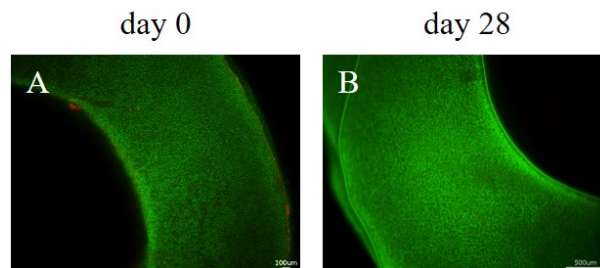


Figure 13 Live–dead staining of osteochondral explants (OCE) at day 0 and after 28 days *ex vivo* culture. Top view on cartilage ring (A) at day 0 and after (B) 28 days static *ex vivo* culture. OCE isolation and *ex vivo* culture did not negatively influence chondrocyte viability. (Scale bar (A) 100 μm , (B) 500 μm)

After 4 weeks *ex vivo* culture in static culture device with tissue specific nutrient supply viability of pChondrocytes was maintained (figure 13). Viability of subchondral bone decreased after 28 days. Further characterization of metabolic activity is shown in the figure 15.

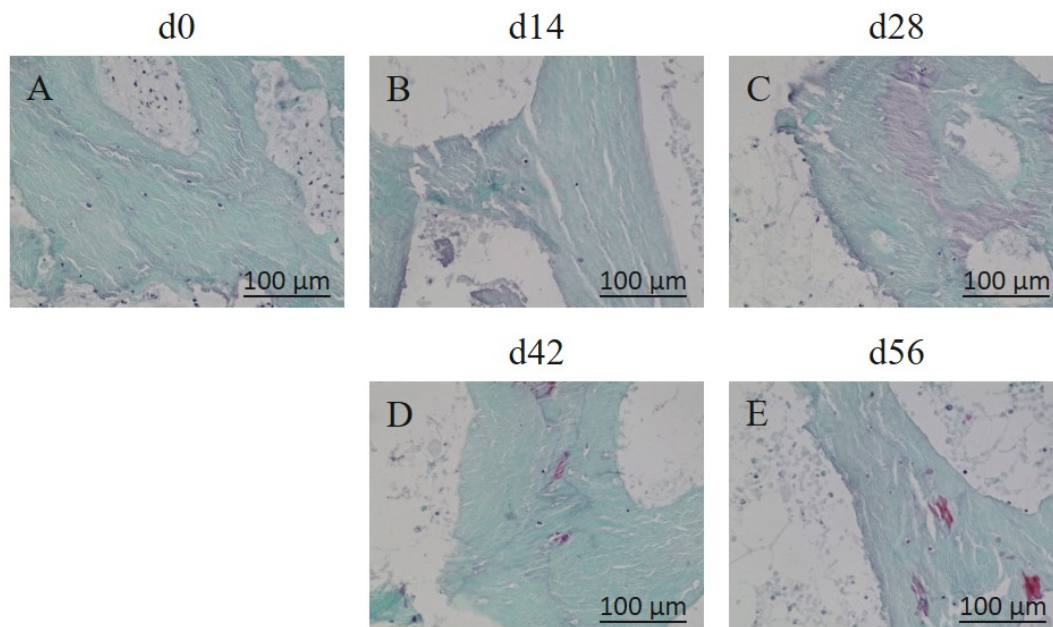


Figure 14 Safranin-O staining of osteochondral explant (diameter 8 mm) without defect cultured for 56 days *ex vivo* with tissue specific media. (A-E) Brightfield images focusing on trabecula of subchondral bone to visualize cell nuclei stained with weigert iron hematoxylin during 56 days *ex vivo* culture. Cell nuclei (stained in black) of bone cells show no changes in morphology during culture time and no indication of fragmented cell nuclei. (Scale bar 100 μm)

Figure 14 illustrates safranin-O stained samples with focus on subchondral bone. To characterize viability and remodeling activity of subchondral bone high magnified images (40x magnification) were taken from subchondral bone trabecula of an explant without defect cultured for up to 8 weeks with tissue specific media in culture platform. Since the cell nuclei of the osteocytes, osteoblasts and osteoclasts residing in the trabecula do not appear to change over culture time in shape and are not fragmented, these cells are viable.

5.1.2 *Ex vivo* critical size defect: Viability, proteoglycan content and cell recruitment

Creation of full thickness defect with a diameter of 6 mm damaged the explant to an extent that the left over cartilage tissue with width of 1 mm broke or was mechanically unstable for fixation in inserts. Due to the extent of damage for 6 mm defects (figure 15 D), largest defect included in study to define critical size defect in the *ex vivo* culture represented a diameter of 4 mm.

No indications of cartilage swelling after isolation, defect creation and culture were observed. Representative macroscopic images of MTT stained OCE at day 0 (no defect, 2 mm defect,

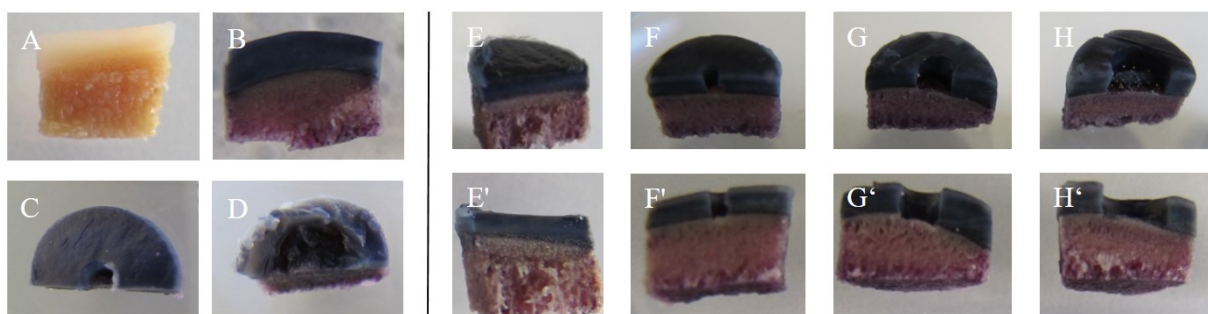


Figure 15 MTT viability staining of osteochondral explants (OCE) with full thickness cartilage defects at day 0 and after 28 days *ex vivo* culture. (A) OCE without MTT staining, (B) MTT stained OCE without defect, (C) OCE with 1 mm and (D) 6 mm defects at day 0 (OCE diameter: 8 mm). MTT staining of OCE at day 28 (E, E') without defect, (F, F') 1 mm, (G, G') 2 mm, (H, H') and 4 mm full thickness cartilage defect. Metabolic active cells in OCE are shown in purple/blue. Reduction in intensity of MTT staining resulted in subchondral bone but not in cartilage at day 28.

6 mm defect) and day 28 (no defect, 1 mm, 2 mm and 4 mm defect) are shown in figure 15 A–H'. Metabolic active cells reduce MTT dye to blue formazan product illustrated by purple to blue staining of the explant. No differences in metabolic activity resulted for cartilage of OCE cultured 28 days in static *ex vivo* system. Subchondral bone showed a decrease in metabolic activity when cultured in static system compared to day 0.

The definition of critical size defect, representing a defect size that does not heal by itself

within 4 weeks *ex vivo* culture in static culture device, was based on histological stainings for safranin-O (figure 16) [152]. Safranin-O stainings after 28 days static culture with

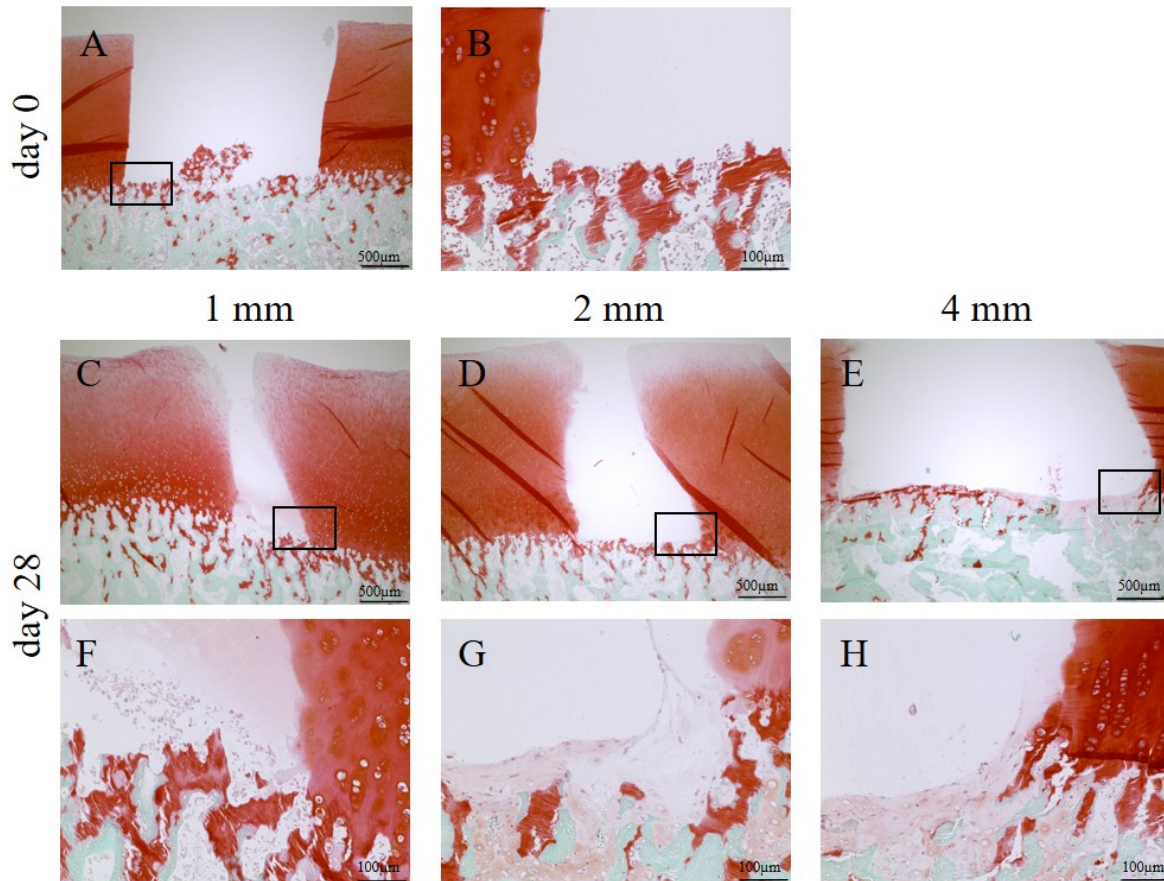


Figure 16 Definition of *ex vivo* critical size cartilage defect. Safranin-O stainings of osteochondral explants (OCE) with full thickness cartilage defects at day 0 and day 28. (A–B) OCE with 2 mm defect at day 0. (C) OCE with 1 mm, (D) 2 mm and (E) 4 mm cartilage defect after 28 days static culture. (F–H) Higher magnification of images (C–E). Safranin-O positive tissue is present in wounding edges and on top of calcified layer. There is no complete filling of defect volumes. Adapted from Schwab *et al.* [152]. (Scale bar (A, C, D, E) 500 μm , (B, F, G, H) 100 μm)

tissue specific media did not result in complete defect healing of full thickness defects (1 mm, 2 mm, 4 mm). At the wounding edges and on top of calcified layer of all samples a thin layer of ECM and cells was present. This intrinsic neo-tissue formation was positive for proteoglycans with a less intense red staining compared to native cartilage tissue. OCE with 4 mm in diameter resulted in cartilage like tissue formation on calcified layer to an extent comparable to OCE with smaller diameter. The left over cartilage in this samples provided sufficient healthy tissue to study cartilage regeneration in this defect model. This lead to the decision to define 4 mm as critical size defect and thus perform all following material testings in explants with this defect diameter. Moreover, 4 mm defects open the possibility to test bi-layered or printed constructs in future work which is hardly possible

for smaller defect diameters. Cell recruitment on calcified layer, wounding edges up to

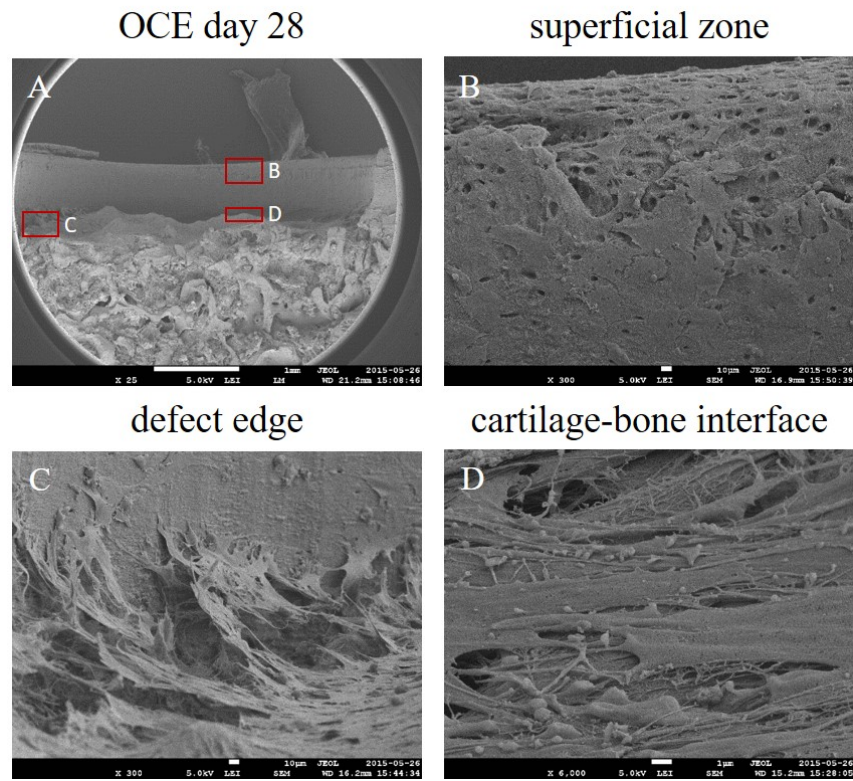


Figure 17 Scanning electron microscopy (SEM) images of osteochondral explant (OCE) with 4 mm defect after 28 days *ex vivo* culture. (A) Overview of OCE cross section (scale bar 1 mm). Rectangles indicate location of higher magnified images presented in B–D. (B) View on cartilage tissue at the superficial zone with flat cells covering the articular surface in the defect (scale bar 10 μm). (C–D) Cartilage–bone interface and calcified layer. (C) cells spread from the subchondral bone to cartilage (scale bar 10 μm). (D) Multilayer of flat and elongated cells on calcified layer. (Scale bar (B, C) 10 μm , (A, D) 1 μm)

the cartilage wall in superficial zone of OCE with full thickness defect was visualized by SEM images. Figure 17 shows representative images of OCE with 4 mm defect. Confluent layers of elongated, flat cells were visualized at the cartilage–matrix interface of the defect. Cells covered the surface of the cartilage in the defect area up to the superficial zone (figure 17 B). Figure 17 C illustrates the bridging of cells between calcified layer and cartilage in the wound edge. On calcified zone, the direct interface between bone and cartilage, multilayer of flat and elongated cells were present.

The separated media compartments of the static culture device allowed the characterization of cartilage media in terms of GAG released from explants during culture in cartilage media compartment (table 19 and figure 18 A–C). Accumulated GAG release of OCE without, 1 mm, 2 mm and 4 mm defects into cartilage media supernatant increased linear over culture time (figure 18 A). Dependency between surface area of cartilage and GAG release resulted when GAG release was normalized to cartilage surface area including surface jacket area at defect side shown by green coloring in figure 18 D.

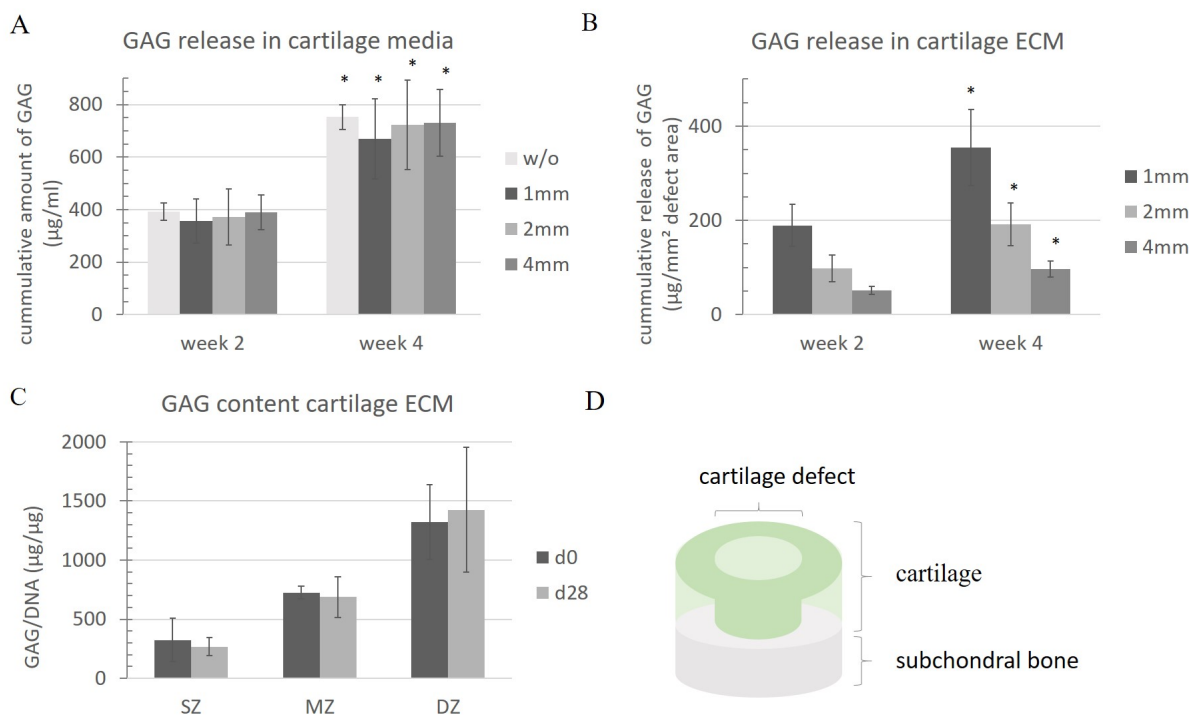


Figure 18 Quantification of proteoglycans in superficial (SZ), middle (MZ) and deep zone (DZ) and GAG release during static *ex vivo* culture. (A) Total amount of cumulative GAG release in cartilage media during static *ex vivo* culture over 28 days ($\mu\text{g}/\text{ml}$). (B) GAG release normalized to cartilage surface area including surface jacket area at defect side ($\mu\text{g}/\text{mm}^2$). (C) GAGs quantified in SZ, MZ and DZ of cartilage at day 0 and after 28 days *ex vivo* culture. There is no significant difference of GAG levels in SZ, MZ and DZ in cartilage tissue over time. OCE with 4 mm defect released less GAG/ mm^2 into cartilage supernatant followed by 2 mm, 1 mm and no defect. (D) Schematic drawing of osteochondral explant with cartilage defect with coloring of defect surface area including defect jacket area in dark green. Statistical significance was determined by student's T-test: * $p < 0.05$ compared to day 0, ($n = 3-5$).

Figure 18 A displays the GAGs released between week 2 and week 4 in OCE with 1 mm, 2 mm and 4 mm defect (each $n = 3$) normalized to defect surface. Highest values were reached by OCE with 1 mm defect, followed by 2 mm and 4 mm defect diameter. The bigger the defect, the smaller the remaining cartilage surface the lower the GAGs found in supernatant.

Quantification of zonal GAG distribution normalized to DNA content cartilage tissue of OCE without defect after 4 week static *ex vivo* culture did not show significant differences compared to freshly isolated samples in superficial zone (0 – 0.2 mm), middle zone (0.2 – 1.0 mm) and deep zone (1.0 – 1.4 mm) measured from cartilage surface (figure 18 C). No significant differences resulted in total GAG/DNA content in the three cartilage zones between day 0 and after 28 days culture.

Table 19 Summary of accumulated (acc.) GAG release from osteochondral explant culture without, 1 mm, 2 mm and 4 mm full thickness defect in cartilage media after 28 days *ex vivo* culture. Statistical significance was determined by student's T-Test between day 0 and day 28, (n=3-5).

defect diameter	acc. GAG ($\mu\text{g/ml}$)	GAG / surface ($\mu\text{g/mm}^2$)
no defect	752.00 (p=0.012)	
1 mm	669.06 (p=0.035)	118.30 (p=0.035)
2 mm	722.28 (p=0.039)	31.90 (p=0.039)
4 mm	744.12 (p=0.025)	131.59 (p=0.025)

5.1.3 Prototype bioreactor: Influence of dynamic culture on viability

A prototype bioreactor for dynamic culture of OCE, developed in collaboration with LifeTec group within HydroZONES consortium, was tested to investigate the potential of constant media flow through bone compartment on bone viability. The bioreactor is manufactured in a similar way to the static culture device displaying two separated media chambers sealed by an O-ring at the cartilage–bone interface.

In collaboration with Research Center for Magnetic Resonance Bavaria e.V in Würzburg gross morphological parameters bone volume, trabecula thickness (TbTh), trabecula space (TbSp) and porosity of porcine subchondral bone were analyzed by μ -computer tomographic scans. Mean values of these parameters were calculated and depicted in the SEM image in figure 19 A. Porcine subchondral bone trabecula displayed a high natural derived variation in TbTh ranging from 35.77 μm to 307.45 μm with mean value of 135.93 ± 40.65 μm . Values for TbSp ranged between 265.36 μm and 509.71 μm with mean value of 265.36 ± 85.64 μm . TbTh and TbSp providing the tissue with inter-connectivity and strength.

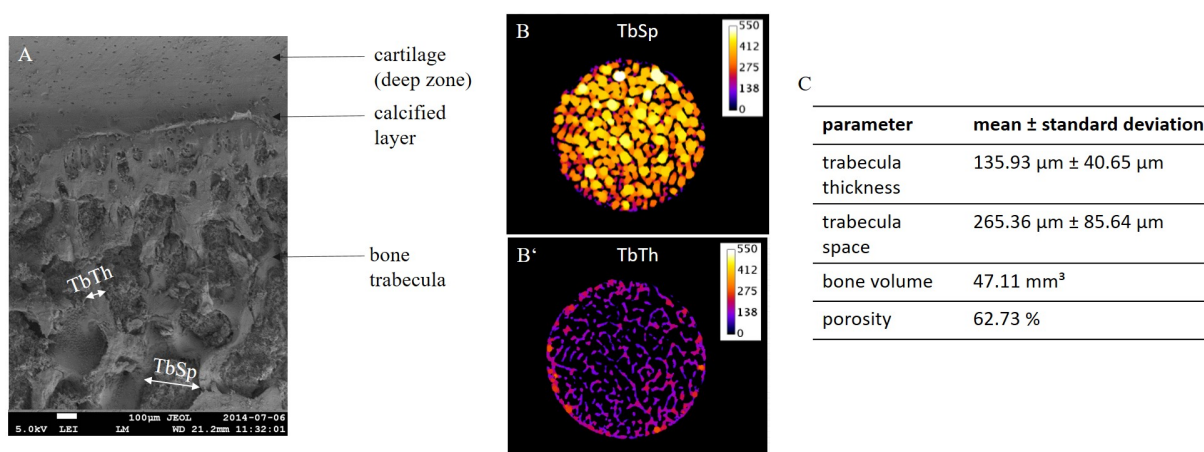


Figure 19 Characterization of subchondral bone of porcine osteochondral explant. (A) Scanning electron microscopical (SEM) image of porcine osteochondral explants cross section. (B–B') Results of μ -computer tomographic analysis of porcine subchondral bone parameters trabecula thickness (TbTh) and trabecula space (TbSp) as well as (C) calculation of subchondral bone volume and porosity based on μ Ct data. TbTh and TbSp are marked by white arrow in SEM image. (Scale bar 100 μ m, n=1)

From theoretical point of view the bone porosity of 62.73 % represented a sample volume suitable to perfuse in a dynamic culture set up for elevated supply of nutrients and removal of waste compared to diffusion processes under static conditions. MTT stainings of subchondral bone in bioreactor system (figure 20 A) did not exceed the result when cultured under static conditions (figure 15 E–H).

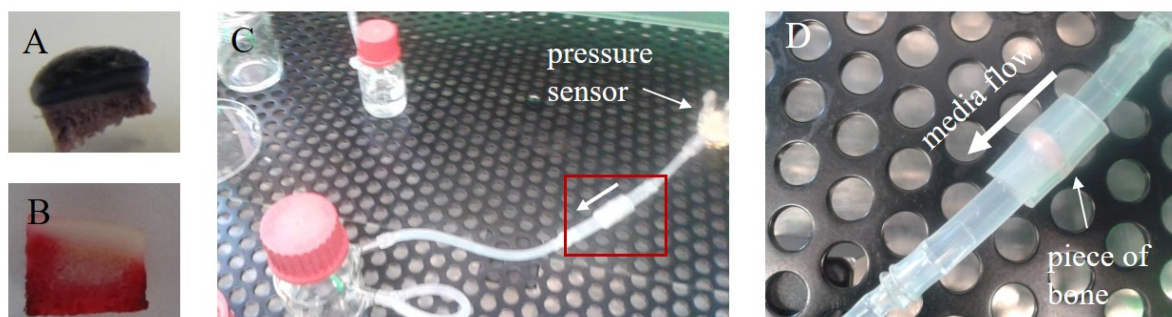


Figure 20 Experimental set up to measure pressure of media through subchondral bone of osteochondral explant (OCE). (A) MTT staining of OCE (diameter: 6.5 mm) after 28 days dynamic culture in bioreactor. (B) Cross section of OCE after constant perfusion in bone compartment with Eosin (2 h, 4 rpm, 1 ml/min). (C–D) Subchondral bone of OCE press fit in silicon tube, connected to pressure sensor and perfused at 4 rpm.

The low perfusion pressure of 7–10 mmHG during dynamic culture (1 ml/min) lead to the assumption that bone media washed around periphery of subchondral bone instead of perfusion the sample. To proof this issue an OCE was perfused with Eosin dissolved in PBS (2 h, 4 rpm, 1 ml/min). After cutting the explant into half the cross section clearly

demonstrated that the dye did not penetrate into the center of subchondral bone (figure 20 B). On the other hand the sealing of cartilage and bone media compartments was successfully since the cartilage did not stain red.

An additional experiment to measure the pressure when media actively perfused subchondral bone was set up shown in figure 20 C–D. A cylindrical disc of porcine subchondral bone was fixed tightly in silicon tube and connected via roller pump with media reservoir. The pressure was measured with a pressure sensor between media reservoir and sample. OCE was perfused at 4 rpm resulting in a rapid elevation of pressure exceeding the maximum measurable pressure of 500 mmHG. Following, there is no perfusion through subchondral bone possible. For all further results shown in the following sections the static culture device was used for *ex vivo* culture of the OCE.

5.2 Characterization of collagen I isolated from rat tail

Characterization of collagen I isolated from rat tails by western blot analysis for presence of collagen type I and structural analysis of polymerized collagen I hydrogel (3 mg/ml) by SEM are shown in figure 21. Collagen I hydrogel revealed fiber mesh of randomly orientated collagen fibers with uniform diameter. The immune blot for collagen I displayed

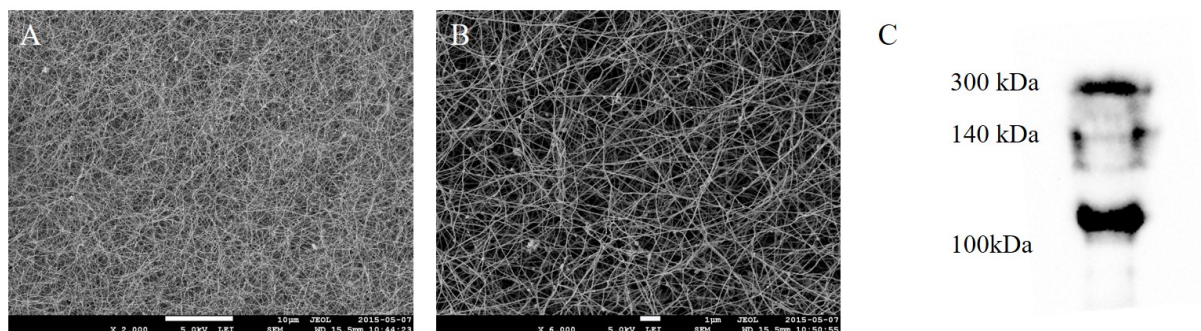


Figure 21 Characterization of collagen I isolated from rat tails. (A–B) Scanning electron microscopical images of collagen I hydrogel (3 mg/ml) display a fiber mesh with homogenous fiber diameter. (C) Western blot analysis of collagen I isolated from rat tail against collagen I shows two characteristic bands at 120 kDa and 300 kDa. (Scale bar (A) 10 μm , (B) 1 μm)

two bands at 120 kDa and 300 kDa as described in the datasheet of collagen I antibody. The 120 kDa represents the single chain of collagen I triple helix. Additionally, the dimeric collagen I protein band is seen at around 300 kDa.

5.3 Characterization of porcine articular cartilage and porcine chondrocytes

pChondrocytes isolated from lateral condyles were phenotypically characterized (5.3.1) and growth behavior during *in vitro* culture was analyzed (5.3.2).

5.3.1 Phenotypical characterization of pChondrocytes and articular cartilage

Primary isolated pChondrocytes were characterized for *in vitro* expansion behavior in terms of morphology and population doubling. Microscopical images were taken at day 3, day 5, day 7 and day 11 to document morphological changes of pChondrocytes (figure 22). During *in vitro* expansion pChondrocytes underwent morphological changes from compact,

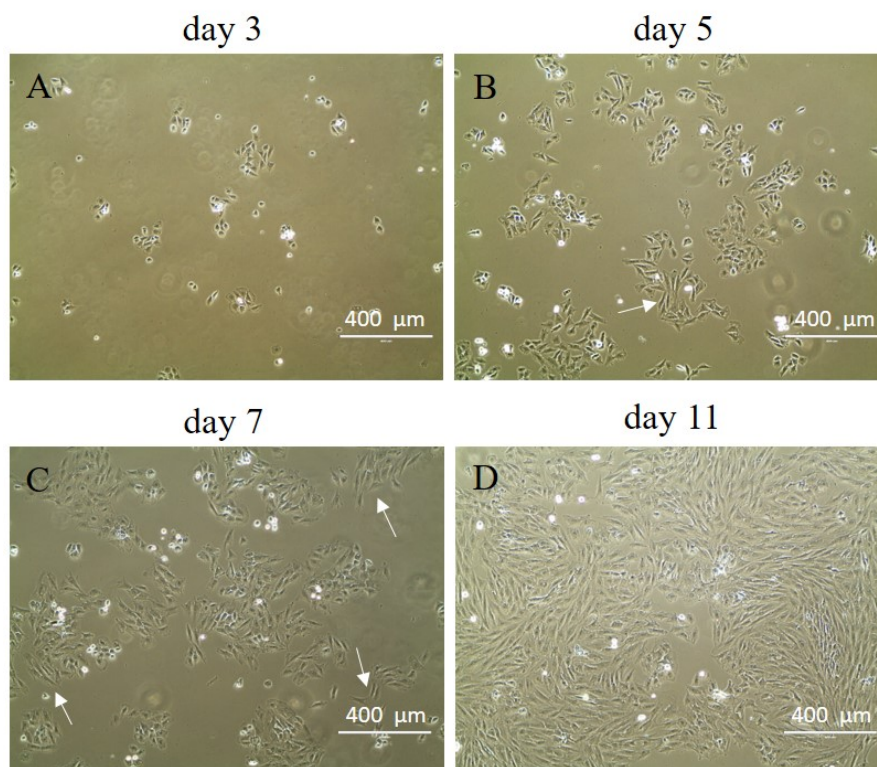


Figure 22 Microscopical images of porcine chondrocytes during *in vitro* expansion. pChondrocytes at (A) day 3, (B) day 5, (C) day 7 and (D) day 11 during expansion became elongated with fibroblastoid morphology from day 5 on (marked by white arrow). (Scale bar (A–D) 400 μm)

round appearance at day 3 to elongated and fibroblastoid morphology from day 5 on (white arrow in figure 22 B and C). In order to keep chondrogenic phenotype and prevent pChondrocyte dedifferentiation, cells were embedded in hydrogels direct after isolation

without seeding and expansion in 2D.

Population doubling of pChondrocytes (passage 0, pooled cells from four lateral condyles) was investigated by counting cells (in triplicates) cultured in 6 well plate (n=3 wells at each time point) and subsequent DNA quantification summarized in table 20. Cell proliferation of *in vitro* expanded pChondrocytes showed exponential growth with a longer time of population doubling when cells became confluent. Population doubling of pChondrocytes based on cell numbers ranges from 41 h between day 3 and day 7 to 48 h between day 3 to day 9. From day 7 to day 9 the population doubling elevated to 75 h.

Table 20 Calculation of cell number of 2D expanded porcine chondrocytes in terms of cell numbers and DNA content at day 3, day 7 and day 9 including standard deviation (n=3).

	day 3	day 7	day 9
cell counting	62 000 ± 7 722	290 357 ± 33 439	371 555 ± 28 333
DNA content (mg)	12.08 ± 1.28	21.39 ± 2.38	32.21 ± 1.58

Phenotypic expression of intra- and extracellular markers and ECM proteins was investigated by IF stainings on porcine articular cartilage for cartilage specific proteins aggrecan, collagen II and VI and transcription factor SOX9 and osteogenic or hypertrophic related markers RunX2, proCollagen I and collagen X. pChondrocytes in native cartilage tissue (fresh isolated samples) were positively stained for all selected cartilage specific markers (see supplementary material figure 37). Collagen II was homogeneously stained throughout cartilage tissue. Collagen X staining increases from superficial zone to deep zone and the osteogenic markers RunX2 and proCollagen I were only weak present.

To control specificity of secondary antibody in IHC and primary antibodies isotype controls (Ms IgG1, IgM, IgG2a) and second antibody only were also stained on porcine material (figure 36 in supplementary data). No stainings implicate specificity of antibody stainings in subsequent histological analysis.

5.3.2 Chondrocyte pellet culture and free swelling culture of collagen I loaded hydrogel

To demonstrate the influence of surrounding osteochondral explant on pChondrocyte phenotype and matrix production a control group of chondrocyte loaded collagen I hydrogel (20 mio cells/ml) and pellet culture (0.5 mio cells/pellet) were *in vitro* cultured for 28 days in cartilage media (free swelling) without TGF- β 1 as it was used for OCE culture. Some results are shown in the supplementary material (figure 37).

SOX9 and collagen VI were mainly present in periphery of pChondrocyte pellet whereas both markers stained positive throughout chondrocyte loaded collagen I hydrogel in absence of TGF- β in culture media. Hyaline cartilage markers aggrecan and collagen II were weak expressed in both groups with higher accumulation in pChondrocyte pellet culture compared to hydrogel but less than in native tissue.

Hypertrophic marker proCollagen I was only expressed in pellet culture but not in collagen I loaded hydrogel cultured under free swelling conditions. RunX2 was negative. Matrix protein collagen X was expressed in both groups with accumulation in pericellular region. In collagen I hydrogel cells expressed collagen X throughout material and in pellet culture primarily in periphery and less in deeper areas. Comparing the stainings with the results of cell loaded collagen I hydrogel implanted in OCE model, the synthesis of collagen II, VI, and aggrecan was more pronounced in the *ex vivo* model compared to the free swelling and pellet culture. Additionally, the chondrogenic transcription factor SOX9 was positively stained in majority of pChondrocytes embedded in hydrogel after *ex vivo* culture whereas it was only locally expressed in the two control groups. Moreover, collagen X, proCollagen I and RunX2 indicating a more hypertrophic phenotype were only weak expressed at the bottom side of the collagen I hydrogel facing to subchondral bone in the OCE defect model. Since the pChondrocyte pellet culture and free swelling control was not cultured in parallel to OCE cultures the results have to be interpreted with caution and no direct correlations should be drawn.

5.4 *Ex vivo* evaluation of novel biomaterials

In the first approach, three novel hydrogel materials starPEGh, MP/HA and (PAGE/G)–HA–SH and the two clinically used materials collagen I isolated from rat tail and fibrin glue were screened cell free to define the baseline results of their regenerative potential in the porcine *ex vivo* osteochondral defect model after 4 weeks static culture with tissue specific media based on (immune–) histological stainings. In a second experimental set up the hydrogel materials were loaded with primary isolated pChondrocytes (20 mio/ml) (passage 0) into the hydrogel materials. Commercially available fibrin glue and collagen I hydrogel, isolated from rat tails, served reference materials.

Additionally, the influence of peptide modification on extracellular matrix synthesis and accumulation was analyzed with chondrocyte loaded (20 mio cells/ml) starPEGh material. Four peptide sequences (2 M in starPEGh), namely WYRGL, KLER, RGD and scrambled (random) RGD were augmented to the starPEGh and cultured in the osteochondral defect model. Histological stainings were performed to characterize the influence of peptide modified starPEGh hydrogels on cartilage matrix synthesis.

5.4.1 Cell free hydrogel material testing

Casted hydrogels transferred press fit into full thickness cartilage defects of OCE maintained shape and size and stayed in place in the defects without glueing. In contrast, collagen I and

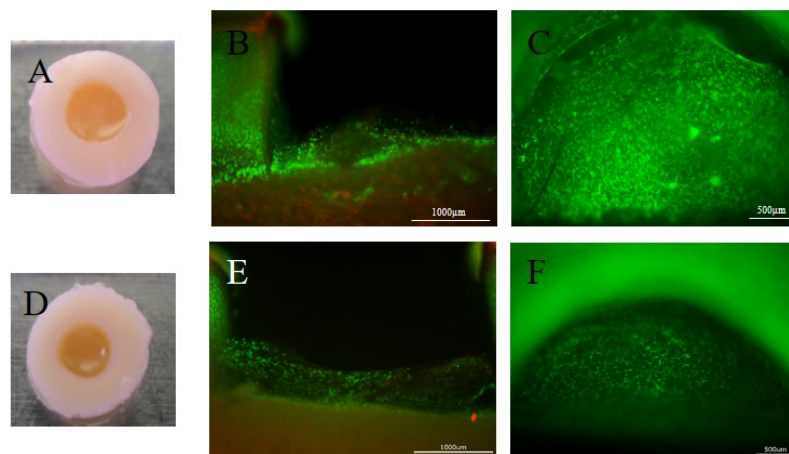


Figure 23 Macroscopic images and live–dead staining of cell free hydrogel (collagen I, fibrin glue) cultured 28 days in *ex vivo* defect model. (A, D) Macroscopic images of explant (OCE diameter: 8 mm) at day 28. (B–C) Live–dead images of cross section and top view of collagen I and (E–F) Fibrin glue. Hydrogel integrated into defect and invasion of cells from surrounding OCE into cell free hydrogels are shown in live–dead images. (Scale bar (B, E) 1000 µm, (A, C, D, F) 500 µm)

fibrin gels shrank in height but remained diameter with good integration to subchondral

bone as it is seen in figure 23 B and E.

Cells migrated into cell free hydrogels displayed an elongated morphology and were

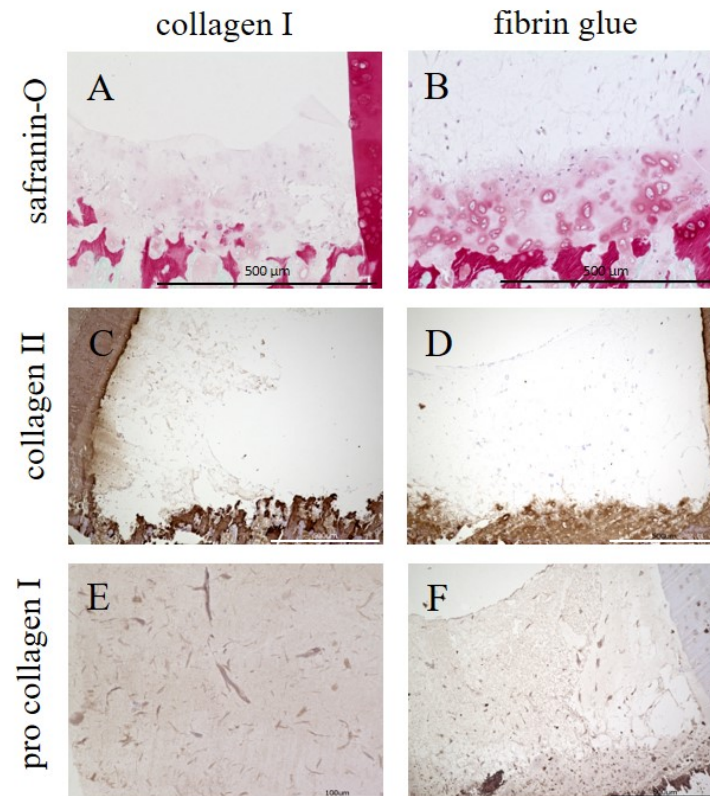


Figure 24 Histological stainings of cell free collagen I hydrogel and fibrin glue cultured 28 days in *ex vivo* defect model. (A–B) Safranin–O staining focusing on hydrogels in cartilage defect. (C–D) Immuno–histological stainings for collagen II and (E–F) proCollagen I. Light red safranin–O and proCollagen I positive staining with elongated cells migrated into cell free collagen I and fibrin glue indicate fibrous cartilage tissue formation. (Scale bar (A–D, F) 500 µm, (E) 100 µm)

homogeneously distributed in hydrogel materials (figure 23) accompanied by shrinkage in hydrogel height during *in vitro* culture.

For further characterization of cartilage defect healing and regeneration in cell free treated OCE after static culture, safranin–O and IHC stainings for collagen II and proCollagen I are shown in figure 24. The red background staining of the scaffold components is caused by presence of negative charged hydrogel components, namely heparin in starPEGh and HA in P(AGE/G)–HA–SH and MP/HA, and does not represent cartilagenous tissue formation. IHC stainings of the cell free tested innovative hydrogels starPEGh, MP/HA and P(AGE/G)–HA–SH showed cells on the calcified layer but no migration into the synthetic hydrogel materials was observed. In safranin–O staining and IHC images stained for proCollagen I and collagen II the presence of cells in cell free implanted materials collage I and fibrin glue was visible. The cells migrated into the natural hydrogels

originating either from the surrounding cartilage or bone tissue of the OCE. Exact origin of these cells remains unclear.

The materials implanted into defect stained positive for proCollagen I, a marker for fibrous tissue formation (figure 24 E–F). IHC stainings for articular cartilage ECM protein collagen II was negative (figure 23 C–D) although light red staining of safranin–O resulted in hydrogel facing to the calcified layer (figure 24 A–B). IHC and safranin–O staining of samples at day 0 were not positively stained. Following, a false positive background staining of the antibodies and dye was excluded. In contrast to the two reference materials the

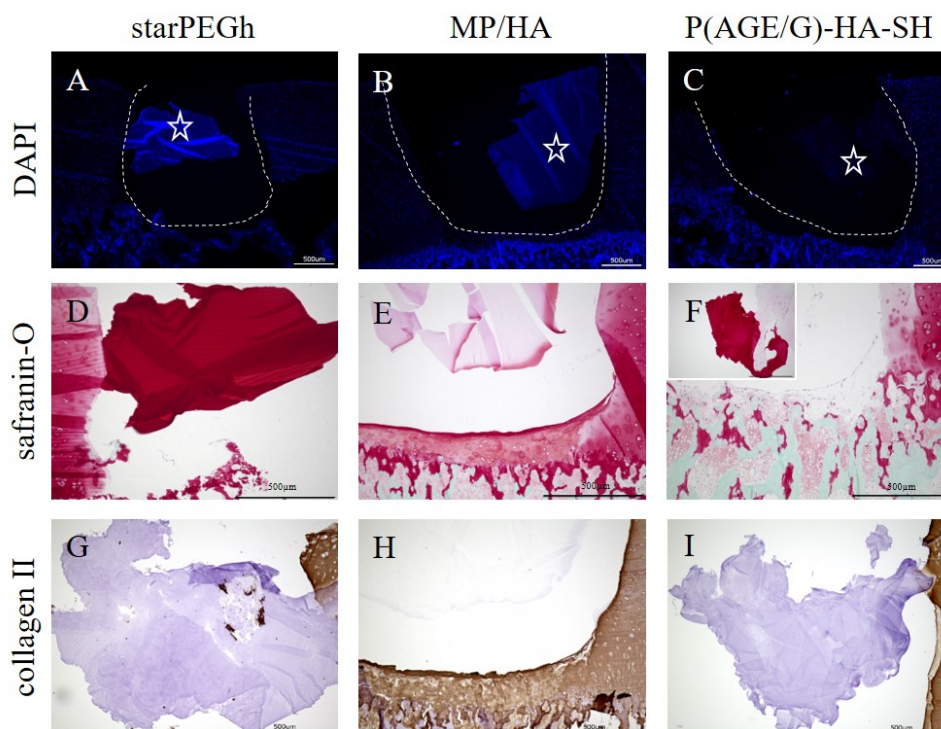


Figure 25 Histological stainings of cell free tested HydroZONES materials in osteochondral model after 28 days. (A–C) DAPI staining to visualize cell nuclei, (D–F) Safranin–O and (G–I) collagen II staining. Cells from surrounding explant do not migrate into cell free hydrogels and no cartilage matrix production is present. Red staining of the hydrogels is due to the presence of negative charged hydrogel components heparin in starPEGh and HA in P(AGE/G)–HA–SH and MP/HA. (Scale bar 500 μ m)

three innovative hydrogel systems starPEGh, MP/HA and P(AGE/G)–HA–SH developed within HydroZONES project did not result in invasion of cells into cell free materials characterized by DAPI staining of sliced samples (figure 25 A–C). The boundary of cartilage defect is marked by white line and the scaffold by a star. Due to the absence of cartilage regeneration in cell free approach of these three materials only selected images for safranin–O and collagen II immuno–histological stainings were included in this section.

5.4.2 Chondrocyte loaded hydrogel material testing

One option to improve the outcome of the three innovative materials regarding cartilage regeneration is the embedding of cells, either porcine chondrocytes or mesenchymal stem cells, prior to implantation to achieve improvement in tissue regeneration. In this study, chondrocyte loaded innovative materials starPEGh, MP/HA and (P/AGE/G)–HA–SH maintained shape and size whereas fibrin glue and collagen I hydrogel shrank when loaded with cells after 4 weeks *ex vivo* culture in static culture platform (figure 26) introduced in figure 7. The characterization and analytical results with focus on cartilage regeneration are presented in the following paragraphs.

5.4.2.1 Characterization of hydrogel materials: histology and proteoglycan content

MTT substrate in pChondrocyte loaded materials was reduced from metabolic active cells embedded in collagen I, fibrin glue and starPEGh materials at day 0 and day 28 resulting in blue formazan product (figure 26). Since MTT assay was negative for MP/HA and P(AGE/G)–HA–SH the two materials were additionally analyzed by live–dead staining which resulted in presence of living but also dead cells (data not shown). The results of

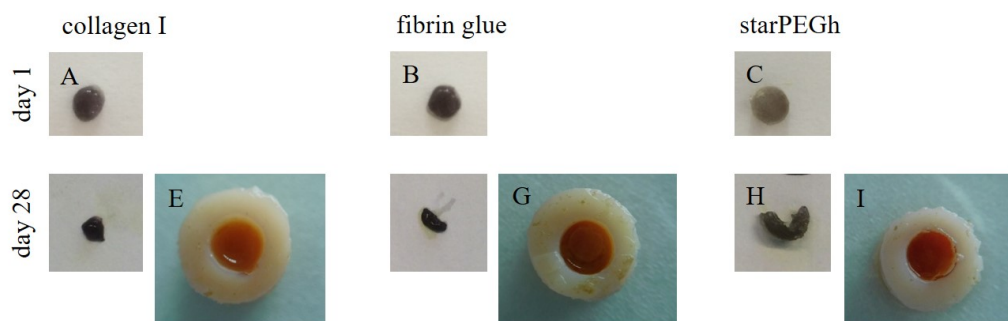


Figure 26 MTT staining and macroscopic images of porcine chondrocyte loaded hydrogels (20 mio/ml). (A) MTT staining of collagen I, (B) fibrin glue and (C) starPEGh at day 1 (hydrogel diameter: 4 mm). (D–E) Macroscopic image and MTT staining of collagen I, (F–G) fibrin glue and (H–I) starPEGh after 28 days *ex vivo* culture in osteochondral explant model (OCE diameter: 8 mm). pChondrocytes in hydrogels were metabolic active at day 1 and day 28 marked by reduction of MTT reagent to purple to blue crystals. Collagen I hydrogel and fibrin glue shrank in diameter.

IHC and IF stainings as well as macroscopic images and MTT outcome from cell loaded approach of the two reference materials collagen I, fibrin glue as well as innovative materials starPEGh, MP/HA and P(AGE/G)–HA–SH are summarized in figure 26. In comparison of all scaffolds the cartilage regenerative potential regarding ECM synthesis revealed material

dependency. pChondrocytes seeded in the two natural materials collagen I and fibrin glue synthesized aggrecan and collagen II being positive stained throughout the whole scaffold matrix (figure 28F–G, K–L). There were no antibody staining visible in control samples at day 0. Following, background staining induced by hydrogel materials is excluded. In contrast, cartilage matrix accumulation in starPEGh was locally concentrated in periphery of pChondrocytes with indication of matrix remodeling starting around pChondrocytes (figure 28 C, H). IHC stainings for starPEGh were weaker than for collagen I hydrogel. Slight indications of collagen II and aggrecan synthesis between cellular aggregates could be detected in MP/HA and P(AGE/G)–HA–SH materials. A subjective summary of the histological stainings in terms of staining intensity compared to native cartilage and amount of positive staining presented in a heat map is shown in figure 27. Chondrogenic

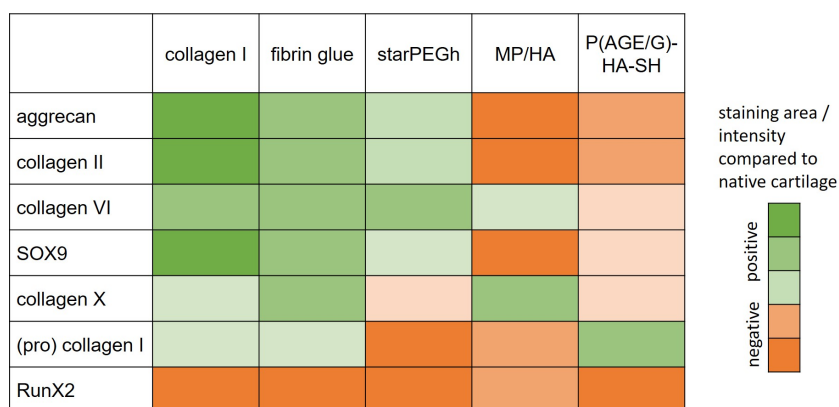


Figure 27 Heat map to qualitatively summarize the immuno-histological and -fluorescent stainings of pChondrocyte loaded hydrogel materials cultured for 28 days *ex vivo* in osteochondral defect model. Intensity of positive staining and/or amount of synthesized extracellular matrix (aggrecan, collagen I, II, VI and X, proCollagen I and transcription factors (SOX9, RunX2) present in hydrogel materials are shown in orange (no staining) to green (light green: slight positive staining, dark green: strong staining) color.

phenotype was maintained during 4 weeks *ex vivo* culture even without supplementation of cartilage media with TGF- β based.

Chondrogenic transcription factor SOX9 and ECM protein collagen VI mostly present in IF staining (figure 29 F–J) in collagen I and fibrin glue, followed by starPEGh. pChondrocytes embedded in MP/HA and P(AGE/G)–HA–SH resulted in reduced expression of SOX9 already at day 0. In IF stainings for SOX9 and collagen VI a reduction in positive staining for starPEGh, MP/HA and P(AGE/G)–HA–SH resulted compared to fibrin glue and collagen I hydrogel at day 0. Collagen VI which is naturally localized in pericellular matrix of articular chondrocyte was most abundantly stained for collagen I hydrogel, followed by fibrin glue and less present in starPEGh at day 28. MP/HA and P(AGE/G)–HA–SH showed a reduced IF staining for SOX9 compared to the other materials.

ProCollagen I and RunX2 were negative for collagen I and starPEGh with a slight positive detection of proCollagen I in fibrin glue at day 28 in IF. Addressing P(AGE/G)-HA-SH and MP/HA cells in these two materials were positive for proCollagen I and RunX2 (figure 29 N, O) accompanied with weak staining for collagen X (figure 29 S, T). Collagen X was visible in collagen I, fibrin glue and starPEGh material with low intensity. pChondrocytes embedded in fibrin glue synthesized more collagen X compared to collagen I and starPEGh. The metabolic activity of pChondrocytes in collagen I, fibrin glue and starPEGh correlates with synthesis of cartilage ECM after 4 weeks *ex vivo* culture. Absence of MTT positive staining in PG-HA-SH and MP-HA indicated no metabolic active cells after hydrogel polymerization that may explain the reduced cartilagenous matrix synthesis compared to collagen I and fibrin glue.

Since the samples at day 0 were negative for RunX2, proCollagen I and collagen X no images are shown in this section. Negative staining of isotype controls (figure 36) and no staining of hydrogel matrix at day 0 excludes non specific antibody binding.

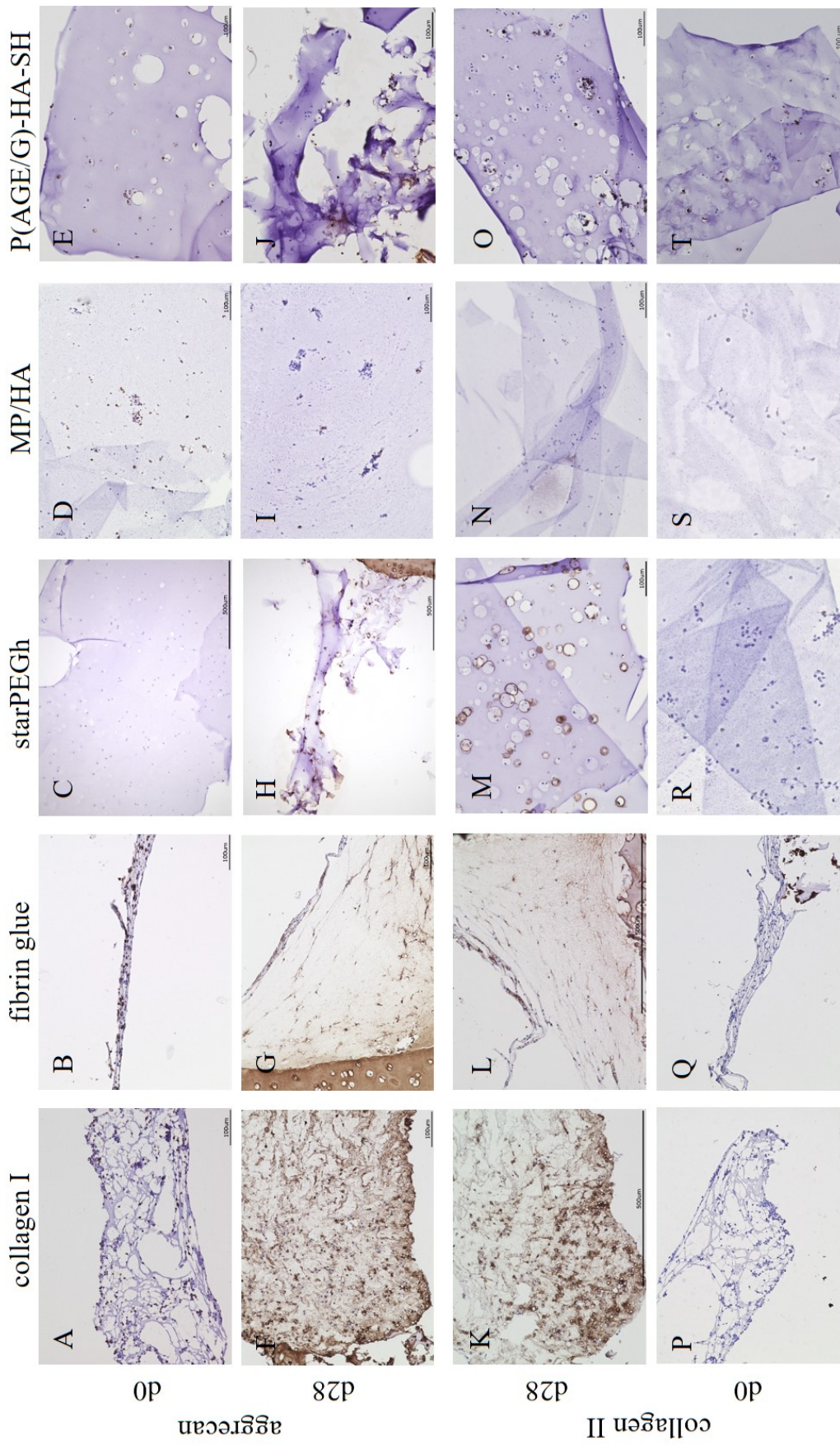


Figure 28 Immuno-histological (IHC) stainings of collagen I, fibrin glue, starPEGh, MP/HA and P(AGE/G)-HA-SH materials at day 0 and after 28 days *ex vivo* culture. (A-E) IHC staining for cartilage matrix protein aggrecan at day 0 and (F-J) after 28 days *ex vivo* culture. (K-O) IHC staining for cartilage matrix protein collagen II at day 0 and (P-T) at day 28. At day 28 pChondrocytes expressed cartilage related ECM markers (aggrecan, collagen II) throughout hydrogels. In starPEGh both proteins are detected locally in pericellular region whereas in MP/HA and P(AGE/G)-HA-SH markers were hardly expressed. (scale bar (C, H, K, L) 500 μ m, (A, B, D-G, I, J, M-T) 100 μ m)

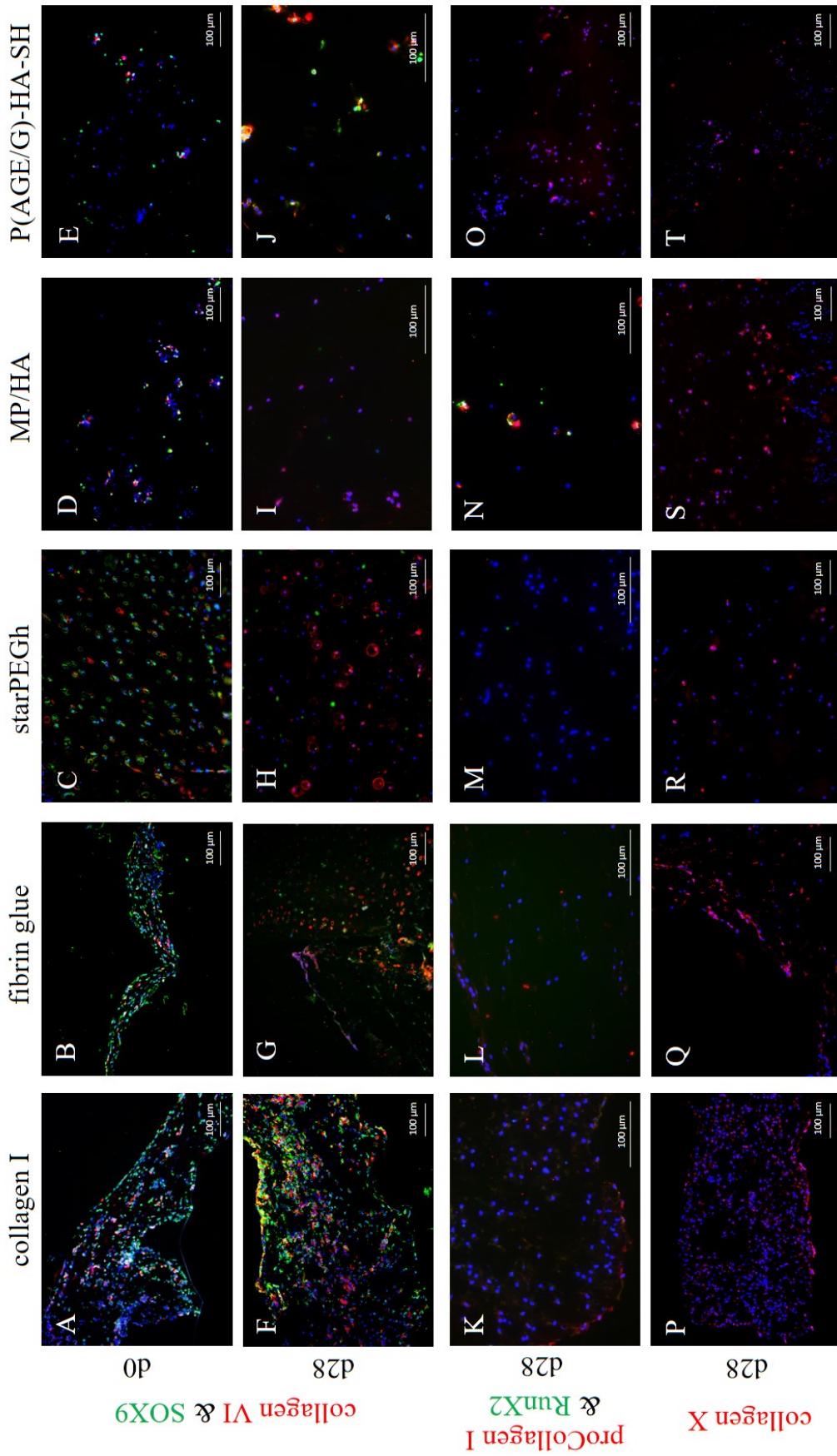


Figure 29 Immune-fluorescent (IF) stainings of collagen I, fibrin glue, starPEGh, MP/HA and P(AGE/G)-HA-SH materials. (A-E) Overlay of IF staining for collagen VI (red), SOX9 (green) and DAPI (blue) at day 0 and (F-J) after 28 days *ex vivo* culture in osteochondral explants. (K-O) Overlay of proCollagen I (red), RunX2 (green) and DAPI (blue) staining at day 28. (P-T) IF stainings for collagen X (red) and DAPI (blue) at day 28. At day 0 cells embedded in hydrogel materials expressed cartilage specific markers (SOX9, collagen VI) which were present in reduced amount in collagen I, fibrin glue and starPEGh at day 28. In MP/HA and P(AGE/G)-HA-SH both cartilage specific markers were less present compared to collagen I. Instead, hypertrophic and osteogenic related protein and transcription factor (proCollagen I, RunX2) were more present in these materials compared to collagen I, fibrin glue and starPEGh. pChondrocytes embedded in fibrin glue synthesized more collagen X than in collagen I hydrogel. (scale bar 100 µm)

Quantification of proteoglycans expressed in GAGs ($\mu\text{g}/\text{mg}$ wet weight) increased within 28 days *ex vivo* culture (figure 30 A) for collagen I ($2.3 \mu\text{g}/\text{mg}$), fibrin glue ($2.3 \mu\text{g}/\text{mg}$) and starPEGh ($4.3 \mu\text{g}/\text{mg}$) materials ($p < 0.0005$ each). The initial GAG content at day 0

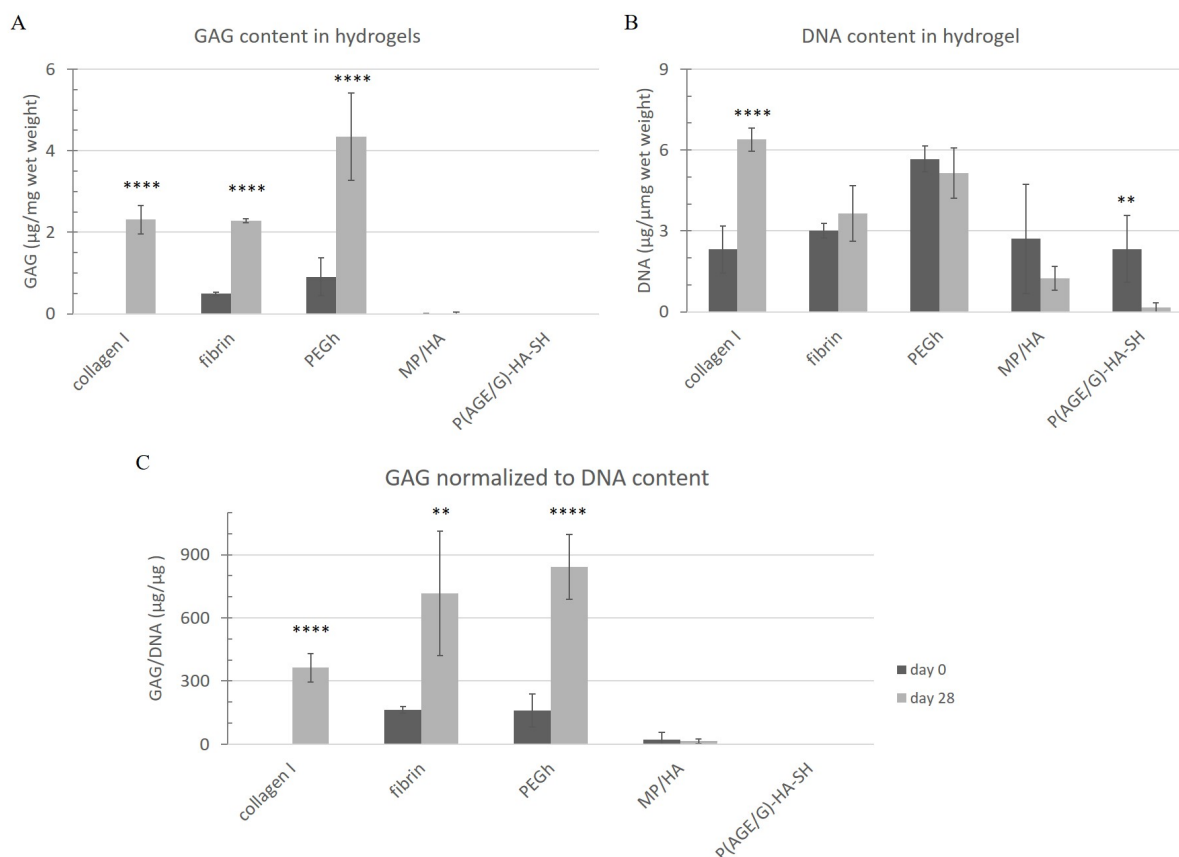


Figure 30 Quantification of proteoglycans (GAG) in chondrocyte loaded hydrogels at day 0 and after 28 days *ex vivo* culture. (A) GAG content in collagen I, fibrin glue, starPEGh, MP/HA and P(AGE/G)-HA-SH materials. (B) DNA content and (C) GAG normalized to DNA content. Total amount of GAG and GAG/DNA content increased in pChondrocyte loaded collagen I, fibrin glue and starPEGh between day 0 and day 28. Statistical significance was determined by student's T-test: * $p < 0.05$, ** $p < 0.005$, *** $p < 0.0005$, **** $p < 0.0001$ compared to day 0, ($n=3/\text{material}$).

in starPEGh is due to the hydrogel component heparin and thus limit the applicability of this quantitative analysis. Proteoglycan content in MP/HA and P(AGE/G)-HA-SH did not result in proteoglycan matrix production after *ex vivo* culture (figure 30 A).

GAG values normalized to DNA content (figure 30 C) displaying comparable trend to GAG content. GAG/DNA increased between day 0 and day 28 in collagen hydrogel by $363.5 \mu\text{g}/\mu\text{g}$ ($p < 0.0001$), in fibrin glue by $554.3 \mu\text{g}/\mu\text{g}$ ($p = 0.001$) and starPEGh by $682.1 \mu\text{g}/\mu\text{g}$ ($p < 0.0001$).

In collagen I gel total DNA content showed a three-fold increase ($p < 0.0005$) and in

firbin glue DNA content was elevated by 0.6 $\mu\text{g}/\text{mg}$ wet weight ($p=0.168$). In contrast, DNA content was reduced in P(AGE/G)–HA–SH from 2.3 $\mu\text{g}/\text{mg}$ at day 0 to 0.2 $\mu\text{g}/\text{mg}$ ($p=0.002$) after *ex vivo* culture. A similar trend was present for MP/HA with a reduction in DNA content of 1,5 $\mu\text{g}/\text{mg}$ ($p=0.114$). Number of cells in starPEGh remained almost stable at 5.1 $\mu\text{g}/\text{mg}$ compared to 5.6 $\mu\text{g}/\text{mg}$ at day 0 ($p=0.258$).

Comparing the IHC stainings and GAG quantification both methods result in a variation of cartilage ECM synthesis in dependency of hydrogel materials.

5.4.2.2 Gene expression analysis

RNA isolation of pChondrocyte loaded hydrogels resulted in 260/280 ratios between 1.5–1.8 indicating a tendency to contain residues of hydrogel. For the interpretation of PCR results this has to be kept in mind to avoid over interpretation of results.

Before performing PCR with gene of interests, the stability of housekeeping genes was tested by calculation of the target stability value, the so called M–value with CFX Software (BioRad). M–value represents the geometric mean of selected combinations of housekeeping genes. In heterogeneous samples (comparison of genes between different hydrogel materials) target stability is given for M–value that does not exceed a value of 1 [161]. In dependency of sampling method for the five hydrogel materials and freshly isolated pChondrocytes the M–values showed differences. A selected choice of housekeeping gene combinations resulted in the most stable M–values are summarized in table 21. In general, the lower the M–value the more stable are the combination of housekeeping genes.

When samples ($n=3/\text{hydrogel}$) were grouped for hydrogel materials (named sampling

Table 21 Calculation of target stability value referred as M–value of selected combinations of housekeeping genes combinations. All samples at three time points (day 0, day 13, day 28) were compared for each hydrogel material (no sampling) or sampled within one hydrogel material before calculation of M–value (sampling material). Mean of M–values are displayed including standard deviation.

gene combination	β –actin HMBS	YWHAZ GAPDH	β –actin GAPDH	β –actin GAPDH YWHAZ
M–value (no sampling)	0,7561 \pm 0.2714	1,2084 \pm 0.4239	1.8758 \pm 0.6310	1.7613 \pm 0.7433
M–value (sampling materials)	0,7354 \pm 0.2530	1,0450 \pm 0.3633	1.3564 \pm 0.4510	1.3876 \pm 0.5529

materials) the M–values were more stable compared to not sampling the three time points, day 0, day 13 and day 28, within one material (table 21). The combination of

β -actin & HMBS resulted in a stable M-value but the melt curve of HMBS resulted in two peaks at different temperatures indicating the formation of a HMBS side product which was confirmed when loaded on an agarose gel (data not shown).

Therefore, for calculation of normalization factor the housekeeping genes YWHAZ and GAPDH were used since they resulted in second most stable combination. The gene expressions were calculated by dividing RQ values of target genes by normalization factor for each sample. Normalized expression is calculated by dividing RQ values of samples with RQ values of freshly isolated pChondrocytes.

In figure 31 normalized gene expressions ($\Delta\Delta$ Ct values) are shown for all materials clustered for every gene of interest over time. Gene expression levels of all materials at day 0, day 13 and day 28 were normalized to respective values of freshly isolated pCZs. Efficiency of primer annealing was assumed equally between materials. No efficiencies of primer pairs are included in analysis because of the limited amount of isolated mRNA and thus not sufficient amounts of cDNA to perform efficiencies for all genes of interest. Collagen II, major collagen component in articular cartilage, shows reduced expression levels for all materials compared to day 0 (day 28, day 13 vs. day 0: $p < 0.0001$ each) with an up-regulation between day 13 ($\Delta\Delta$ Ct=4.4) and day 28 ($\Delta\Delta$ Ct=9.9) only for starPEGh material (day 28 vs day 13: $p = 0.777$).

Chondrogenic transcription factor SOX9 increases over culture time for MP/HA (day 0: $\Delta\Delta$ Ct=9.1 and day 28: $\Delta\Delta$ Ct=16.4, $p = 0.221$) and P(AGE/G)-HA-SH (day 0: $\Delta\Delta$ Ct=1.7 and day 28: $\Delta\Delta$ Ct=8.5, $p = 0.010$). Additionally, aggrecan levels were elevated at day 28 with $\Delta\Delta$ Ct=7.3 for MP/HA and $\Delta\Delta$ Ct=3.9 for P(AGE/G)-HA-SH compared to day 0. SOX9 and aggrecan levels in collagen I, fibrin glue and starPEGh decreased slightly between day 0 to day 13. From day 13 on expression remained constant accompanied by an increase for SOX9 displaying values of $\Delta\Delta$ Ct=1.3 at day 0, $\Delta\Delta$ Ct=1.2 at day 13 and $\Delta\Delta$ Ct=3.7 at day 28. In starPEGh material aggrecan gene expression level was elevated at day 28 ($\Delta\Delta$ Ct=1.6) compared to day 13 ($\Delta\Delta$ Ct=0.9).

The osteogenic transcription factor RunX2 and ECM protein collagen X were significantly up-regulated for MP/HA and P(AGE/G)-HA-SH at day 13 and day 28 compared to day 0. pChondrocytes embedded in MP/HA resulted in strong increase of $\Delta\Delta$ Ct=208.4 for RunX2 ($p < 0.0001$) and $\Delta\Delta$ Ct=62.7 for collagen X ($p < 0.0001$) at day 13. At day 28 both genes of interest remained significantly upregulated (RunX2: $\Delta\Delta$ Ct=265.8, $p < 0.0001$; collagen X: $\Delta\Delta$ Ct=46.9, $p < 0.0001$) compared to day 0 but at lower level compared to day 13. The hypertrophic differentiation of pChondrocyte in P(AGE/G)-HA-SH resulted in continuous increase over culture time with maximum normalized gene expression at day 28 for RunX2: $\Delta\Delta$ Ct=118.5, $p = 0.002$ and collagen X: $\Delta\Delta$ Ct=41.2, $p = 0.002$). In

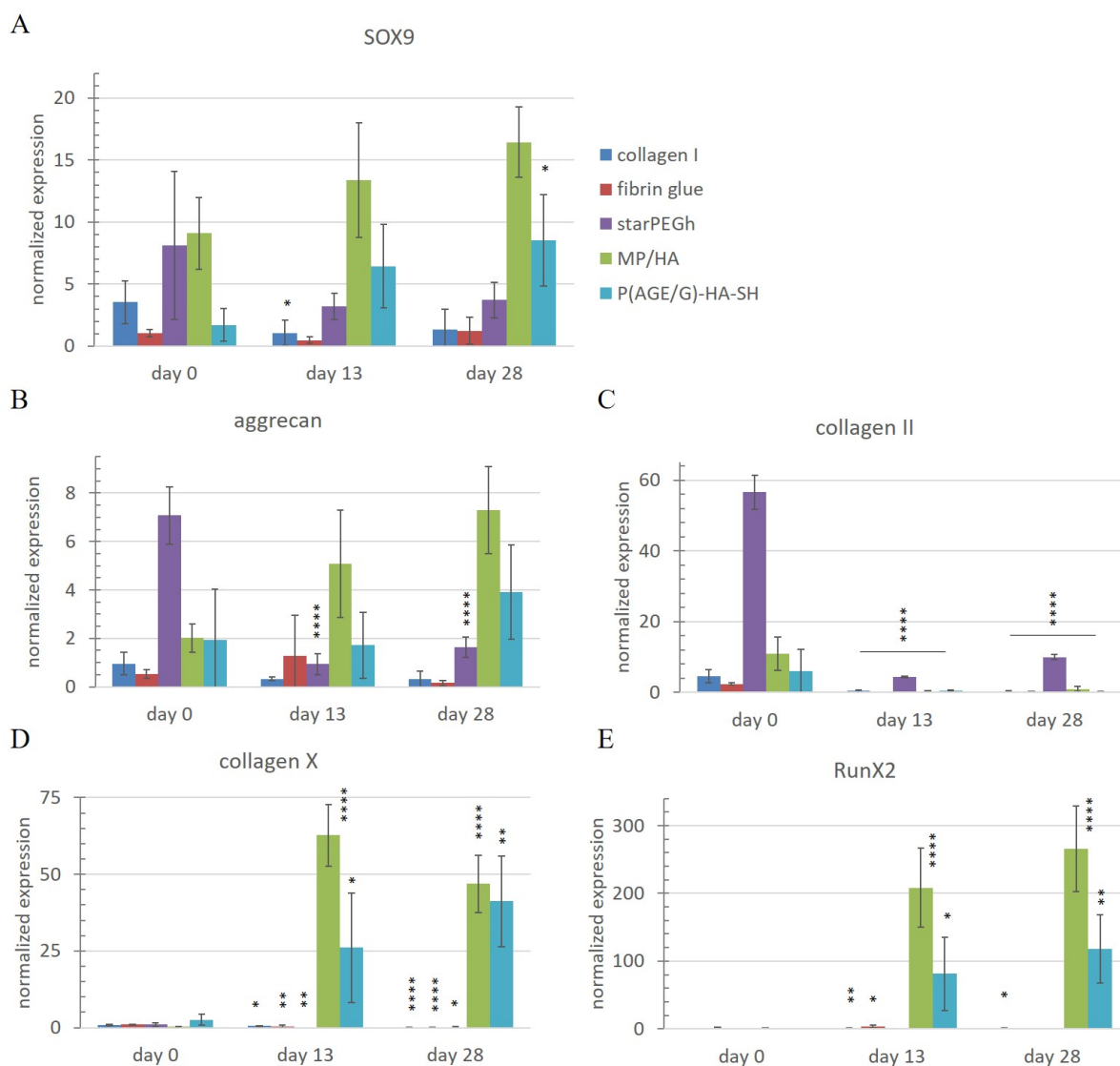


Figure 31 Gene expression analysis of chondrocyte loaded hydrogels culture 28 days in *ex vivo* system. Normalized gene expression ($\Delta\Delta C_t$ values) of (A) SOX9, (B) aggrecan (C) collagen II, (D) collagen X and (E) RunX2. C_t values are corrected for house keeping genes (GAPDH, YWHAZ) and normalized to gene expression of pChondrocytes. Collagen II gene expression remains upregulated over 28 days in starPEGh. MP/HA and P(AGE/G)-HA-SH resulted in SOX9 and aggrecan upregulation which is accompanied by elevation in collagen X and RunX2 levels over time. Cells embedded in collagen I and fibrin glue resulted in upregulation of cartilage genes (aggrecan, collagen II) which decrease with culture time. Collagen X and RunX2 were downregulated in starPEGh, collagen I and fibrin glue. Statistical significance was determined by one-way-ANOVA over time with Bonferroni post hoc test: * $p < 0.05$, ** $p < 0.005$, **** $p < 0.0001$ compared to day 0. Horizontal line means same significance of all materials at respective time point compared to day 0, ($n=3$ /material).

contrast, the expression of collagen X and RunX2 in collagen I, fibrin glue and starPEGh were only weak present. Normalized gene expression of RunX2 was down-regulated for

collagen I (day 13: $\Delta\Delta Ct=1.4$ $p=0.001$, day 28: $\Delta\Delta Ct=0.9$ $p=0.032$ compared to day 0), fibrin glue (day 13: $\Delta\Delta Ct=3.5$ $p=0.016$, day 28: $\Delta\Delta Ct=0.2$ $p=0.243$ compared to day 0) and starPEGh (day 13: $\Delta\Delta Ct=0.1$ $p=0.331$, day 28: $\Delta\Delta Ct=0.3$ $p=1.000$ compared to day 0). Same trend resulted for collagen X ($p<0.0001$ each compared to day 0).

5.4.2.3 Influence of peptide augmented starPEGh material on ECM synthesis

pChondrocyte loaded starPEGh hydrogel resulted in most promising results regarding cartilage ECM synthesis in the osteochondral defect model based on immuno-histological and -fluorescent stainings (figure 28 and 29), matrix production (figure 30) and gene expression analysis (figure 31). Therefore, an additional study was performed with peptide augmented starPEGh (2 M of each peptide: KLER, WYRGL, RGD and scrambled RGD). These peptides were chosen due to the fact that KLER and WYRGL are described in literature to elevate ECM production whereas RGD increases cell adhesion. Scrambled RGD represented a control peptide.

The augmentation of the peptides with starPEGh material did not harm pCZ viability. Live–dead vitality assay with pCZ loaded materials showed no differences, neither between materials groups nor over *ex vivo* culture in OCE at day 0 and day 28. Cells maintained CZ specific round morphology.

Influence of peptide modification on ECM formation in the cartilage defect model did not result in different IHC stainings for aggrecan. Aggrecan was present for all peptide modified hydrogels to an extent comparable to starPEGh without peptide functionalization. On the other hand, collagen II stainings revealed tendency of differences dependent on peptide augmentation. For scrambled RGD no collagen II was present in $n=3$ independent experiments. Intensity and collagen II positive area in the other groups differed between experimental repetitions. In two out of three OCE cultures collagen II synthesis indicated higher collagen II production in RGD and WYRGL group compared to KLER, without peptide and scrambled RGD. Results of this study were part of the Bachelor Thesis performed by Sebastian Naczenski [162].

5.4.3 Migration of cells in hydrogels: time lapse experiments

Hydrogel in which cells are embedded influence cell behavior in terms of migration velocity ($\mu\text{m}/\text{min}$) in cartilage media (as it is used in OCE cultures) shown in figure 32 B. To visualize experimental set up a schematic drawing is shown in figure 32 A. The diagram displays the mean velocity ($\mu\text{m}/\text{min}$) including standard deviation. Since there was no obvious difference in migration distance and velocity when chemo–attractant either 10 ng/ml TGF- β 1 or 10 % (v/v) FCS was supplemented in both compartments or left

out, the illustrated data refers to mean values ($n=10$ cells) without chemo-attractant. In the positive control, represented by pMSC embedded in collagen I hydrogel, cells migrated over an accumulated distance up to $300\ \mu\text{m}$ with a mean speed of $0.58\ \mu\text{m}/\text{min}$. pCZs

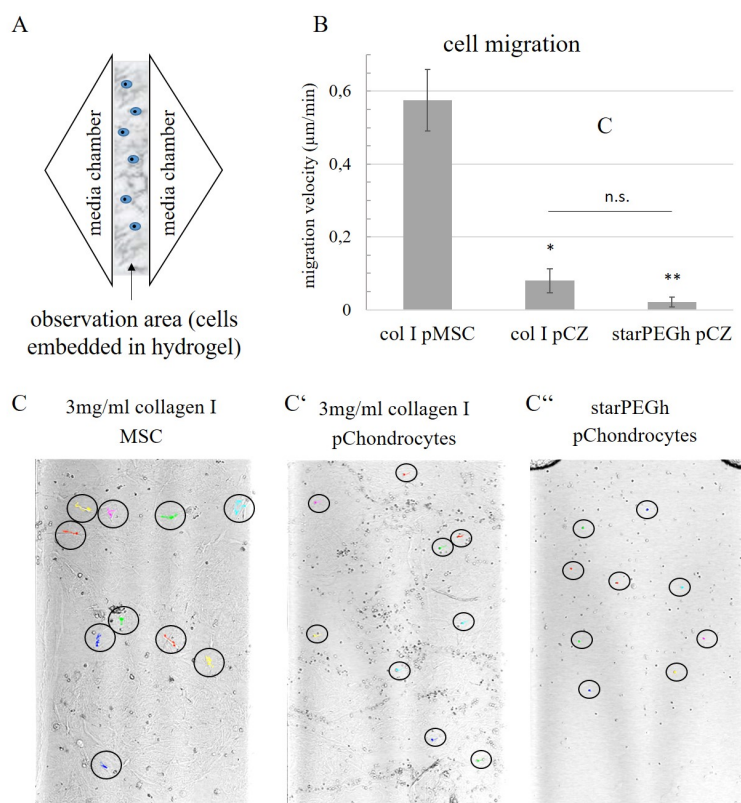


Figure 32 Cell migration in hydrogel materials displaying maximum migration distance and velocity as bar chart with mean values including standard deviation. (A) Schematic drawing of a μ -slide illustrating two media chambers separated by observation channel (containing hydrogel and cells). (B) Migration velocity of pCZs (pCZ) in hydrogel materials with pMSC in collagen I gel as positive control. (C–C'') microscopic images of observation area of hMSC embedded in collagen I and pCZs embedded in (C') collagen I or (C'') starPEGh material. Colored lines mark migration path of tracked cells (highlighted by black circle). pCZ migration velocity is decreased to less than 1/10 in collagen I hydrogel and further decreased in innovative hydrogels (1/29 in starPEGh) compared to values of pMSC in cartilage media without growth factor supplementation. Statistical significance was determined by student's T-test: n.s. no significance, * $p<0.05$, ** $p<0.005$, ($n=10$ cells).

showed a reduced mobility to migrate ($0.08\ \mu\text{m}/\text{min}$) compared to pMSC in collagen I hydrogel ($0.58\ \mu\text{m}/\text{min}$). Mean velocity of pMSC was ap. 7 fold higher than that of pCZs in collagen I hydrogel ($p=0.020$) and 29 fold higher than is starPEGh ($p=0.004$). pCZ movement in starPEGh resulted in a more pronounced decrease of $0.02\ \mu\text{m}/\text{min}$ compared to $0.06\ \mu\text{m}/\text{min}$ collagen I ($p=0.449$). In starPEGh pCZ indicated spinning instead of migration. The microscopic images of the observation channel in figure 32 C–C'' visualize the migration path of pMSC marked by colored lines within black circles. In samples with

pCZs embedded in hydrogels no lines were present due to absence of cell movement.

5.5 Influence of defect depth on cartilage regeneration

In this section (part III) the osteochondral defect model was modified in terms of standardized defects with defined geometry to simulate cartilage fissures in early stage of OA. Partial thickness and full thickness defects were left untreated or cell free collagen I hydrogel (3 mg/ml) was implanted to investigate the influence of cartilage defect depth on the cartilage regeneration.

5.5.1 Viability and cell migration in chondral defects

Live–dead staining did not reveal cell damage after drilling 1 mm chondral defects with ARTcut® at cartilage surface and in chondral defects (figure 33). The intact cell membranes of viable CZs in cartilage tissue were stained by Calcein–AM in green. In contrast to

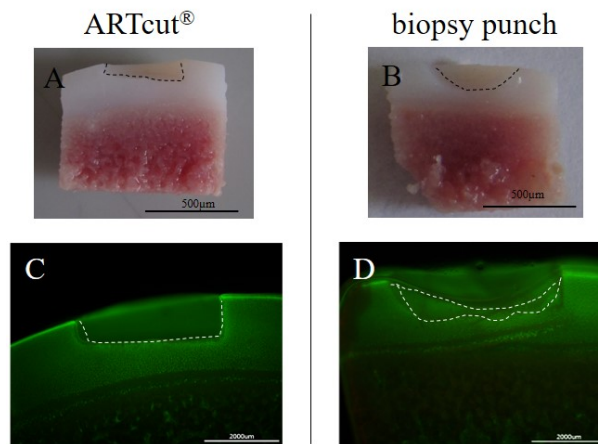


Figure 33 Creation of 1 mm chondral defects in osteochondral explant with ARTcut®. (A–B) Macroscopic images of explant cross section (OCE diameter: 8 mm) after defect creation (A) with ARTcut® and (B) biopsy punch (boundary of 4 mm defect is marked with white dotted line). Live–dead images did not show negative influence on cell viability due to (C) automated or (D) manual defect creation. (Scale bar (A–B) 500 µm, (C–D) 200 µm)

manual defect creation with biopsy punch the bottom of defect is characterized by flat boundary marked with black / white line in figure 33 which cannot be achieved manually with biopsy punch and sharp spoon. The chondral defects induced with ARTcut® were classified based on ICRS standard score (see table 1) as ICRS grade 2 since the defect size does not exceed more than 50 % of cartilage thickness. After 28 days *ex vivo* culture in

static culture system OCE with chondral defect, either left untreated or implantation of cell free collagen I hydrogel, recruitment of cells at defect boundary and cell migration into cell free collagen I hydrogel was observed in live–dead–staining (figure 34).

In the top view of untreated OCE a cell layer at the boundary of chondral defects is clearly shown (day 28). In the OCE treated with cell free collagen I (figure 34 D–D') cells are characterized by an elongated morphology. These results were in coincidence with findings of study in which cell free materials were implanted in full thickness cartilage defects (figure 23 B–C).

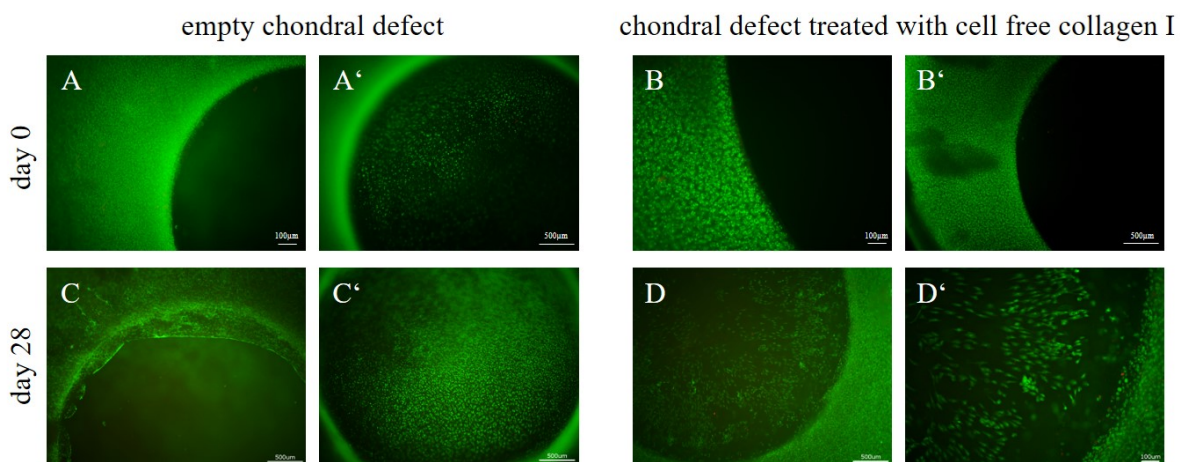


Figure 34 Live–dead images of osteochondral explants (OCE) with chondral defects (4 mm x 1 mm) either left untreated or with cell free collagen I hydrogel. (A–B) Top view focusing on the cartilage ring or (A'–B') on the bottom of chondral defects at day 0. (C–C') OCE with untreated chondral defect or (D–D') implanted cell free collagen I hydrogel after 28 days static culture. Migration of cells with elongated shape from cartilage into defects was seen. (Scale bar (A', B', C–D) 500 μm , (A, B, D') 100 μm)

To further analyze cell origin, cell morphology and cell phenotype of invaded cells histological analysis of cross sections (day 0 and day 28) followed. The chondral defects without treatment and cell free collagen I hydrogel did not result in cartilage neo tissue formation after 28 days *ex vivo* culture compared to day 0. Due to the low cell number that were recruited into defect side of chondral lesions seen in live–dead staining, only few single cells could be visualized in safranin–O staining (see figure 38 in supplementary data). Due to the low cell numbers in the defect present on histological slices, a further detailed phenotypic characterization of recruited cells was not possible.

6. Discussion

Regeneration of cartilage defects with mechanically long term stable hyaline tissue has been focusing long time in *in vivo* and *in vitro* studies. Till now there is no answer which cell type(s) like MSCs or CZs, material assisted or material free treatment strategy and which external stimuli are necessary to result in formation of hyaline cartilage tissue [163,164]. One reason are signaling pathways of cartilage during development and changes in regenerative capacity with age which have not been fully understood [165].

The establishment of a predictive *ex vivo* cartilage model was the focus of this thesis. This test system was based on OCE isolated from porcine femoral condyle to mimic the native physiological conditions in anatomy and culture conditions that allow to study clinical relevant cartilage defect scenarios.

The relevance of subchondral bone and necessity of tissue specific media supply in cartilage ECM characteristics during *ex vivo* culture of OCE is discussed in section 6.1. Cartilage critical defect size and regeneration is topic in section 6.2. Results of biomaterial screening in cartilage defects and the influence of defect geometry in terms of chondral vs. full thickness defects on cartilage regeneration in the OCE model is also discussed in this paragraph.

An outlook and future perspective for further applications and possible modifications of the osteochondral defect model are addressed in chapter 7.

6.1 Osteochondral explant model: Relevance of subchondral bone and tissue specific media supply

The decision to build up the cartilage test system on a two tissue model is accounted by lessons learned from clinical practice highlighting the role of subchondral bone in cartilage regeneration. In order to meet the requirements of bone and cartilage tissue during *ex vivo* culture, the static culture platform (chapter 6.1.2) was developed allowing tissue specific nutrient supply.

6.1.1 Role of subchondral bone in cartilage regeneration

Addressing the application of the test system as platform to better understand mechanisms involved in cartilage regeneration it is of interest to maintain communication between the two tissues bone and cartilage on cellular and protein level.

Cartilage and subchondral bone are directly connected via calcified layer and thus affecting each other in disease and regeneration. The importance of subchondral bone as a critical factor in cartilage repair became prominent in the 20th century when microfracture was introduced as treatment option for cartilage defects [48, 132]. Subchondral bone provides not only a cell source after cartilage damage but interferes and influences bio-mechanical properties and biological factors and thus cartilage metabolism. Based on this knowledge it is obvious that a predictive *ex vivo* model to study cartilage diseases and defect regeneration necessarily needs to consist of the complex two tissue model, comprising bone and cartilage. Moreover, CZs are naturally exposed to a gradient in nutrients and oxygen decreasing from the superficial layer to the deep zone [22, 23]. These physiological conditions are not addressed in cartilage only models as the deep zone of cartilage is also exposed to culture medium and oxygen resulting in a different gradient to *in vivo* situation. From this perspective, an osteochondral explant mimics the diffusion driven processes *in vivo* more closely than cartilage only explants.

The stimulative effect of the surrounding cartilage and bone tissue on cell recruitment but also matrix production in the cartilage defect model were proven in different experimental setups being discussed in more detail in section 6.2.2 and 6.2.4. Osteophyte formation that are described in literature to occur in subchondral bone as characteristic structural change during OA were not seen in the *ex vivo* model [166, 167].

De Vries-van Melle *et al.* first investigated an *ex vivo* culture of bovine osteochondral biopsies to characterize the explant. They published promising results regarding its feasibility in cartilage repair. Comparing the relative gene expression levels of cartilage matrix proteins collagen II and aggrecan, the expression levels in cartilage only explants with relative expression of 0.5 for collagen II and 1.0 for aggrecan decreased to a more pronounced extent than in cartilage of osteochondral explants with relative expression of 1.0 for collagen II and 3.0 for aggrecan after 4 weeks culture. These results highlight the importance of subchondral bone during *ex vivo* culture [134].

Based on these data it is obvious that separation of subchondral bone for preparation of cartilage only explants as simplified model do not adequately represent *in vivo* situation due to lack of bone. However, limitation of this model is the lack of tissue specific media supply that plays a critical role with regard to maintain cartilage ECM composition.

6.1.2 Tissue specific media is critical to maintain cartilage ECM during *ex vivo* culture

The osteochondral model issued a challenge to *ex vivo* culture due to the presence of the two different tissues - cartilage and bone. *In vitro* cultures of primary isolated cells require cell specific media to maintain cell phenotype during 2D expansion. For CZ culture the supplementation of cartilage media with ascorbic acid, dexamethasone, insulin, transferrin and selenic acid is crucial to maintain the cartilaginous matrix production and CZ functional properties [168, 169]. In contrast to CZs, osteogenic phenotype of bone cells requires β -glycerophosphate, ascorbic acid, dexamethasone and serum, providing growth factors to maintain phenotype [170, 171].

The solution allowing tissue specific media supply was the development of the custom made culture device (introduced in chapter 4.1.2). The main characteristic of the static culture platform developed for *ex vivo* culture of osteochondral explants are the separated media compartments. Following, the exchange of both media compartments is restricted to diffusional processes through calcified layer of the OCE. The importance of tissue specific media on viability and ECM composition and mechanical properties of OCE has been extensively characterized [152]. It was shown that tissue specific nutrient supply and separation of bone and cartilage media is crucial to maintain proteoglycan content in cartilage ECM of explants during culture. In this study three culture conditions – agarose embedding according to protocols of de-Vries van Melle *et al.*, tissue specific media or cartilage media in both compartments of the static culture device - were compared regarding viability and ECM characteristics [134]. Only in the set-up with cartilage media without TGF- β supplementation in the upper compartment and osteogenic media for subchondral bone cartilage degeneration was delayed and inhibited for a period of 8 weeks whereas decrease in GAGs was observed from day 14 on when the OCE was embedded in agarose (day 14: 31 %, day 28: 60 % GAG loss) or cultured in culture device with cartilage media in both compartments (day 14, 28: 23 % GAG loss). The samples differed only in the amount of proteoglycans but not in DNA and collagen content or metabolic activity of cartilage. Following the restriction of bone-cartilage crosstalk to natural barrier, the calcified layer, and no longer via the culture media lead to a less pronounced ECM degradation. But the separation of both compartments alone is not sufficient in this two-tissue explant model. If subchondral bone is not supplied with tissue specified nutrients a loss in cartilage GAG content was the consequence but not for samples cultured with tissue specific media [152]. These results lead to the conclusion that the decisive point to improve the *ex vivo* culture of osteochondral explants even over long term up to 8 weeks is the separated and tissue specific media.

So far, this characteristic of the static culture device is unique for culture of osteochondral explants and mimics native situation within the knee more closely than other cartilage and osteochondral cultures. The separated and sealed compartments allow for better control during culture in terms of tissue specific nutrient supply, media supplementation of stimulative factors and studying release of growth factors and proteins in supernatant that can be included in further experiments. One possible application of the static culture platform would be the optimization of culture media. Since there is no comparable culture device published or commercially available continuative studies have to be done for better understanding what are the mechanisms inducing cartilage degeneration and also address cross talk of cartilage and bone in more detail.

Proteoglycan loss after 8-10 weeks *ex vivo* culture from 330 $\mu\text{g}/\text{mg}$ at day 0 to 250 $\mu\text{g}/\text{mg}$ dry weight at day 56 may display a symptom in early cartilage degeneration. Cartilage degeneration is also marked by loss in collagen content which was not seen in our model during 84 days long term culture. The stable amount of collagen in OCE did not indicate severe matrix degradation as it occurs in OA [172].

Furthermore, the correlation of cartilage proteoglycan loss and decrease in mechanical properties after 8 weeks *ex vivo* was also demonstrated in the OCE model [152]. Due to absence of mechanical triggers the cartilage matrix homeostasis is not balanced resulting in matrix degradation and thinning. The correlation of reduced GAG content and decrease in mechanical properties has been characterized by many groups [173,174]. In rat experiments the thinning of articular cartilage was significant compared to continuous passive motion [175]. The absence of mechanical loading of the osteochondral model is one limitation. On cellular level many groups demonstrated the dependency of CZ metabolism and mechanical stimulation *in vitro* [112,176,177]. Possibilities to overcome this issue are topic in chapter 7.2.2.

Metabolic activity and viability of subchondral bone decreased after 4 weeks static culture shown by less intense MTT staining compared to day 0. The viability of subchondral bone after OCE isolation is principally dominated by cells of bone marrow hosted in the inter trabecula space. The bone cells (osteoblasts, osteoclasts, osteocytes) residing in the trabecula of subchondral bone make only a few percentage of the total cells in the subchondral bone being responsible for the bone remodeling [136]. With a porosity of ap. 63 % and bone volume of 47 mm^3 bone cells are most likely not visible in the MTT staining.

A common determination of cell viability from pathologists is to distinguish life and dead cells by the appearance of cell nuclei in hematoxylin staining. Fragmented cell

nuclei are a sign for dead cells whereas living cells are characterized by their ellipsoidal to round shape. A detailed look on bone cells in the subchondral bone of the OCE did not indicate changes in morphology and thus presence of dead bone cells (characterized by fragmented cell nuclei) after *ex vivo* culture (figure 14). Focusing on bone marrow cells in the inter trabecula space the amount of cells showed tendency to decrease over time. Additionally, the bone remodeling in terms of deposition of mineralized matrix was investigated by calcein-AM labeling OCE (see supplementary data figure 35). The images show incorporation of calcein in subchondral bone synthesized between day 28-42 and day 42-56. Following, the subchondral bone is metabolic active and cells are remodelling the matrix even during *ex vivo* long-term culture.

6.1.3 Bioreactor for dynamic culture of explants

Bioreactors are culture devices to overcome limitations due to diffusional problems of nutrients in TE products by active and homogenous perfusion in a closed circulating system [178]. The micro-structural characterization by SEM addressing porosity in subchondral bone lead to the development of a bioreactor system that allowed for controlled perfusion of bone part to enhance metabolic activity and thus positive affect cartilage matrix composition. The hypothesis to increase and maintain bone viability over longer time period could not be achieved with this prototype. Additional perfusion experiments to measure pressure of media flow through bone explains the presumption that the media did not perfuse the bone. This lead to the conclusion that the bone media in the bioreactor goes the way with least resistance which is around the periphery of the explant and circulated in the gap between flow chamber and explant. In order to force media flow through the explant the bone compartment need to be adjusted to tightly fix subchondral bone boundary in e.g. a silicon tube. If the subchondral bone boundary is sealed the only way of media flow will be through pores of the explant.

The possibility to perfused bovine cancellous bone with similar bone density of 65 % to porcine material was demonstrated by Kohles *et al.* [179]. Kleinhans *et al.* demonstrated in a computational modeling of a perfusion bioreactor system that the numbers of media streamlines through a porous bone scaffolds is reduced to a minimum if the boundaries are not sealed [153]. Following, a re-design similar to the perfusion system of Kleinhans *et al.* would overcome the diffusion problem with the OCE prototype bioreactor. On the other side, the redesign of bioreactor means a sophisticated technical challenge that also requires more complex software for control.

Moreover, the sample numbers that can be run in parallel in bioreactor systems is limited and thus decreases the throughput compared to static culture device. Additional to

the discussed limitation of the prototype bioreactor, evaporation issues in the cartilage compartment and decrease in controllability of culture conditions lead to the decision not to investigate the issue further in the light of this thesis. Considering the outcome in case perfusion issue would be improved, the effort and support to re-design the bioreactor prototype was valued to be too vague.

6.2 *Ex vivo* evaluation of cartilage regeneration in the osteochondral defect model

The establishment of the *ex vivo* osteochondral defect model investigated in the first part of this thesis represents a tool to address clinically relevant questions by testing novel cartilage implant materials and developing new treatment approaches *ex vivo*. Creation of full thickness cartilage defects following clinical standard with a biopsy punch and subsequent removal of residual cartilage at calcified layer (chapter 6.2.1) opened the possibility to screen novel hydrogel materials in critical sized defects (chapter 6.2.3). For deeper insight on how defect depth influences cartilage repair standardized 4 mm chondral defects were created with the help of custom developed wounding machine ARTcut[®] (chapter 6.2.4).

6.2.1 Definition of *ex vivo* critical size diameter in osteochondral defect model

First application of the *ex vivo* osteochondral cartilage defect model was the definition of the *ex vivo* critical size diameter to exclude spontaneous intrinsic self repair in subsequent material testings. Based on histological stainings cartilage defect with 4 mm in diameter was defined in this thesis as critical size diameter.

Defects exceeding 50 % of OCE diameter as it was given for 6 mm defects decreased stability of left over cartilage. Maximum possible defect size that did not harm OCE in stability and viability was in this study was 4 mm. Due to the fact that this model will be used as platform to test innovative cartilage materials the smaller defect diameter of 1 mm and 2 mm are not further considered as critical size diameter, even if they also did not fully regenerate. One further reason to define *ex vivo* critical size defect to be 4 mm is the fact that this diameter allows to test bio-printed and even bi-layered hydrogel materials. Number of layers in width and height of printed materials are dependent on diameter and spacing of printed fibers. The larger the defect geometry the more layers and fibers can be printed to generate a hierarchical implant.

In literature critical size defect in göttinger minipigs is defined dependent on location size

but ranges in comparable lesion sizes of the 4 mm defects *ex vivo*. Chang *et al.* reported critical size defects in young miniature pigs damage more than 40 % of femoral condyle width or 4.5 mm full thickness defects [180]. Gotterbarm *et al.* defined full thickness and osteochondral defects with 6.3 mm to not spontaneous self repair [181]. In an adult pig critical size defects start from 6 mm [182].

The comparison of physiology in the reported animals and the OCE model explains the smaller defect diameters that do not spontaneous self repair since it represents a simplified model compared to native knee physiology. In humans and animals the knee capsule provides an additional and natural source of progenitor cells in the synovial fluid and synovial membrane but also the blood supply from subchondral bone that is not reflected in the OCE model. Another reason for no obvious differences in amount of neo-tissue formation can be the limited culture period of 28 days. Moreover, volume of matrix synthesis is dependent on the amount of cells recruited into defect side. Anyhow, if no cell recruitment takes place within first days of injury there will be no regeneration. Therefore an *ex vivo* culture period of 4 weeks is sufficient addressing the cellular response and healing process in early stage after injury.

OCE with cartilage defect did not show evidence of physical damage resulting from OCE isolation and defect creation. Viable and metabolic active cells in the tissue of the OCE are important to maintain ECM characteristics and tissue homeostasis. By safranin-O staining the feasibility of the model that allows migration of cells from the explant into defect side was shown. Based on the hypothesis that cells hosted in the OCE represent a natural source to induce, stimulate or recruit migration of cells into defect side the explant need to be able to provide the cells and allow cell-cell communication and cell migration. This characteristic will be further discussed in chapter 6.2.3 and 6.2.4.

Preservation of proteoglycans in cartilage tissue of OCE was proven by quantification of GAGs in the three cartilage zones with only minor differences between day 0 to day 28 when cultured with tissue specific media. The natural increase in proteoglycan content normalized to DNA from superficial over middle to deep zone in cartilage was shown not to vary significantly between day 0 and day 28. At day 28 GAG content was lowest in the superficial zone with 269 $\mu\text{g}/\mu\text{g}+\text{DNA}$, increased to 688 $\mu\text{g}/\mu\text{g} \text{DNA}$ in the middle zone and reached the maximum value of 1 425 $\mu\text{g}/\mu\text{g} \text{DNA}$ in the deep zone.

The release of GAGs into cartilage culture media showed a dependency on defect size and thus surface area of cartilage. Due to the fact that the GAG content quantified in cartilage ECM maintained at comparable levels after *ex vivo* culture and GAGs measured in supernatant outweighs the differences observed in cartilage matrix CZs in the OCE

constantly remodel the matrix. The reduced intense red staining in safranin-O of OCE superficial zone can be explained by loss of proteoglycans during drilling or decalcification or polymer embedding for histological processing rather than tissue degeneration because this phenomena was also seen in freshly isolated samples.

Pretzel *et al.* published similar observations on GAG leaching of bovine cartilage only explants into culture media over time of ap. 15 mg/g cartilage wet weight after 4 weeks [129].

6.2.2 Stimulative effect of osteochondral explant on cartilage matrix production

The OCE model represents a complex two-tissue model that stimulates hyaline cartilage matrix production of pCZs embedded in collagen I hydrogel and does not necessarily need supplementation of cartilage media with additional growth factors like TGF- β to stimulate cartilage matrix production.

A comparable experiment in which pCZs were embedded in collagen I hydrogel that was cultured in chondrogenic media without TGF- β under free swelling conditions demonstrates the stimulative effect of OCE on CZ matrix synthesis. Hyaline neo-cartilage matrix production in terms of collagen VI, SOX9, collagen II and aggrecan was less present under free swelling conditions compared to immuno-histological and immuno-fluorescent stainings after implantation in full thickness defects of OCE (supplementary data figure 37). Comparing the synthesis of the hypertrophic related protein collagen X this was less stained in the hydrogel cultured in the *ex vivo* model with locally enhanced presence at the interface to subchondral bone (figure 37). Following, the presence of porcine explant material induced CZ matrix production and showed indications to suppress collagen X production without supplementation of cartilage media with TGF- β .

Comparing the histological findings of free swelling cell laden collagen I hydrogel and pCZ pellet culture the pellet culture showed an increase in collagen X expression and presence of RunX2 [33,34]. Expression of hypertrophic markers indicate the maturation or de-differentiation of CZs towards osteogenic lineage via endochondral ossification [34,35]. In native tissue hypertrophic CZs are located in the deeper zones close to calcified layer [33]. Advantage of surrounding tissue of explant cultures on cartilage matrix synthesis were investigated by Vinardell *et al.* and de Vries-van Melle *et al.* [130,183]. De Vries-van Melle *et al.* showed that differences in chondrogenesis of human bone marrow derived MSC encapsulated in alginate hydrogel were present when cultured under free swelling conditions in dependence of exogenous supplementation with TGF- β 1. They showed that the presence of the bovine osteochondral explant does not require additional TGF- β supplementation to induce MSC chondrogenesis when implanted in the model. Collagen II

and aggrecan expression in hMSC in both groups, free swelling in alginate with TGF- β 1 and osteochondral biopsy without TGF- β 1, did not show significant differences. Levels of GAG production and gene expression of aggrecan and collagen II were more elevated in hMSC embedded in alginate cultured in media containing 10 ng/ml TGF- β 1 than without TGF- β 1. Astonishingly, free swelling culture with TGF- β 1 supplementation or implanted in cartilage defects of bovine osteochondral explant resulted in comparable GAG/DNA content of ap. 11 $\mu\text{g}/\mu\text{g}$ DNA and ap. 12 $\mu\text{g}/\mu\text{g}$ DNA respectively that were ap. 10-fold higher than in alginate beads with ap. 1 $\mu\text{g}/\mu\text{g}$ cultured without TGF- β 1 [135]. In comparison to free swelling condition without TGF- β 1 the relative gene expression level were downregulated. From this study it can be concluded that the stimulative effect by presence of subchondral bone outweighs TGF- β supplementation in culture media [183]. These results are comparable to the outcome of the free swelling cultures presented in 5.3.2. During osteochondral explant culture CZs synthesize amongst others TGF- β being released into cartilage media. The presence of native cartilage matrix and the soluble factors released from the explant tissue into media have a beneficial effect on cartilage matrix production.

In contrast to the results of de Vries-van Melle *et al.* and our findings, Vinardell *et al.* compared an *in vitro* and *ex vivo* cartilage model and obtained different outcomes after 6 weeks of culture. They showed a higher matrix production (GAG, collagen in terms of hydroxyproline) and DNA content of pCZs embedded in 2 % agarose hydrogels (15 mio/ml) under free swelling conditions (GAG: ap. 1.70 % wet weight) than cultured in chondral disks (GAG: ap. 1.27 % wet weight) isolated from femoro patellar joint of 4 month young pigs in cartilage media containing 10 ng/ml TGF- β 3 after 42 days [130]. Similar trend was observed when MSCs were embedded in agarose gels. The reason for different outcomes may rise from the fact that they removed superficial and deep zone of cartilage disks before injecting cell-agarose mixture. The controversial results can be explained by the scaffold materials in which cells were embedded and differences in cellular response due to donor related reasons like age, disease, passage number, species, cell phenotype or cell numbers. On the other hand no differences in the study of Vinardell *et al.* may be a result due to the absence of subchondral bone in their model which was shown by de Vries-van Melle *et al.* to play an important role in mediating MSC chondrogenesis [135,183].

6.2.3 Hydrogel materials revealed differences in repair of full thickness cartilage defects

Material assisted treatment of full thickness defects resulted in a material dependent ECM deposition in terms of presence and distribution of hyaline cartilage matrix (aggrecan, collagen II).

In two studies (cell free and pCZ loaded materials) the three innovative hydrogel materials starPEGh, MP/HA and P(AGE/G)–HA–SH that were developed within the consortium of the EU project HydroZONES (see table 7 for details) and kindly provided by the partners were screened as cartilage implant in the *ex vivo* model against 3 mg/ml collagen I isolated from rat tail and commercially available fibrin glue.

The invasion of cells from the surrounding tissue of the OCE into cell free collagen I and fibrin glue indicated the preference of natural polymers collagen I and fibrin glue compared to the innovative but synthetic based polymers starPEGh, MP/HA and P(AGE/G)–HA–SH. A comparable trend that cells favor the two natural hydrogels was also seen in CZ loaded approach referring to the increase in DNA content for collagen and fibrin, stable amount in starPEGh and decrease in MP–HA and P(AGE–G)–HA–SH (figure 30 B).

Bio-compatible properties of implant materials are of importance to allow or stimulate cell in-growth and thus matrix synthesis. Materials not being attractive for cells pose the risk to fail due to missing matrix remodeling. *In vitro* and *in vivo* testings ectopically in mice of all HydroZONES materials within the project consortium were performed to evaluate effect of materials on differentiation of MSC and / or CZs (human, equine or porcine) under free swelling conditions stimulated with TGF- β 1 (10 ng/ml). From these studies no adverse effects or signs of cytotoxicity were reported.

In cell free approach the invasion of elongated and more fibroblast like cells into fibrin glue and collagen I hydrogel demonstrated the attractiveness of the natural polymers for cells that did not result in innovative materials. Instead, formation of cell multilayer on bottom of full thickness cartilage defects on calcified layer was characteristic for the three innovative synthetic based materials. Immuno-histological staining indicated the formation of mechanical inferior fibrous tissue marked by presence of collagen I that was indirect shown for proCollagen I as pre stage of collagen I formation and absence of collagen II in figure 24 and 25.

Colonialization of cells from surrounding tissue in commercially available cell free collagen I hydrogel (Arthro Kinetics) has been reported for animal studies in miniature pigs [103,104]. In contrast to the *ex vivo* results the immuno-histological stainings for collagen II were positive one year post-operative in the *in vivo* study with round CZ like cells but less

present compared to cell loaded collagen implant [104]. Based on this comparison of the *ex vivo* and *in vivo* results with cell free collagen I hydrogel the OCE defect model holds promise to predict success of implanted materials with comparable outcome to *in vivo* studies. Possible origin of the recruited cells is discussed in chapter 6.2.4.

The results of cell free testing in OCE demonstrated that hydrogel materials have to be seeded with cells prior to implantation to regenerate cartilage defects in the *ex vivo* cartilage defect model. Therefore, all materials were tested in a second study as CZ loaded implant materials in critical size defects of the OCE defect model.

In coincidence with cell free testing material dependent regenerative properties of CZ loaded hydrogels resulted after 4 weeks *ex vivo* culture. Articular cartilage matrix synthesis in terms of aggrecan, collagen II and collagen VI stainings was only present in the natural polymers collagen I and fibrin glue and starPEGh with the most pronounced increase in GAG between day 0 and day 28 content for starPEGh with 3.4 $\mu\text{g}/\text{mg}$ wet weight, followed by collagen I displaying an elevation of 2.3 $\mu\text{g}/\text{mg}$ wet weight and fibrin glue with 1.8 $\mu\text{g}/\text{mg}$ wet weight.

In MP/HA and P(AGE/G)–HA–SH no cartilagenous matrix synthesis was visible and thus quantified. The decrease in total DNA content in MP/HA and P(AGE/G)–HA–SH support these findings in the way that cell migrated out of the hydrogel due to insufficient nutrient supply or underwent apoptosis. In contrast, the strong 2.8 fold increase in collagen gel and the most likely stable amount for fibrin glue with 1.2 fold and 0.9 fold increase for starPEGh highlight the cell attractiveness of these polymers.

Cell specific differences in the outcome of cell loaded approach is excluded because pCZs embedded in all five hydrogel materials derived from same pool of tissue digests of pCZ isolation. From the cell free and pCZ loaded testing the collagen I performed best in terms of cartilage regenerative properties followed by fibrin glue and starPEGh.

Comparing collagen I hydrogel and fibrin glue with starPEGh material the location of synthesized ECM was different (figure 28 and 29). In these materials pCZs maintained chondrogenic phenotype marked by presence of SOX9, collagen II and aggrecan [8, 16]. Especially presence of SOX9 is of importance, since this chondrogenic transcription factor regulates aggrecan synthesis [18].

In contrast to collagen I gel and fibrin glue, histological stainings for collagen II and aggrecan were locally present in pericellular region in starPEGh. Additionally, tendency for hydrogel degradation during *ex vivo* culture of starPEGh CZs was visible marked by formation of holes in which ECM is accumulated. The degradation of this material takes place by enzymatic activity of MMPs that access MMP cleavable sides incorporated in starPEGh hydrogel. The implant geometry is maintained while the porosity increases

during remodeling.

Comparing gene expression results of the natural polymers collagen I and fibrin glue with starPEGh the normalized expression of pCZs in starPEGh exceeds the one in the natural polymers over culture time (figure 31). The absence of RunX2 and collagen X, two markers related to endochondral ossification, confirms results of histology that pCZs maintained chondrogenic phenotype in these materials. Collagen X was not upregulated on gene expression level but present on protein level in IF stainings. The increased collagen X positive staining of cells embedded in fibrin glue compared to collagen I may be interpreted as sign of fibrous neo-cartilage tissue formation. In figure 25 P the collagen X presence in collagen I hydrogel is localized at the side which the scaffold was in contact to underlying bone. Thus the expression may be stimulated by the direct interface to calcified layer in the OCE model.

The characterization of *in vitro* bio-compatibility of starPEGh showed the chondrogenic potential of starPEGh in terms of supporting chondrogenesis in MSC loaded materials and the positive effect of MMP-degradability on cell viability and distribution of synthesized matrix. Variation in hydrogel degradability by different amounts of MMP in starPEGh demonstrated that the distribution of collagen II and aggrecan was more even in 100 % MMP compared to 0 % and 50 % MMP cleaving sites. In these *in vitro* studies cartilage proteins were also predominantly localized in pericellular region of hydrogels. Once the materials were implanted subcutaneously in mice this could be overcome and matrix proteins were stained more homogeneously in hydrogel [155].

CZs seeded in MP/HA and P(AGE/G)-HA-SH may have experienced cell alteration during hydrogel embedding and UV light polymerization. The more than 200 fold increase in RunX2 on gene expression level accompanied by 50 fold elevation in collagen X gene expression. This finding indicates the differentiation towards mature and hypertrophic CZs [32, 33]. The reduced presence of SOX9 staining at day 0 compared to three other materials the UV cross-linking may have induced cell alteration. On the other hand, increase of chondrogenic gene expression for aggrecan and SOX9 compared to day 0 in MP/HA and P(AGE/G)-HA-SH can be explained by cell recovering from stress during hydrogel embedding. Furthermore, a mixed population of metabolic active, necrotic and senescent CZs can be present in MP/HA and P(AGE/G)-HA-SH hydrogels that may explain the high standard deviations in qRT gene expression analysis. In literature, hypertrophy of mature CZs is characterized with high levels of RunX2 and collagen X expressed by CZs in deep zone [33, 35].

Abbadessa *et al.* compared chondrogenic potential of equine MSC in MP/HA to fibrin glue with the result that this material showed chondrogenic potential. However, comparing the immuno-histological stainings of MP/HA and fibrin in the study of Abbadessa *et*

al. the cartilage matrix formation (safranin-O, collagen II, VI, aggrecan) was clearly reduced in MP/HA and locally expressed in pericellular region at day 42. GAG/DNA content in equine embedded CZs (20 mio/ml) after free swelling culture with TGF- β 1 supplementation in MP/HA gel was comparable after 42 days with values obtained in fibrin glue control. While at day 28 amount of GAG in MP/HA was higher with 27 $\mu\text{g}/\mu\text{g}$ DNA compared to 16 $\mu\text{g}/\mu\text{g}$ DNA, at day 42 GAG content in fibrin glue outweighed with 30 $\mu\text{g}/\mu\text{g}$ DNA the values in MP/HA hydrogel with 26 $\mu\text{g}/\mu\text{g}$ DNA [157]. Within HydroZONES consortium *in vitro* experiments of encapsulated hMSC in (PAGE/G)-HA-SH revealed viability and TGF- β mediated chondrogenesis resulted in cartilaginous ECM production *in vitro* (data not shown).

The differences of the *ex vivo* testings in the OCE model and the *in vitro* experiments are related to several factors. On the one hand, cells originating from different species e.g. equine, young pig or human and passage numbers are different compared to the testings presented in this thesis. While the *ex vivo* testing were all done with primary pCZs without expansion (passage 0) the *in vitro* characterization were performed with expanded CZs. Second major difference is the culture media. While the cartilage media of the OCE is not chemically modified with serum or growth factors to mimic physiological conditions the *in vitro* cultures were all supplemented with 10 ng/ml TGF- β 1. TGF- β has been extensively characterized and enhances cartilage matrix production. Recently, Bianchi *et al.* published the influence of human CZ passage (passage 0 vs. passage 2) and TGF- β 3 on cartilage matrix production. They showed a significant less amount of GAG/DNA and reduced collagen II staining in primary passage 0 CZ high density cultures and also when no TGF- β 3 was added to culture media [184].

Moreover, the stiffness of material and mesh width of hydrogel has an influence on diffusion of nutrients and waste products and on cell-hydrogel behavior. If the hydrogel material is a dense network that does not allow for diffusion of nutrients cells in the center die due to starvation.

In order to get a closer insight into cell material interaction in terms of migration characteristics time lapse experiments were performed and resulted in a dependency of cell migration speed in hydrogels on cell type and hydrogel material. On the one hand CZs showed a 10 fold decrease in migration velocity in collagen I hydrogel compared to pMSC. Additionally, the further reduction of 3 fold in CZ velocity in innovative hydrogel, represented by starPEGh, compared to collagen I when CZs were embedded explains the absence of cell infiltration during cell free material implantation. Reason for reduced migration speed are material properties indicating that the stiffness of innovative materials

slows down cell movement.

In an *in vitro* studies of Hesse *et al.* the influence of material properties of starPEGh on cell proliferation was demonstrated. starPEGh with 100 % MMP linker resulted in increase in hMSC proliferation compared to 50 % MMP linker [155].

From the point of a material scientist a dependency of material properties and cell migration and ECM synthesis was expected. The five materials differ in the polymers itself. Collagen I and fibrin glue are natural polymers whereas starPEGh, MP/HA and (PAGE/G)–HA–SH are made of synthetic polymer PEG or PG modified with natural components. Following, the material structure of the natural and synthetic materials differ in the way that fibrin and collagen I hydrogels display a fibrous network mimicking the native ECM of articular cartilage but lack in mechanical stability. Based on the cell free material testings, the natural hydrogels fibrin glue and collagen I showed a stimulating effect on cell recruitment and defect regeneration. In contrast, the synthetic materials PEG or PG itself are inert materials with tailorable mechanical properties but they are not degradable. The PEG or PG modification by incorporation of natural components as they are HA or MMP resulted in a partially (enzymatically) biodegradable hydrogel materials that opened the way for application as cartilage materials shown by HydroZONES collaboration partners for *in vitro* cultures [155,157].

These three innovative materials do not have a fibrous structure. They display a more inert structure with naturally derived components (HA) or incorporated MMP–cleaving sites to enhance biodegradability. Hydrogels with a mesh width smaller than the protein size of newly synthesized ECM hinders homogenous distributed throughout the hydrogels which was the case for starPEGh. In that case the starPEGh hydrogel first had to be degraded by the embedded CZs before cartilagenous ECM, rich in collagen II and aggrecan, was synthesized in pericellular holes. The absence of matrix production in CZs embedded in MP/HA and (PAGE/G)–HA–SH may be explained by material properties. pCZs seemed to be embedded in a hydrogel that was too stiff for remodeling and / or not porous enough to deliver cells with nutrients. This would explain the expression and protein synthesis of hypertrophic markers collagen X and RunX2. On the other hand, the HydroZONES material do not allow direct cell–cell contact once cells are embedded. They are encapsulated as isolated cells meaning that the hydrogels present a boundary between cells. Due to naturally derived low activity of pCZs they do not migrate in these materials. CZs in mature articular cartilage, in contrast to most other cells in the body, show low motility. In literature it is not fully understood which stimuli (growth factors, environment, cell signaling) induces CZ migration. Morales *et el.* reviewed literature available on CZ motility and presented in single CZ time lapse experiments that CZ have signs of movement

kinetics in presence of e.g. TGF- β , fibroblast growth factor and insulin-like growth factor-I [185]. Hopper *et al.* investigated human CZ migration of cartilage explants in co-culture with mono-nucleated cells. The results showed that CZ migration rate and number of migrating CZs after 3 h was 2.6 times higher and increased 9.7 times, respectively in direct contact with mono-nucleated cells. In a scratch assay wound closure rate of CZs co-cultured with mono-nucleated cells outweighed with 31.5 $\mu\text{m}/\text{h}$ the 14.1 $\mu\text{m}/\text{h}$ in CZ mono-culture [186]. There are hints for CZ motility which need to be further studied.

One option to increase cell attachment and matrix synthesis is the modification of implants with peptide sequences. First results of peptide augmented starPEGh with RGD, KLER, WYRGL did not show a stimulative effect on cartilage ECM production in that context. Adverse effects on pCZ viability were excluded by live-dead staining. In an *in vitro* and *in vivo* study of hMSC or pCZ loaded starPEGh materials RGD functionalization resulted in cell spreading with and elevated network formation [155]. In coincidence with our findings KLER and WYRGL did not enhance significantly collagen II production in cell loaded starPEGh material compared to RGD starPEGh. Regarding distribution of collagen II in CZ loaded starPEGh Hesse *et al.* reported of a more even distribution *in vitro* and *in vivo* for RGD modified starPEGh than the other materials modifications. Additionally, spreading of hMSC and pCZs were reported for RGD group [155].

Three major differences, TGF- β 1 vs. no growth factor supplementation in cell culture media, cell type as they were MSC or CZs and passage number (passage 0 vs. passage 1) are not comparable between above discussed studies of Hesse *et al.* and the OCE model. The overall higher matrix accumulation in the *in vitro* experiments are related to supplementation of culture media with TGF- β 1 that was not added in the cartilage media of the OCE model.

In contrast to Hesse *et al.* Villanueva *et al.* reported that RGD ligands (0.8 mM) in PEG hydrogels stimulates bovine CZ matrix synthesis only when mechanical loaded. Under free swelling conditions they did not see any changes in morphology [187].

6.2.4 Partial thickness defects: Repair and cell recruitment

Beside relation of defect regeneration and ECM deposition with materials defect geometry and depth influences formation of repair tissue.

To simulate focal lesions chondral defects were created by implementation of automated device ARTcut[®]. Main advantage of this device was depicted in macroscopic images comparing automated vs. manual defect creation with a defined and reproducible defect geometry after using ARTcut[®] (figure 34). Full thickness defects created with biopsy punch are classified based on outerbridge classification as defect grade ICRS 4. In contrast, chondral defects represent lesions that do not reach subchondral bone. Since the defect depth does not exceed 50 % of articular cartilage height in OCE they are grade ICRS 2 [41]. The difference in environment of chondral and osteochondral defects influenced defect regeneration.

The observation of cell invasion in live–dead staining into empty chondral defects and after treatment with cell free collagen I hydrogels after 28 days *ex vivo* culture lead to the assumption that cell migrated into defect side did not solely originate from subchondral bone.

Due to the findings that cells migrated into defect was only visible in viability staining but not in histological staining, the number of cells in chondral defects are little compared to full thickness defects. In full thickness cartilage defects subchondral bone is opened resulting in a direct communication between bone and defect area to recruit cells out of the bone into lesion. If only low numbers of cells are recruited into defect there is not enough matrix synthesized to visualize by histological stainings. In contrast, higher amount of spindle shaped and elongated cells and regenerative tissue were present in full thickness defects treated with cell free collagen I hydrogel or left untreated. However, the positive staining of proCollagen I indicates the formation of fibrous tissue instead of hyaline ECM. This experiment demonstrates that majority of recruited cells originate from subchondral bone tissue and minor cells numbers from cartilage which is in correlation with other studies. Shapiro *et al.* analyzed origin of cells in repair of full thickness defects in rabbits to come from subchondral bone. They found spindle shaped precursor cells in the defects from week 2 on that synthesized fibrous tissue [188]. The presence of cells in chondral only defects supports above discussed topic that CZs do migrate to some extend.

In the here reported study no immuno–histological characterization was possible to phenotypically characterize the origin of cells in chondral defects. Cells from subchondral bone are excluded due to the natural barrier presented by the intact deep zone and calcified layer that prevents communication between bone marrow and defect are. It is

unclear whether the cells came from the cartilage since CZs are low metabolic active. The localization of cells in chondral defects preferentially at the defect edges was also reported by Hunziker *et al.* in *in vivo* studies of partial thickness articular cartilage defects in adult rabbits and minipigs. They showed that cells in partial thickness articular cartilage defects are recruited from synovial membrane [189]. However, these cell population are not present in the OCE model.

In vitro culture of immature vs. mature bovine cartilage explants did result in formation of neo-cartilage around the explants with significant higher outgrowth from immature compared to mature samples. Bos *et al.* further investigated the origin of the migrated cells by culturing superficial zone and deep zone samples of immature bovine articular cartilage only with the result that cell outgrowth was present for deep zone with only minor cells in superficial zone explants. The higher amount of migrated cells in deep zone is comparable with results of full and partial thickness cartilage defects in our defect model. In agreement with the study of Bos *et al.* opening the deep zone in cartilage defects leads to an increase in cell invasion. By Ki67 immuno-histological staining they found proliferative CZs being present in the deep zone [190]. Additional to proliferation issue Tew *et al.* reported a second response mechanisms of CZs in cartilage explants after wounding, namely cell death (combination of necrosis and apoptosis) [191]. These experiments clearly demonstrate the proliferative and migratorial character of CZ sub-populations exclusively present in immature tissue.

6.2.5 Conclusion

Preservation of ECM components and viability but also physiological complexity of the porcine cartilage test system are of high relevance for predictive (pre-) clinical testings. The osteochondral defect model established in this thesis represents the articular cartilage in thickness with mean value of 1.5 mm, anatomy and hierarchy more closely than small animal studies.

A clinical relevant cartilage test system should allow to simulate defects that do not heal spontaneous and being comparable in middle size to large animal models e.g. horse, sheep, dog. This issue is overcome in the OCE model which showed its feasibility in screenings of scaffolds assisted treatments (chapter 6.2.3). Before a new drug or medical device is translated into clinics the safety and efficacy need to be evaluated in animal studies. Test systems can be an alternative to animal models and at least overcome some limitations and disadvantages of small animal models. Due to differences in tissue thickness the hierarchical structure but also nutrient and oxygen gradients are different in small animals compared to humans [22, 23]. Following, chondral defects which are discussed in chapter 6.2.4 are

hardly to realize in small animals. Moreover, the high costs accompanied for animal caring and facility are no longer issue for studies with the OCE model. On the other hand, one limitation of the OCE model are safety related material or compound testing due to lack of immune system.

Taken together the results of this thesis the osteochondral cartilage defect model positively stimulated chondrogenic phenotype and cartilage matrix synthesis of implanted pCZ loaded natural hydrogels. The presence of the OCE does not only stimulate cartilage tissue formation but also provides a natural cell source shown my recruitment of cells into cell free natural hydrogels in full thickness and chondral defects. The defect creation with the ARTcut[®] opens opportunity to induce standardized and reproducible defects varying in geometry and thus to simulate different defect scenarios. This osteochondral cartilage defect model can be used as predictive platform to further investigate cartilage healing, defect progression and treatment approaches under controlled conditions.

7. Outlook

The osteochondral defect model represents a platform to address novel strategies in cartilage regeneration. The model can be used as predictive tool in pre-clinical testing for a variety of applications ranging from cellular only treatment to material assisted treatments to adjustment of culture device on clinical demands. Moreover, the model can be used to validate human *ex vivo* models.

7.1 Clinical relevance: cartilage therapies and simulated OA

The *ex vivo* osteochondral (defect) model allows for further investigating the influence of defect geometry but also inflammatory conditions on cartilage metabolism and regeneration. Selected modifications as well as applications are summarized in the following paragraphs.

7.1.1 Defect geometry and treatment approaches

With regard to defect creation the ARTcut[®] allows to control further defect geometries like scratches and fibrillation or address trauma induced defects. Modifications include induction of multiple small diameter defects, roughening of surface and mechanical induced trauma. In a second approach, the influence of defect geometry can be studied to find alternative cell types e.g. CZs, arthritic CZs, MSC or synoviocytes for the regeneration may end up in a dependency of cell type and lesion depth. Furthermore, seeding strategies, namely layered seeding, homogenous or localized seeding and their impact in defect regeneration in dependence of defect severity and depth can be addressed in further studies.

Beside comparing different materials the question of which cell type/s is most promising in cartilage defect healing can be studied in more detail. The model allows to investigate different cell types like MSC, cartilage progenitor cells or synovial derived MSC and combinations thereof with different cell ratios. First results of IHC stainings indicate a stimulative effect of surrounding tissue of OCE on cartilage regeneration with pCZs loaded collagen I hydrogel. IHC staining for aggrecan showed the tendency to be more expressed in full thickness cartilage defects. On the other hand, collagen II was not influenced by defect depth and was expressed in full thickness and chondral defects.

Referring to the controversially reported outcome of using periosteal flap or commercially

available membranes like Collagen I–III membrane, Cartipatch, Bioseed C or NovoCart[®] 3D in ACI, the model presents a standardized test system to compare the different materials in terms of integration and hypertrophic tissue formation. Covering defects with different membranes and subsequent histological analysis may help to better characterize and understand formation of hyaline or fibrous neo-cartilage tissue.

7.1.2 Inflammatory conditions

In a different approach, the media could be supplemented with different cytokines found in synovial fluid of OA patients or introduce bacteria into cartilage compartment to investigate the influence of inflammatory milieu on cartilage ECM of explants or during defect regeneration. For histopathologic assessment OA is induced *in vivo* in small animals like mice, rat, rabbit or guinea pig and larger animals including sheep, dog, goat, horse or pig by genetic modification (knock-out). Furthermore OA can be induced surgically by joint destabilization including meniscectomy, anterior crucial ligament transection, chemically via intra-articular injection of pro-inflammatory or cartilage and CZ toxic substances or combinations thereof [148, 192].

Chemically induced OA can be adapted into our *ex vivo* model by supplementation of cartilage media with enzymes as they are collagenase or chondroitinase or inflammatory substances like lipopolysaccharide. An *ex vivo* OA model would allow to better understand disease onset and progression. But also the regeneration of cartilage lesions under OA conditions can be investigated in more detail. Here, the stimulative effect of pharmaceutical products to slow down degenerative processes are of interest.

Based on the knowledge that OA starts by alterations in subchondral bone, the separation of the static culture device presented in this thesis allows for further characterization of cartilage–bone cross talk for example after application of pharmaceuticals in bone compartment, respectively cartilage compartment. To sum up, the model offers opportunity to define markers and/or develop methods to identify OA in early stage that will allow to better understand cartilage turnover.

7.2 Influence of culture conditions: Low oxygen tension and cartilage biomechanics

In order to become a more functional model the *ex vivo* osteochondral test system can be adapted by culture under hypoxic conditions or implementation of biomechanical stimulation during period of culture.

7.2.1 Oxygen tension

Oxygen tension in articular cartilage varies between pigs, rabbits and humans and is characterized by decreasing gradient from superficial to deep zone. The oxygen tension in human knee in superficial zone accounts with 6 % and decreases to less than 2 % in the deep zone [23].

Ex vivo culture of the model under hypoxic conditions allows to study the effect of oxygen tension on cartilage regeneration but also on cell phenotype and ECM synthesis. Studies of MSC micro-pellets cultured *in vitro* under hypoxic conditions (1 % or 5 % O₂) promoted chondrogenic differentiation marked by increase in matrix production and proteoglycan synthesis and reduction in MSCs undergoing apoptosis and thus endochondral ossification [193, 194].

Preliminary results of pCZs embedded in collagen I hydrogel showed an improvement in hydrogel material stiffness with indication of better integration into defects when cultured under hypoxic conditions with 2 % oxygen compared to normoxic conditions in the osteochondral defect model.

7.2.2 Cartilage biomechanics

The hierarchical architecture of hyaline cartilage is the result of zonal variations in experiencing mechanical load influencing biochemical mechanisms. This results in depth dependent cellular arrangement, cell shape and ECM synthesis. CZs in articular cartilage are exposed to different strain levels as a result of transmission compression along collagen fibers from surface to deeper zones. Following, shear stress is highest in superficial zone with a Young's modulus of 460 ± 220 Pa that decreases to the deeper regions marked by lower modulus of 260 ± 140 Pa for middle and deep zone cells. The values result from atomic force microscopy measurements on articular CZs isolated from femoral condyles of skeletally mature pigs [195–197].

Applying mechanical forces is discussed as a critical factor for cartilage metabolism and thus to maintain cartilage ECM properties and prevent degenerative processes. Many

groups have shown the positive effect of mechanical stimulation on cartilage matrix synthesis [112, 176, 177]. The mechanical properties of TE cartilage scaffolds correlates with the ECM synthesis and is stimulated by mechanical stimulation [177, 198, 199]. Bleuel *et al.* found a positive effect on collagen fiber diameter under loading in CZ *in vitro* studies [111]. In a numerical model Khoshgoftar *et al.* showed that sliding indentation lead to parallel fiber alignment of TE cartilage in superficial zone [198]. Aisenbrey *et al.* published that mechanical loading can suppress hypertrophic differentiation of MSC encapsulated in hydrogel [200].

The biomechanics in the knee are a complex interplay of shear, tension, hydrostatic pressure and compression [113]. So far, there is only one device published that allows for induction of combined mechanical stimulation, namely shear and compression [114]. This multi-axial loading stimulates cartilage matrix synthesis of hMSC seeded scaffolds on protein and gene expression level that outweighs results if only compression or shear alone is applied. On the other hand, Gardner *et al.* showed that the multi-axial loading leads to endogenous production of TGF- β 1 that can drive MSC chondrogenesis [201]. In clinical practice Wilk *et al.* discussed the need for patient specific rehabilitation program after microfracture treatment dependent on the lesion, patient and surgical procedure [63]. To conclude, mechanical loading can have beneficial effect in cartilage tissue engineering but in case the loading regime exceeds physiological range and does not meet the needs of the specific cells, scaffold or tissue it can have an inhibitory effect on matrix synthesis, chondrogenesis and differentiation [200, 202–204]. The implementation of a mechanical loading device to the *ex vivo* osteochondral model would allow to investigate amongst others the mechanisms and molecular response in cartilage after overloading or the relation of cartilage ECM composition and properties and loading protocol. Moreover, it would be beneficial if the mechanical properties could be monitored as additional readout during *ex vivo* culture with the same loading device.

Bibliography

- [1] “Diagnosedaten der Krankenhäuser ab 2000 ICD10: M17 Gonarthrose [Arthrose des Kniegelenkes],” Robert Koch Institut, Primärquelle: Statistisches Bundesamt (In www.gbe-bund.de - Startseite > Krankheiten/ Gesundheitsprobleme > Krankheiten allgemein > Tabelle (gestaltbar): Diagnosedaten der Krankenhäuser nach Wohnsitz (ICD10-3-Steller, ab 2000)), 2016.
- [2] “Gesundheit in Deutschland, Reihe Gesundheitsberichterstattung des Bundes,” *Gemeinsam getragen von RKI und Destatis. RKI, Berlin ++ Gesundheitsbericht GBE, Robert Koch Institut (Primärquelle: Statistisches Bundesamt)*, 2015.
- [3] M. Tabenberg, *Robert Koch Institut, Gesundheitsberichterstattung des Bundes: Themenhefte/Schwerpunktberichte Heft 54: Arthrose*. Robert Koch Institut, 2013.
- [4] “Diagnosedaten der Krankenhäuser nach Behandlungsort (ICD10-4-steller, ab 2000),” Robert Koch Institut, Primärquelle: Statistisches Bundesamt (In www.gbe-bund.de - Startseite > Krankheiten/ Gesundheitsprobleme > Tabelle (gestaltbar): Diagnosedaten der Krankenhäuser nach Wohnsitz (ICD10-4-Steller, ab 2000)), 2016.
- [5] “Diagnosedaten der Krankenhäuser ab 2000 ICD10: S83.3 Riss des Kniegelenkknorpels,” Robert Koch Institut, Primärquelle: Statistisches Bundesamt (In www.gbe-bund.de - Startseite > Krankheiten/ Gesundheitsprobleme > Krankheiten allgemein > Tabelle (gestaltbar): Diagnosedaten der Krankenhäuser (Eckdaten der vollstationären Patienten und Patientinnen)), 2016.
- [6] W. Widuchowski, J. Widuchowski, and T. Trzaska, “Articular cartilage defects: study of 25,124 knee arthroscopies,” *The Knee*, vol. 14, no. 3, pp. 177–182, 2007.
- [7] V. Mow, E. Flatow, and G. Ateshian, *Biomechanics*, pp. 140–142. Amer Acad of Orthopaedic Surgeons, 2000.
- [8] N. P. Cohen, R. J. Foster, and V. C. Mow, “Composition and dynamics of articular cartilage: structure, function, and maintaining healthy state,” *J. Orthop. Sports Phys. Ther.*, vol. 28, no. 4, pp. 203–215, 1998.
- [9] K. Boettcher, S. Kienle, J. Nachtsheim, R. Burgkart, T. Hugel, and O. Lieleg, “The structure and mechanical properties of articular cartilage are highly resilient towards transient dehydration,” *Acta Biomater.*, vol. 29, pp. 180–187, 2016.

- [10] J. A. Buckwalter and H. J. Mankin, "Articular cartilage: tissue design and chondrocyte-matrix interactions," *Instr. Course Lect.*, vol. 47, pp. 477–486, 1998.
- [11] D. R. Eyre, "The collagens of articular cartilage," *Semin. Arthritis Rheum.*, vol. 21, no. 3 Suppl 2, pp. 2–11, 1991.
- [12] D. R. Eyre and J. J. Wu, "Collagen structure and cartilage matrix integrity," *J. Rheumatol. Suppl.*, vol. 43, pp. 82–5, 1995.
- [13] C. A. Poole, S. Ayad, and J. R. Schofield, "Chondrons from articular cartilage: I. immunolocalization of type VI collagen in the pericellular capsule of isolated canine tibial chondrons," *J. Cell Sci.*, vol. 90 (Pt 4), pp. 635–643, 1988.
- [14] C. R. Flannery, C. E. Hughes, B. L. Schumacher, D. Tudor, M. B. Aydelotte, K. E. Kuettner, and B. Caterson, "Articular cartilage superficial zone protein (szp) is homologous to megakaryocyte stimulating factor precursor and is a multifunctional proteoglycan with potential growth-promoting, cytoprotective, and lubricating properties in cartilage metabolism," *Biochem. Biophys. Res. Commun.*, vol. 254, no. 3, pp. 535–41, 1999.
- [15] H. Muir, "Proteoglycans of cartilage," *J. Clin. Pathol. Suppl.*, vol. 12, pp. 67–81, 1978.
- [16] H. Muir, "Proteoglycans as organizers of the intercellular matrix," *Biochem. Soc. Trans.*, vol. 11, no. 6, pp. 613–22, 1983.
- [17] C. Kiani, L. Chen, Y. J. Wu, A. J. Yee, and B. B. Yang, "Structure and function of aggrecan," *Cell Res.*, vol. 12, no. 1, pp. 19–32, 2002.
- [18] I. Sekiya, K. Tsuji, P. Koopman, H. Watanabe, Y. Yamada, K. Shinomiya, A. Nifuji, and M. Noda, "SOX9 enhances aggrecan gene promoter/enhancer activity and is up-regulated by retinoic acid in a cartilage-derived cell line, TC6," *J. Biol. Chem.*, vol. 275, no. 15, pp. 10738–10744, 2000.
- [19] A. Maroudas, "Balance between swelling pressure and collagen tension in normal and degenerate cartilage," *Nature*, vol. 260, no. 5554, pp. 808–809, 1976.
- [20] E. Hunziker, T. Quinn, and H.-J. Häuselmann, "Quantitative structural organization of normal adult human articular cartilage," *Osteoarthritis Cartilage*, vol. 10, no. 7, pp. 564–572, 2002.

- [21] W. Knudson and R. F. Loeser, "Cd44 and integrin matrix receptors participate in cartilage homeostasis," *Cell. Mol. Life Sci.*, vol. 59, no. 1, pp. 36–44, 2002.
- [22] D. Pfander and K. Gelse, "Hypoxia and osteoarthritis: how chondrocytes survive hypoxic environments," *Curr. Opin. Rheumatol.*, vol. 19, no. 5, pp. 457–462, 2007.
- [23] S. Zhou, Z. Cui, and J. P. G. Urban, "Factors influencing the oxygen concentration gradient from the synovial surface of articular cartilage to the cartilage–bone interface: A modeling study," *Arthritis Rheum.*, vol. 50, no. 12, pp. 3915–3924, 2004.
- [24] G. Js, M. Pi, W. R, F. Tp, and W. Rj, "Oxygen and reactive oxygen species in articular cartilage: modulators of ionic homeostasis.," *Pflugers Arch - Eur J Physiol*, vol. 455, no. 4, pp. 563–573, 2007.
- [25] H. Muir, P. Bullough, and A. Maroudas, "The distribution of collagen in human articular cartilage with some of its physiological implications," *J. Bone Joint Surg. Br.*, vol. 52, no. 3, pp. 554–63, 1970.
- [26] J. A. Buckwalter, V. C. Mow, and A. Ratcliffe, "Restoration of injured or degenerated articular cartilage," *J. Am. Acad. Orthop. Surg.*, vol. 2, no. 4, pp. 192–201, 1994.
- [27] G. Meachim and S. R. Sheffield, "Surface ultrastructure of mature adult human articular cartilage," *J. Bone Joint Surg. Br.*, vol. 51, no. 3, pp. 529–39, 1969.
- [28] E. B. Hunziker, M. Michel, and D. Studer, "Ultrastructure of adult human articular cartilage matrix after cryotechnical processing," *Microsc. Res. Tech.*, vol. 37, no. 4, pp. 271–84, 1997.
- [29] M. Venn and A. Maroudas, "Chemical composition and swelling of normal and osteoarthrotic femoral head cartilage. i. chemical composition," *Ann. Rheum. Dis.*, vol. 36, no. 2, pp. 121–9, 1977.
- [30] R. A. Stockwell, "The interrelationship of cell density and cartilage thickness in mammalian articular cartilage," *J. Anat.*, vol. 109, no. Pt 3, pp. 411–21, 1971.
- [31] R. S. Gilmore and A. J. Palfrey, "Chondrocyte distribution in the articular cartilage of human femoral condyles.," *J. Anat.*, vol. 157, pp. 23–31, 1988.
- [32] T. Aigner, E. Reichenberger, W. Bertling, T. Kirsch, H. Stoss, and K. von der Mark, "Type x collagen expression in osteoarthritic and rheumatoid articular cartilage," *Virchows Arch. B Cell Pathol. Incl. Mol. Pathol.*, vol. 63, no. 4, pp. 205–11, 1993.

- [33] K. von der Mark, T. Kirsch, A. Nerlich, A. Kuss, G. Weseloh, K. Glückert, and H. Stöss, "Type x collagen synthesis in human osteoarthritic cartilage. indication of chondrocyte hypertrophy," *Arthritis Rheum.*, vol. 35, no. 7, pp. 806–811, 1992.
- [34] S. Takeda, J. P. Bonnamy, M. J. Owen, P. Ducy, and G. Karsenty, "Continuous expression of *cbfa1* in nonhypertrophic chondrocytes uncovers its ability to induce hypertrophic chondrocyte differentiation and partially rescues *cbfa1*-deficient mice," *Genes Dev.*, vol. 15, no. 4, pp. 467–481, 2001.
- [35] M. Ding, Y. Lu, S. Abbassi, F. Li, X. Li, Y. Song, V. Geoffroy, H.-J. Im, and Q. Zheng, "Targeting *runx2* expression in hypertrophic chondrocytes impairs endochondral ossification during early skeletal development," *J. Cell. Physiol.*, vol. 227, no. 10, pp. 3446–3456, 2012.
- [36] K. Chen, T. K. H. Teh, S. Ravi, S. L. Toh, and J. C. H. Goh, "Osteochondral interface generation by rabbit bone marrow stromal cells and osteoblasts coculture," *Tissue Eng. Part A*, vol. 18, no. 17, pp. 1902–1911, 2012.
- [37] L. Hangody and P. Füles, "Autologous osteochondral mosaicplasty for the treatment of full-thickness defects of weight-bearing joints," *J. Bone Joint Surg. Am.*, vol. 85, pp. 25–32, 2003.
- [38] S. B. Abramson and M. Attur, "Developments in the scientific understanding of osteoarthritis," *Arthritis Res. Ther.*, vol. 11, no. 3, p. 227, 2009.
- [39] Y. Zhang and J. M. Jordan, "Epidemiology of osteoarthritis," *Clin. Geriatr. Med.*, vol. 26, no. 3, pp. 355–369, 2010.
- [40] D. T. Felson, R. C. Lawrence, P. A. Dieppe, R. Hirsch, C. G. Helmick, J. M. Jordan, R. S. Kington, N. E. Lane, M. C. Nevitt, Y. Zhang, M. Sowers, T. McAlindon, T. D. Spector, A. R. Poole, S. Z. Yanovski, G. Ateshian, L. Sharma, J. A. Buckwalter, K. D. Brandt, and J. F. Fries, "Osteoarthritis: new insights. part 1: the disease and its risk factors," *Ann. Intern. Med.*, vol. 133, no. 8, pp. 635–646, 2000.
- [41] M. Brittberg and C. S. Winalski, "Evaluation of cartilage injuries and repair," *J. Bone Joint Surg. Br.*, vol. 85, no. suppl 2, pp. 58–69, 2003.
- [42] L. A. Setton, D. M. Elliott, and V. C. Mow, "Altered mechanics of cartilage with osteoarthritis: Human osteoarthritis and an experimental model of joint degeneration," *Osteoarthritis Cartilage*, vol. 7, no. 1, pp. 2–14, 1999.

- [43] R. J. Lories and F. P. Luyten, "The bone-cartilage unit in osteoarthritis," *Nat. Rev. Rheumatol.*, vol. 7, pp. 43–49, dec 2010.
- [44] M. R. Shah, K. M. Kaplan, R. J. Meislin, and J. A. Bosco, "Articular cartilage restoration of the knee," *Bull NYU Hosp Jt Dis*, vol. 65, no. 1, pp. 51–60, 2007.
- [45] E. A. Makris, A. H. Gomoll, K. N. Malizos, J. C. Hu, and K. A. Athanasiou, "Repair and tissue engineering techniques for articular cartilage," *Nat. Rev. Rheumatol.*, vol. 11, no. 1, pp. 21–34, 2014.
- [46] B. J. Cole, C. Pascual-Garrido, and R. C. Grumet, "Surgical management of articular cartilage defects in the knee," *J. Bone Joint Surg. Am.*, vol. 91, no. 7, pp. 1778–1790, 2009.
- [47] J. R. Steadman, K. K. Briggs, J. J. Rodrigo, M. S. Kocher, T. J. Gill, and W. G. Rodkey, "Outcomes of microfracture for traumatic chondral defects of the knee: average 11-year follow-up," *Arthroscopy*, vol. 19, no. 5, pp. 477–484, 2003.
- [48] J. R. Steadman, W. G. Rodkey, S. B. Singleton, and K. K. Briggs, "Microfracture technique for full-thickness chondral defects: Technique and clinical results," *Operative Techniques in Orthopaedics*, vol. 7, no. 4, pp. 300–304, 1997.
- [49] J. R. Steadman, W. G. Rodkey, and J. J. Rodrigo, "Microfracture: surgical technique and rehabilitation to treat chondral defects," *Clin. Orthop.*, no. 391, pp. S362–369, 2001.
- [50] P. C. Kreuz, M. R. Steinwachs, C. Erggelet, S. J. Krause, G. Konrad, M. Uhl, and N. Südkamp, "Results after microfracture of full-thickness chondral defects in different compartments in the knee," *Osteoarthritis Cartilage*, vol. 14, no. 11, pp. 1119–1125, 2006.
- [51] G. Knutsen, L. Engebretsen, T. C. Ludvigsen, J. O. Drogset, T. Grontvedt, E. Solheim, T. Strand, S. Roberts, V. Isaksen, and O. Johansen, "Autologous chondrocyte implantation compared with microfracture in the knee. a randomized trial," *J. Bone Joint Surg. Am.*, vol. 86-A, no. 3, pp. 455–64, 2004.
- [52] M. Steinwachs, "New technique for cell-seeded collagen-matrix-supported autologous chondrocyte transplantation," *Arthroscopy*, vol. 25, no. 2, pp. 208–211, 2009.
- [53] C. Ossendorf, M. R. Steinwachs, P. C. Kreuz, G. Osterhoff, A. Lahm, P. P. Ducommun, and C. Erggelet, "Autologous chondrocyte implantation (ACI) for the treatment of large and complex cartilage lesions of the knee," *SMART*, vol. 3, p. 11, 2011.

- [54] C. R. Gooding, W. Bartlett, G. Bentley, J. A. Skinner, R. Carrington, and A. Flanagan, "A prospective, randomised study comparing two techniques of autologous chondrocyte implantation for osteochondral defects in the knee: Periosteum covered versus type I/III collagen covered," *The Knee*, vol. 13, no. 3, pp. 203–210, 2006.
- [55] H. S. McCarthy and S. Roberts, "A histological comparison of the repair tissue formed when using either chondrogide((r)) or periosteum during autologous chondrocyte implantation," *Osteoarthritis Cartilage*, vol. 21, no. 12, pp. 2048–57, 2013.
- [56] P. Cherubino, F. A. Grassi, P. Bulgheroni, and M. Ronga, "Autologous chondrocyte implantation using a bilayer collagen membrane: a preliminary report," *J. Orthop. Surg.*, vol. 11, no. 1, pp. 10–5, 2003.
- [57] W. Bartlett, J. A. Skinner, C. R. Gooding, R. W. Carrington, A. M. Flanagan, T. W. Briggs, and G. Bentley, "Autologous chondrocyte implantation versus matrix-induced autologous chondrocyte implantation for osteochondral defects of the knee: a prospective, randomised study," *J. Bone Joint Surg. Br.*, vol. 87, no. 5, pp. 640–5, 2005.
- [58] F. Zeifang, D. Oberle, C. Nierhoff, W. Richter, B. Moradi, and H. Schmitt, "Autologous chondrocyte implantation using the original periosteum-cover technique versus matrix-associated autologous chondrocyte implantation: a randomized clinical trial," *Am. J. Sports Med.*, vol. 38, no. 5, pp. 924–933, 2010.
- [59] R. Jeuken, A. Roth, R. Peters, C. van Donkelaar, J. Thies, L. van Rhijn, and P. Emans, "Polymers in cartilage defect repair of the knee: Current status and future prospects," *Polymers*, vol. 8, no. 6, p. 219, 2016.
- [60] A. E. Gross, N. Shasha, and P. Aubin, "Long-term followup of the use of fresh osteochondral allografts for posttraumatic knee defects," *Clin. Orthop.*, no. 435, pp. 79–87, 2005.
- [61] J. D. Wylie, M. K. Hartley, A. L. Kapron, S. K. Aoki, and T. G. Maak, "Failures and reoperations after matrix-assisted cartilage repair of the knee: A systematic review," *Arthroscopy*, vol. 32, no. 2, pp. 386–92, 2016.
- [62] C. E. Quatman, J. D. Harris, and T. E. Hewett, "Biomechanical outcomes of cartilage repair of the knee," *J. Knee Surg.*, vol. 25, no. 3, pp. 197–206, 2012.
- [63] K. E. Wilk, L. C. Macrina, and M. M. Reinold, "Rehabilitation following microfracture of the knee," *Cartilage*, vol. 1, no. 2, pp. 96–107, 2010.

- [64] M. Benjamin and J. R. Ralphs, "Biology of fibrocartilage cells," *Int. Rev. Cytol.*, vol. 233, pp. 1–45, 2004.
- [65] A. Barbero, S. Grogan, D. Schäfer, M. Heberer, P. Mainil-Varlet, and I. Martin, "Age related changes in human articular chondrocyte yield, proliferation and post-expansion chondrogenic capacity," *Osteoarthritis Cartilage*, vol. 12, no. 6, pp. 476–484, 2004.
- [66] M. M. J. Caron, P. J. Emans, M. M. E. Coolen, L. Voss, D. a. M. Surtel, A. Cremers, L. W. van Rhijn, and T. J. M. Welting, "Redifferentiation of dedifferentiated human articular chondrocytes: comparison of 2d and 3d cultures," *Osteoarthritis Cartilage*, vol. 20, no. 10, pp. 1170–1178, 2012.
- [67] E. M. Darling and K. A. Athanasiou, "Rapid phenotypic changes in passaged articular chondrocyte subpopulations," *J. Orthop. Res.*, vol. 23, no. 2, pp. 425–32, 2005.
- [68] M. Barandun, L. D. Iselin, F. Santini, M. Pansini, C. Scotti, D. Baumhoer, O. Bieri, U. Studler, D. Wirz, M. Haug, M. Jakob, D. J. Schaefer, I. Martin, and A. Barbero, "Generation and characterization of osteochondral grafts with human nasal chondrocytes," *J. Orthop. Res.*, vol. 33, no. 8, pp. 1111–1119, 2015.
- [69] A. G. Tay, J. Farhadi, R. Suetterlin, G. Pierer, M. Heberer, and I. Martin, "Cell yield, proliferation, and postexpansion differentiation capacity of human ear, nasal, and rib chondrocytes," *Tissue Eng.*, vol. 10, no. 5, pp. 762–770, 2004.
- [70] M. Mumme, A. Barbero, S. Miot, A. Wixmerten, S. Feliciano, F. Wolf, A. M. Asnaghi, D. Baumhoer, O. Bieri, M. Kretschmar, G. Pagenstert, M. Haug, D. J. Schaefer, I. Martin, and M. Jakob, "Nasal chondrocyte-based engineered autologous cartilage tissue for repair of articular cartilage defects: an observational first-in-human trial," *Lancet*, vol. 388, no. 10055, pp. 1985–1994, 2016.
- [71] C.-Y. Li, X.-Y. Wu, J.-B. Tong, X.-X. Yang, J.-L. Zhao, Q.-F. Zheng, G.-B. Zhao, and Z.-J. Ma, "Comparative analysis of human mesenchymal stem cells from bone marrow and adipose tissue under xeno-free conditions for cell therapy," *Stem Cell Res. Ther.*, vol. 6, p. 55, 2015.
- [72] A. Santhagunam, F. Dos Santos, C. Madeira, J. B. Salgueiro, and J. M. S. Cabral, "Isolation and ex vivo expansion of synovial mesenchymal stromal cells for cartilage repair," *Cytherapy*, vol. 16, no. 4, pp. 440–453, 2014.

- [73] R. Secunda, R. Vennila, A. M. Mohanashankar, M. Rajasundari, S. Jeswanth, and R. Surendran, "Isolation, expansion and characterisation of mesenchymal stem cells from human bone marrow, adipose tissue, umbilical cord blood and matrix: a comparative study," *Cytotechnology*, vol. 67, no. 5, pp. 793–807, 2015.
- [74] M. Dominici, K. Le Blanc, I. Mueller, I. Slaper-Cortenbach, F. Marini, D. Krause, R. Deans, A. Keating, D. Prockop, and E. Horwitz, "Minimal criteria for defining multipotent mesenchymal stromal cells. the international society for cellular therapy position statement," *Cytotherapy*, vol. 8, no. 4, pp. 315–317, 2006.
- [75] B. Johnstone, T. M. Hering, A. I. Caplan, V. M. Goldberg, and J. U. Yoo, "In vitro chondrogenesis of bone marrow-derived mesenchymal progenitor cells," *Exp. Cell. Res.*, vol. 238, no. 1, pp. 265–272, 1998.
- [76] M. J. Farrell, M. B. Fisher, A. H. Huang, J. I. Shin, K. M. Farrell, and R. L. Mauck, "Functional properties of bone marrow-derived msc-based engineered cartilage are unstable with very long-term in vitro culture," *J. Biomech.*, vol. 47, no. 9, pp. 2173–82, 2014.
- [77] S. Shirasawa, I. Sekiya, Y. Sakaguchi, K. Yagishita, S. Ichinose, and T. Muneta, "In vitro chondrogenesis of human synovium-derived mesenchymal stem cells: optimal condition and comparison with bone marrow-derived cells," *J. Cell. Biochem.*, vol. 97, no. 1, pp. 84–97, 2006.
- [78] T. Vinardell, E. J. Sheehy, C. T. Buckley, and D. J. Kelly, "A comparison of the functionality and in vivo phenotypic stability of cartilaginous tissues engineered from different stem cell sources," *Tissue Eng. Part A*, vol. 18, no. 11-12, pp. 1161–70, 2012.
- [79] M. M. Pleumeekers, L. Nimeskern, W. L. Koevoet, M. Karperien, K. S. Stok, and G. J. van Osch, "Cartilage regeneration in the head and neck area: Combination of ear or nasal chondrocytes and mesenchymal stem cells improves cartilage production," *Plast. Reconstr. Surg.*, vol. 136, no. 6, pp. 762e–74e, 2015.
- [80] C. Acharya, A. Adesida, P. Zajac, M. Mumme, J. Riesle, I. Martin, and A. Barbero, "Enhanced chondrocyte proliferation and mesenchymal stromal cells chondrogenesis in coculture pellets mediate improved cartilage formation," *J. Cell. Physiol.*, vol. 227, no. 1, pp. 88–97, 2012.

- [81] L. Wu, J. C. H. Leijten, N. Georgi, J. N. Post, C. A. van Blitterswijk, and M. Karperien, "Trophic effects of mesenchymal stem cells increase chondrocyte proliferation and matrix formation," *Tissue Eng. Part A*, vol. 17, no. 9, pp. 1425–1436, 2011.
- [82] S. Nuernberger, N. Cyran, C. Albrecht, H. Redl, V. Vecsei, and S. Marlovits, "The influence of scaffold architecture on chondrocyte distribution and behavior in matrix-associated chondrocyte transplantation grafts," *Biomaterials*, vol. 32, no. 4, pp. 1032–40, 2011.
- [83] Z. Izadifar, X. Chen, and W. Kulyk, "Strategic design and fabrication of engineered scaffolds for articular cartilage repair," *J. Funct. Biomater.*, vol. 3, no. 4, pp. 799–838, 2012.
- [84] J. T. Connelly, A. J. García, and M. E. Levenston, "Inhibition of in vitro chondrogenesis in RGD-modified three-dimensional alginate gels," *Biomaterials*, vol. 28, no. 6, pp. 1071–1083, 2007.
- [85] F. Fuertges and A. Abuchowski, "The clinical efficacy of poly(ethylene glycol)-modified proteins," *J. Controlled Release*, vol. 11, no. 1, pp. 139–148, 1990.
- [86] A. Watarai, L. Schirmer, S. Thones, U. Freudenberg, C. Werner, J. C. Simon, and U. Anderegg, "Tgfbeta functionalized starpeg-heparin hydrogels modulate human dermal fibroblast growth and differentiation," *Acta Biomater.*, vol. 25, pp. 65–75, 2015.
- [87] J. Zhu, "Bioactive modification of poly(ethylene glycol) hydrogels for tissue engineering," *Biomaterials*, vol. 31, no. 17, pp. 4639–4656, 2010.
- [88] M. P. Lutolf and J. A. Hubbell, "Synthetic biomaterials as instructive extracellular microenvironments for morphogenesis in tissue engineering," *Nat. Biotechnol.*, vol. 23, no. 1, pp. 47–55, 2005.
- [89] A. Zieris, K. Chwalek, S. Prokoph, K. R. Levental, P. B. Welzel, U. Freudenberg, and C. Werner, "Dual independent delivery of pro-angiogenic growth factors from starPEG-heparin hydrogels," *J. Controlled Release*, vol. 156, no. 1, pp. 28–36, 2011.
- [90] M. V. Tsurkan, K. R. Levental, U. Freudenberg, and C. Werner, "Enzymatically degradable heparin-polyethylene glycol gels with controlled mechanical properties," *Chem. Commun.*, vol. 46, no. 7, pp. 1141–1143, 2010.
- [91] Y. Park, M. P. Lutolf, J. A. Hubbell, E. B. Hunziker, and M. Wong, "Bovine primary chondrocyte culture in synthetic matrix metalloproteinase-sensitive poly(ethylene

- glycol)-based hydrogels as a scaffold for cartilage repair,” *Tissue Eng.*, vol. 10, no. 3, pp. 515–522, 2004.
- [92] S. J. Bryant and K. S. Anseth, “Controlling the spatial distribution of ecm components in degradable peg hydrogels for tissue engineering cartilage,” *J. Biomed. Mater. Res. A*, vol. 64, no. 1, pp. 70–9, 2003.
- [93] S. B. Anderson, C.-C. Lin, D. V. Kuntzler, and K. S. Anseth, “The performance of human mesenchymal stem cells encapsulated in cell-degradable polymer-peptide hydrogels,” *Biomaterials*, vol. 32, no. 14, pp. 3564–3574, 2011.
- [94] J. E. Frith, D. J. Menzies, A. R. Cameron, P. Ghosh, D. L. Whitehead, S. Gronthos, A. C. W. Zannettino, and J. J. Cooper-White, “Effects of bound versus soluble pentosan polysulphate in PEG/HA-based hydrogels tailored for intervertebral disc regeneration,” *Biomaterials*, vol. 35, no. 4, pp. 1150–1162, 2014.
- [95] N. J. Steinmetz and S. J. Bryant, “Chondroitin sulfate and dynamic loading alter chondrogenesis of human MSCs in PEG hydrogels,” *Biotechnol. Bioeng.*, vol. 109, no. 10, pp. 2671–2682, 2012.
- [96] T. Re’em, O. Tsur-Gang, and S. Cohen, “The effect of immobilized RGD peptide in macroporous alginate scaffolds on TGFbeta1-induced chondrogenesis of human mesenchymal stem cells,” *Biomaterials*, vol. 31, no. 26, pp. 6746–6755, 2010.
- [97] D. L. Elbert and J. A. Hubbell, “Conjugate addition reactions combined with free-radical cross-linking for the design of materials for tissue engineering,” *Biomacromolecules*, vol. 2, no. 2, pp. 430–441, 2001.
- [98] A. Sukarto, C. Yu, L. E. Flynn, and B. G. Amsden, “Co-delivery of adipose-derived stem cells and growth factor-loaded microspheres in RGD-grafted n-methacrylate glycol chitosan gels for focal chondral repair,” *Biomacromolecules*, vol. 13, no. 8, pp. 2490–2502, 2012.
- [99] D. Eyrich, F. Brandl, B. Appel, H. Wiese, G. Maier, M. Wenzel, R. Staudenmaier, A. Goepferich, and T. Blunk, “Long-term stable fibrin gels for cartilage engineering,” *Biomaterials*, vol. 28, no. 1, pp. 55–65, 2007.
- [100] R. L. Mauck, C. C.-B. Wang, E. S. Oswald, G. A. Ateshian, and C. T. Hung, “The role of cell seeding density and nutrient supply for articular cartilage tissue engineering with deformational loading,” *Osteoarthritis Cartilage*, vol. 11, no. 12, pp. 879–890, 2003.

- [101] A. L. Aulthouse, M. Beck, E. Griffey, J. Sanford, K. Arden, M. A. Machado, and W. A. Horton, "Expression of the human chondrocyte phenotype in vitro," *In Vitro Cell. Dev. Biol.*, vol. 25, no. 7, pp. 659–668, 1989.
- [102] T. Efe, C. Theisen, S. Fuchs-Winkelmann, T. Stein, A. Getgood, M. B. Rominger, J. R. Paletta, and M. D. Schofer, "Cell-free collagen type i matrix for repair of cartilage defects-clinical and magnetic resonance imaging results," *Knee Surg. Sports Traumatol. Arthrosc.*, vol. 20, no. 10, pp. 1915–22, 2012.
- [103] K. Gavenis, U. Schneider, U. Maus, T. Mumme, R. Muller-Rath, B. Schmidt-Rohlfing, and S. Andereya, "Cell-free repair of small cartilage defects in the goettinger minipig: which defect size is possible?," *Knee Surg. Sports Traumatol. Arthrosc.*, vol. 20, no. 11, pp. 2307–14, 2012.
- [104] U. Schneider, B. Schmidt-Rohlfing, K. Gavenis, U. Maus, R. Mueller-Rath, and S. Andereya, "A comparative study of 3 different cartilage repair techniques," *Knee Surg. Sports Traumatol. Arthrosc.*, vol. 19, no. 12, pp. 2145–2152, 2011.
- [105] S. Andereya, U. Maus, K. Gavenis, R. Müller-Rath, O. Miltner, T. Mumme, and U. Schneider, "[first clinical experiences with a novel 3d-collagen gel (CaReS) for the treatment of focal cartilage defects in the knee]," *Z. Orthop. Ihre Grenzgeb.*, vol. 144, no. 3, pp. 272–280, 2006.
- [106] K. F. Schüettler, J. Struwer, M. B. Rominger, P. Rexin, and T. Efe, "Repair of a chondral defect using a cell free scaffold in a young patient - a case report of successful scaffold transformation and colonisation," *BMC Surgery*, vol. 13, no. 1, p. 11, 2013.
- [107] M. Kesti, C. Eberhardt, G. Pagliccia, D. Kenkel, D. Grande, A. Boss, and M. Zenobi-Wong, "Bioprinting complex cartilaginous structures with clinically compliant biomaterials," *Adv. Funct. Mater.*, vol. 25, no. 48, pp. 7406–7417, 2015.
- [108] F. Zhao, P. Pathi, W. Grayson, Q. Xing, B. R. Locke, and T. Ma, "Effects of oxygen transport on 3-d human mesenchymal stem cell metabolic activity in perfusion and static cultures: experiments and mathematical model," *Biotechnol. Progr.*, vol. 21, no. 4, pp. 1269–1280, 2005.
- [109] J. Hansmann, F. Groeber, A. Kahlig, C. Kleinhans, and H. Walles, "Bioreactors in tissue engineering - principles, applications and commercial constraints," *Biotechnol. J.*, vol. 8, no. 3, pp. 298–307, 2013.

- [110] G. Vunjak-Novakovic, L. Meinel, G. Altman, and D. Kaplan, “Bioreactor cultivation of osteochondral grafts,” *Orthod. Craniofac. Res.*, vol. 8, no. 3, pp. 209–18, 2005.
- [111] J. Bleuel, F. Zaucke, G.-P. Brüggemann, J. Heilig, M.-L. Wolter, N. Hamann, S. Firner, and A. Niehoff, “Moderate cyclic tensile strain alters the assembly of cartilage extracellular matrix proteins in vitro,” *J. Biomech. Eng.*, vol. 137, no. 6, 2015.
- [112] L. M. Kock, K. Ito, and C. C. van Donkelaar, “Sliding indentation enhances collagen content and depth-dependent matrix distribution in tissue-engineered cartilage constructs,” *Tissue Eng. Part A*, vol. 19, no. 17, pp. 1949–1959, 2013.
- [113] S. Grad, D. Eglin, M. Alini, and M. J. Stoddart, “Physical stimulation of chondrogenic cells in vitro: a review,” *Clin. Orthop.*, vol. 469, no. 10, pp. 2764–2772, 2011.
- [114] O. Schätti, S. Grad, J. Goldhahn, G. Salzmann, Z. Li, M. Alini, and M. J. Stoddart, “A combination of shear and dynamic compression leads to mechanically induced chondrogenesis of human mesenchymal stem cells,” *Eur. Cell. Mater.*, vol. 22, pp. 214–225, 2011.
- [115] K. Shahin and P. M. Doran, “Shear and compression bioreactor for cartilage synthesis,” *Methods Mol. Biol.*, vol. 1340, pp. 221–233, 2015.
- [116] A. Cochis, S. Grad, M. J. Stoddart, S. Farè, L. Altomare, B. Azzimonti, M. Alini, and L. Rimondini, “Bioreactor mechanically guided 3d mesenchymal stem cell chondrogenesis using a biocompatible novel thermo-reversible methylcellulose-based hydrogel,” *Sci Rep.*, vol. 7, p. 45018, 2017.
- [117] A. Ratcliffe and L. E. Niklason, “Bioreactors and bioprocessing for tissue engineering,” *Ann. N.Y. Acad. Sci.*, vol. 961, pp. 210–215, 2002.
- [118] J. L. Cook, C. T. Hung, K. Kuroki, A. M. Stoker, C. R. Cook, F. M. Pfeiffer, S. L. Sherman, and J. P. Stannard, “Animal models of cartilage repair,” *Bone Joint. Res.*, vol. 3, no. 4, pp. 89–94, 2014.
- [119] M. B. Hurtig, M. D. Buschmann, L. A. Fortier, C. D. Hoemann, E. B. Hunziker, J. S. Jurvelin, P. Mainil-Varlet, C. W. McIlwraith, R. L. Sah, and R. A. Whiteside, “Preclinical studies for cartilage repair: Recommendations from the international cartilage repair society,” *Cartilage*, vol. 2, no. 2, pp. 137–52, 2011.

- [120] B. J. Ahern, J. Parvizi, R. Boston, and T. P. Schaer, "Preclinical animal models in single site cartilage defect testing: a systematic review," *Osteoarthritis Cartilage*, vol. 17, no. 6, pp. 705–713, 2009.
- [121] E. J. Sheehy, T. Mesallati, T. Vinardell, and D. J. Kelly, "Engineering cartilage or endochondral bone: a comparison of different naturally derived hydrogels," *Acta Biomater.*, vol. 13, pp. 245–53, 2015.
- [122] K. Benders, W. Boot, S. Cokelaere, P. Van Weeren, D. Gawlitta, H. Bergman, D. Saris, W. Dhert, and J. Malda, "Multipotent stromal cells outperform chondrocytes on cartilage-derived matrix scaffolds," *Cartilage*, vol. 5, no. 4, pp. 221–230, 2014.
- [123] M. Endres, K. Neumann, B. Zhou, U. Freymann, D. Pretzel, M. Stoffel, R. W. Kinne, and C. Kaps, "An ovine in vitro model for chondrocyte-based scaffold-assisted cartilage grafts," *J. Orthop. Surg. Res.*, vol. 7, p. 37, 2012.
- [124] S. Zamani, B. Hashemibeni, E. Esfandiari, A. Kabiri, H. Rabbani, and R. Abutorabi, "Assessment of TGF-3 on production of aggrecan by human articular chondrocytes in pellet culture system," *Adv Biomed Res.*, vol. 3, no. 1, p. 54, 2014.
- [125] J. A. Buckwalter, M. J. Glimcher, R. R. Cooper, and R. Recker, "Bone biology. i: Structure, blood supply, cells, matrix, and mineralization," *Instr. Course Lect.*, vol. 45, pp. 371–86, 1996.
- [126] J. A. Buckwalter, M. J. Glimcher, R. R. Cooper, and R. Recker, "Bone biology. ii: Formation, form, modeling, remodeling, and regulation of cell function," *Instr. Course Lect.*, vol. 45, pp. 387–99, 1996.
- [127] T. Mesallati, C. T. Buckley, and D. J. Kelly, "A comparison of self-assembly and hydrogel encapsulation as a means to engineer functional cartilaginous grafts using culture expanded chondrocytes," *Tissue Eng. Part C*, vol. 20, no. 1, pp. 52–63, 2014.
- [128] J. Wardale, L. Mullen, D. Howard, S. Ghose, and N. Rushton, "An ex vivo model using human osteoarthritic cartilage demonstrates the release of bioactive insulin-like growth factor-1 from a collagen-glycosaminoglycan scaffold," *Cell Biochem. Funct.*, vol. 33, no. 5, pp. 277–84, 2015.
- [129] D. Pretzel, S. Linss, H. Ahrem, M. Endres, C. Kaps, D. Klemm, and R. W. Kinne, "A novel in vitro bovine cartilage punch model for assessing the regeneration of focal cartilage defects with biocompatible bacterial nanocellulose," *Arthritis Res. Ther.*, vol. 15, no. 3, p. R59, 2013.

- [130] T. Vinardell, S. D. Thorpe, C. T. Buckley, and D. J. Kelly, "Chondrogenesis and integration of mesenchymal stem cells within an in vitro cartilage defect repair model," *Ann. Biomed. Eng.*, vol. 37, no. 12, pp. 2556–65, 2009.
- [131] T. R. Oegema, R. J. Carpenter, F. Hofmeister, and R. C. Thompson, "The interaction of the zone of calcified cartilage and subchondral bone in osteoarthritis," *Microsc. Res. Tech.*, vol. 37, no. 4, pp. 324–332, 1997.
- [132] D. D. Frisbie, J. T. Oxford, L. Southwood, G. W. Trotter, W. G. Rodkey, J. R. Steadman, J. L. Goodnight, and C. W. McIlwraith, "Early events in cartilage repair after subchondral bone microfracture," *Clin. Orthop. Relat. Res.*, no. 407, pp. 215–27, 2003.
- [133] D. D. Frisbie, M. W. Cross, and C. W. McIlwraith, "A comparative study of articular cartilage thickness in the stifle of animal species used in human pre-clinical studies compared to articular cartilage thickness in the human knee," *Vet. Comp. Orthop. Traumatol.*, vol. 19, no. 3, pp. 142–6, 2006.
- [134] M. L. de Vries-van Melle, E. W. Mandl, N. Kops, W. J. Koevoet, J. A. Verhaar, and G. J. van Osch, "An osteochondral culture model to study mechanisms involved in articular cartilage repair," *Tissue Eng. Part C*, vol. 18, no. 1, pp. 45–53, 2012.
- [135] M. L. de Vries-van Melle, R. Narcisi, N. Kops, W. J. Koevoet, P. K. Bos, J. M. Murphy, J. A. Verhaar, P. M. van der Kraan, and G. J. van Osch, "Chondrogenesis of mesenchymal stem cells in an osteochondral environment is mediated by the subchondral bone," *Tissue Eng. Part A*, vol. 20, no. 1-2, pp. 23–33, 2014.
- [136] R. S. Taichman, "Blood and bone: two tissues whose fates are intertwined to create the hematopoietic stem-cell niche," *Blood*, vol. 105, no. 7, pp. 2631–2639, 2005.
- [137] D. Lajeunesse and P. Reboul, "Subchondral bone in osteoarthritis: a biologic link with articular cartilage leading to abnormal remodeling," *Curr. Opin. Rheumatol.*, vol. 15, no. 5, pp. 628–633, 2003.
- [138] H. Madry, C. N. van Dijk, and M. Mueller-Gerbl, "The basic science of the subchondral bone," *Knee Surg. Sports Traumatol. Arthrosc.*, vol. 18, no. 4, pp. 419–433, 2010.
- [139] P. K. Bos, J. a. N. Verhaar, and G. J. V. M. van Osch, "Age-related differences in articular cartilage wound healing: a potential role for transforming growth factor beta1 in adult cartilage repair," *Adv. Exp. Med. Biol.*, vol. 585, pp. 297–309, 2006.

- [140] M. Lotz and R. F. Loeser, "Effects of aging on articular cartilage homeostasis," *Bone*, vol. 51, no. 2, pp. 241–248, 2012.
- [141] P. A. Guerne, F. Blanco, A. Kaelin, A. Desgeorges, and M. Lotz, "Growth factor responsiveness of human articular chondrocytes in aging and development," vol. 38, no. 7, pp. 960–968, 1995.
- [142] D. A. Rothenfluh, H. Bermudez, C. P. O'Neil, and J. A. Hubbell, "Biofunctional polymer nanoparticles for intra-articular targeting and retention in cartilage," *Nat. Mater.*, vol. 7, no. 3, pp. 248–254, 2008.
- [143] S. E. D'Souza, M. H. Ginsberg, and E. F. Plow, "Arginyl-glycyl-aspartic acid (RGD): a cell adhesion motif," *Trends Biochem. Sci.*, vol. 16, pp. 246–250, 1991.
- [144] C. N. Salinas and K. S. Anseth, "Decorin moieties tethered into PEG networks induce chondrogenesis of human mesenchymal stem cells," *Journal of Biomedical Materials Research Part A*, vol. 90, no. 2, pp. 456–464, 2009.
- [145] R. Tenni, M. Viola, F. Welser, P. Sini, C. Giudici, A. Rossi, and M. E. Tira, "Interaction of decorin with CNBr peptides from collagens I and II. evidence for multiple binding sites and essential lysyl residues in collagen," *Eur. J. Biochem.*, vol. 269, no. 5, pp. 1428–1437, 2002.
- [146] D. D. Frisbie, S. Morisset, C. P. Ho, W. G. Rodkey, J. R. Steadman, and C. W. McIlwraith, "Effects of calcified cartilage on healing of chondral defects treated with microfracture in horses," *Am. J. Sports Med.*, vol. 34, no. 11, pp. 1824–31, 2006.
- [147] P. Vodicka, K. Smetana, B. Dvoránková, T. Emerick, Y. Z. Xu, J. Ourednik, V. Ourednik, and J. Motlík, "The miniature pig as an animal model in biomedical research," *Ann. N.Y. Acad. Sci.*, vol. 1049, pp. 161–171, may 2005.
- [148] E. Teeple, G. D. Jay, K. A. Elsaid, and B. C. Fleming, "Animal models of osteoarthritis: Challenges of model selection and analysis," *AAPS J.*, vol. 15, no. 2, pp. 438–446, 2013.
- [149] S. Reinwald and D. Burr, "Review of nonprimate, large animal models for osteoporosis research," *J. Bone Miner. Res.*, vol. 23, no. 9, pp. 1353–1368, 2008.
- [150] C. C. Jiang, H. Chiang, C. J. Liao, Y. J. Lin, T. F. Kuo, C. S. Shieh, Y. Y. Huang, and R. S. Tuan, "Repair of porcine articular cartilage defect with a biphasic osteochondral composite," *J. Orthop. Res.*, vol. 25, no. 10, pp. 1277–90, 2007.

- [151] A. I. Vasara, M. M. Hyttinen, O. Pulliainen, M. J. Lammi, J. S. Jurvelin, L. Peterson, A. Lindahl, H. J. Helminen, and I. Kiviranta, “Immature porcine knee cartilage lesions show good healing with or without autologous chondrocyte transplantation,” *Osteoarthritis Cartilage*, vol. 14, no. 10, pp. 1066–74, 2006.
- [152] A. Schwab, A. Meeuwse, F. Ehlicke, J. Hansmann, L. Mulder, A. Smits, H. Walles, and L. Kock, “Ex vivo culture platform for assessment of cartilage repair treatment strategies,” *ALTEX*, vol. 34, pp. 267–277, 2017.
- [153] C. Kleinhans, R. R. Mohan, G. Vacun, T. Schwarz, B. Haller, Y. Sun, A. Kahlig, P. Kluger, A. Finne-Wistrand, H. Walles, and J. Hansmann, “A perfusion bioreactor system efficiently generates cell-loaded bone substitute materials for addressing critical size bone defects,” *Biotechnol. J.*, vol. 10, no. 11, pp. 1727–1738, 2015.
- [154] A. Rossi, A. Appelt-Menzel, S. Kurdyn, H. Walles, and F. Groeber, “Generation of a three-dimensional full thickness skin equivalent and automated wounding,” *J Vis Exp*, no. 96, 2015.
- [155] E. Hesse, U. Freudenberg, T. Niemietz, C. Greth, M. Weisser, S. Hagmann, M. Binner, C. Werner, and W. Richter, “Peptide-functionalized starPEG/heparin hydrogels direct mitogenicity, cell morphology and cartilage matrix distribution in vitro and in vivo,” *J. Tissue Eng. Regener. Med.*, 2017.
- [156] C. N. Salinas, “Photoinitiated thiol -acrylate polymerizations to tailor PEG microenvironments with peptide moieties to direct chondrogenic differentiation of hMSCs,” PhD Thesis, University of Colorado at Boulder, 2007.
- [157] A. Abbadessa, V. H. Mouser, M. M. Blokzijl, D. Gawlitta, W. J. Dhert, W. E. Hennink, J. Malda, and T. Vermonden, “A synthetic thermosensitive hydrogel for cartilage bioprinting and its biofunctionalization with polysaccharides,” *Biomacromolecules*, vol. 17, no. 6, pp. 2137–47, 2016.
- [158] S. Stichler, T. Jungst, M. Schamel, I. Zilkowski, M. Kuhlmann, T. Böck, T. Blunk, J. Teßmar, and J. Groll, “Thiol-ene clickable poly(glycidol) hydrogels for biofabrication,” *Ann. Biomed. Eng.*, pp. 1–13, 2016.
- [159] R. W. Farndale, C. A. Sayers, and A. J. Barrett, “A direct spectrophotometric microassay for sulfated glycosaminoglycans in cartilage cultures,” *Connect. Tissue Res.*, vol. 9, no. 4, pp. 247–8, 1982.

- [160] E. Aescht, S. Büchl-Zimmermann, A. Burmester, S. Dänhardt-Pfeiffer, C. Desel, C. Hamers, G. Jach, M. Kässens, J. Makovitzky, M. Mulisch, B. Nixdorf-Bergweiler, D. Pütz, B. Riedelsheimer, F. van den Boom, R. Wegerhoff, and U. Welsch, *Romeis Mikroskopische Technik*. Spektrum Akademischer Verlag, 18 ed., 2010.
- [161] K. J. Livak and T. D. Schmittgen, “Analysis of relative gene expression data using real-time quantitative PCR and the $2^{-(\Delta\Delta C_t)}$ method,” *Methods*, vol. 25, no. 4, pp. 402–408, 2001.
- [162] S. Naczenski, “Untersuchung modifizierter starPEG/Heparin Hydrogele im osteochondralen Testsystem,” Bachelor Thesis, Julius-Maximilians-University Würzburg, Department Tissue Engineering and Regenerative Medicine, 2016.
- [163] M. Brittberg, “Cellular and acellular approaches for cartilage repair: A philosophical analysis,” *Cartilage*, vol. 6, no. 2, pp. 4S–12S, 2015.
- [164] E. B. Hunziker, K. Lippuner, M. J. B. Keel, and N. Shintani, “An educational review of cartilage repair: precepts & practice—myths & misconceptions—progress & prospects,” *Osteoarthritis Cartilage*, vol. 23, no. 3, pp. 334–350, 2015.
- [165] C. Sanchez, A.-C. Bay-Jensen, T. Pap, M. Dvir-Ginzberg, H. Quasnicka, R. Barrett-Jolley, A. Mobasheri, and Y. Henrotin, “Chondrocyte secretome: a source of novel insights and exploratory biomarkers of osteoarthritis,” *Osteoarthritis Cartilage*, 2017.
- [166] M. B. Goldring and S. R. Goldring, “Osteoarthritis,” *J. Cell. Physiol.*, vol. 213, no. 3, pp. 626–634, 2007.
- [167] S. R. Goldring, “Role of bone in osteoarthritis pathogenesis,” *Med. Clin. North Am.*, vol. 93, no. 1, pp. 25–35, 2009.
- [168] A. G. Clark, A. L. Rohrbaugh, I. Otterness, and V. B. Kraus, “The effects of ascorbic acid on cartilage metabolism in guinea pig articular cartilage explants,” *Matrix Biol.*, vol. 21, no. 2, pp. 175–84, 2002.
- [169] L. Bian, A. M. Stoker, K. M. Marberry, G. A. Ateshian, J. L. Cook, and C. T. Hung, “Effects of dexamethasone on the functional properties of cartilage explants during long-term culture,” *Am. J. Sports Med.*, vol. 38, no. 1, pp. 78–85, 2010.
- [170] K. Urban, H. J. Hohling, B. Luttenberg, T. Szuwart, U. Plate, and U. Biomineralisation Research, “An in vitro study of osteoblast vitality influenced by the vitamins c and e,” *Head Face Med*, vol. 8, p. 25, 2012.

- [171] F. Langenbach and J. Handschel, "Effects of dexamethasone, ascorbic acid and beta-glycerophosphate on the osteogenic differentiation of stem cells in vitro," *Stem Cell Res. Ther.*, vol. 4, no. 5, p. 117, 2013.
- [172] A. Poole, M. Kobayashi, T. Yasuda, S. Lavery, F. Mwale, T. Kojima, T. Sakai, C. Wahl, S. El-Maadawy, G. Webb, E. Tchetina, and W. Wu, "Type II collagen degradation and its regulation in articular cartilage in osteoarthritis," *Ann. Rheum. Dis.*, vol. 61, no. Supplement 2, pp. ii78–ii81, 2002.
- [173] M. A. LeRoux, J. Arokoski, T. P. Vail, F. Guilak, M. M. Hyttinen, I. Kiviranta, and L. A. Setton, "Simultaneous changes in the mechanical properties, quantitative collagen organization, and proteoglycan concentration of articular cartilage following canine meniscectomy," *J. Orthop. Res.*, vol. 18, no. 3, pp. 383–392, 2000.
- [174] J. Mansour, *Biomechanics of cartilage. In Kinesiology: The Mechanics and Pathomechanics of Human Movement*. Wolters Kluwer Health, 2nd ed., 2013.
- [175] J. Sakamoto, T. Origuchi, M. Okita, J. Nakano, K. Kato, T. Yoshimura, S.-i. Izumi, T. Komori, H. Nakamura, H. Ida, A. Kawakami, and K. Eguchi, "Immobilization-induced cartilage degeneration mediated through expression of hypoxia-inducible factor-1alpha, vascular endothelial growth factor, and chondromodulin-i," *Connect. Tissue Res.*, vol. 50, no. 1, pp. 37–45, 2009.
- [176] F. Guilak, B. Fermor, F. J. Keefe, V. B. Kraus, S. A. Olson, D. S. Pisetsky, L. A. Setton, and J. B. Weinberg, "The role of biomechanics and inflammation in cartilage injury and repair," *Clin. Orthop.*, no. 423, pp. 17–26, 2004.
- [177] T. Vinardell, R. Rolfe, C. Buckley, E. Meyer, M. Ahearne, P. Murphy, and D. Kelly, "Hydrostatic pressure acts to stabilise a chondrogenic phenotype in porcine joint tissue derived stem cells," *Eur. Cell. Mater.*, vol. 23, pp. 121–134, 2012.
- [178] E. C. Novosel, C. Kleinans, and P. J. Kluger, "Vascularization is the key challenge in tissue engineering," *Adv. Drug Delivery Rev.*, vol. 63, no. 4, pp. 300–311, 2011.
- [179] S. S. Kohles, J. B. Roberts, M. L. Upton, C. G. Wilson, L. J. Bonassar, and A. L. Schlichting, "Direct perfusion measurements of cancellous bone anisotropic permeability," *J. Biomech.*, vol. 34, no. 9, pp. 1197–1202, 2001.
- [180] C.-H. Chang, Y.-M. Hsu, C.-N. Hsiao, T.-F. Kuo, and M.-H. Chang, "Critical-sized osteochondral defects of young miniature pigs as a preclinical model for articular cartilage repair," *Biomed. Eng.*, vol. 26, no. 1, p. 1450003, 2014.

- [181] T. Gotterbarm, S. J. Breusch, U. Schneider, and M. Jung, “The minipig model for experimental chondral and osteochondral defect repair in tissue engineering: Retrospective analysis of 180 defects,” *Lab. Anim.*, vol. 42, no. 1, pp. 71–82, 2008.
- [182] B. D. Harman, S. H. Weeden, D. K. Lichota, and G. W. Brindley, “Osteochondral autograft transplantation in the porcine knee,” *Am. J. Sports Med.*, vol. 34, no. 6, pp. 913–918, 2006.
- [183] M. L. de Vries-van Melle, M. S. Tihaya, N. Kops, W. J. L. M. Koevoet, J. M. Murphy, J. a. N. Verhaar, M. Alini, D. Eglin, and G. J. V. M. van Osch, “Chondrogenic differentiation of human bone marrow-derived mesenchymal stem cells in a simulated osteochondral environment is hydrogel dependent,” *Eur. Cell. Mater.*, vol. 27, pp. 112–123; discussion 123, 2014.
- [184] V. J. Bianchi, J. F. Weber, S. D. Waldman, D. Backstein, and R. A. Kandel, “Formation of hyaline cartilage tissue by passaged human osteoarthritic chondrocytes,” *Tissue Eng. Part A*, vol. 23, no. 3, pp. 156–165, 2017.
- [185] T. Morales, “Chondrocyte moves: clever strategies?,” *Osteoarthritis Cartilage*, vol. 15, no. 8, pp. 861–871, 2007.
- [186] N. Hopper, F. Henson, R. Brooks, E. Ali, N. Rushton, and J. Wardale, “Peripheral blood derived mononuclear cells enhance osteoarthritic human chondrocyte migration,” *Arthritis Res. Ther.*, vol. 17, no. 1, p. 199, 2015.
- [187] I. Villanueva, C. A. Weigel, and S. J. Bryant, “Cell-matrix interactions and dynamic mechanical loading influence chondrocyte gene expression and bioactivity in PEG-RGD hydrogels,” *Acta Biomater.*, vol. 5, no. 8, pp. 2832–2846, 2009.
- [188] F. Shapiro, S. Koide, and M. J. Glimcher, “Cell origin and differentiation in the repair of full-thickness defects of articular cartilage,” *J. Bone Joint Surg. Am.*, vol. 75, no. 4, pp. 532–53, 1993.
- [189] E. B. Hunziker and L. C. Rosenberg, “Repair of partial-thickness defects in articular cartilage: cell recruitment from the synovial membrane,” *J Bone Joint Surg Am.*, vol. 78, no. 5, pp. 721–733, 1996.
- [190] P. K. Bos, N. Kops, J. a. N. Verhaar, and G. J. V. M. van Osch, “Cellular origin of neocartilage formed at wound edges of articular cartilage in a tissue culture experiment,” *Osteoarthritis Cartilage*, vol. 16, no. 2, pp. 204–211, 2008.

- [191] S. R. Tew, A. P. Kwan, A. Hann, B. M. Thomson, and C. W. Archer, “The reactions of articular cartilage to experimental wounding: role of apoptosis,” *Arthritis Rheum.*, vol. 43, no. 1, pp. 215–225, 2000.
- [192] E. L. Kuyinu, G. Narayanan, L. S. Nair, and C. T. Laurencin, “Animal models of osteoarthritis: classification, update, and measurement of outcomes,” *J. Orthop. Surg. Res.*, vol. 11, no. 1, 2016.
- [193] H. H. Lee, C. C. Chang, M. J. Shieh, J. P. Wang, Y. T. Chen, T. H. Young, and S. C. Hung, “Hypoxia enhances chondrogenesis and prevents terminal differentiation through pi3k/akt/foxo dependent anti-apoptotic effect,” *Sci. Rep.*, vol. 3, p. 2683, 2013.
- [194] B. D. Markway, G. K. Tan, G. Brooke, J. E. Hudson, J. J. Cooper-White, and M. R. Doran, “Enhanced chondrogenic differentiation of human bone marrow-derived mesenchymal stem cells in low oxygen environment micropellet cultures,” *Cell Transplant.*, vol. 19, no. 1, pp. 29–42, 2010.
- [195] E. M. Darling, S. Zauscher, and F. Guilak, “Viscoelastic properties of zonal articular chondrocytes measured by atomic force microscopy,” *Osteoarthritis Cartilage*, vol. 14, no. 6, pp. 571–9, 2006.
- [196] W. Wilson, J. M. Huyghe, and C. C. van Donkelaar, “Depth-dependent compressive equilibrium properties of articular cartilage explained by its composition,” *Biomech. Model. Mechanobiol.*, vol. 6, no. 1, pp. 43–53, 2007.
- [197] K. A. Athanasiou, E. M. Darling, G. D. DuRaine, J. C. Hu, and A. H. Reddi, *Articular Cartilage*. CRC Press, 2013.
- [198] M. Khoshgoftar, C. C. van Donkelaar, and K. Ito, “Mechanical stimulation to stimulate formation of a physiological collagen architecture in tissue-engineered cartilage: a numerical study,” *Comput. Methods Biomech. Biomed. Engin.*, vol. 14, no. 2, pp. 135–144, 2011.
- [199] M. Khoshgoftar, W. Wilson, K. Ito, and C. C. van Donkelaar, “Influence of the temporal deposition of extracellular matrix on the mechanical properties of tissue-engineered cartilage,” *Tissue Eng. Part A*, vol. 20, no. 9, pp. 1476–1485, 2014.
- [200] E. A. Aisenbrey and S. J. Bryant, “Mechanical loading inhibits hypertrophy in chondrogenically differentiating hMSCs within a biomimetic hydrogel,” *J. Mater. Chem. B*, vol. 4, no. 20, pp. 3562–3574, 2016.

- [201] O. F. W. Gardner, N. Fahy, M. Alini, and M. J. Stoddart, “Joint mimicking mechanical load activates TGF1 in fibrin-poly(ester-urethane) scaffolds seeded with mesenchymal stem cells,” *J. Tissue Eng. Regener. Med.*, 2016.
- [202] N. J. Steinmetz and S. J. Bryant, “The effects of intermittent dynamic loading on chondrogenic and osteogenic differentiation of human marrow stromal cells encapsulated in RGD-modified poly(ethylene glycol) hydrogels,” *Acta Biomater.*, vol. 7, no. 11, pp. 3829–3840, 2011.
- [203] L. Bian, D. Y. Zhai, E. C. Zhang, R. L. Mauck, and J. A. Burdick, “Dynamic compressive loading enhances cartilage matrix synthesis and distribution and suppresses hypertrophy in hMSC-laden hyaluronic acid hydrogels,” *Tissue Eng. Part A*, vol. 18, no. 7, pp. 715–724, 2012.
- [204] G. D. Nicodemus and S. J. Bryant, “Mechanical loading regimes affect the anabolic and catabolic activities by chondrocytes encapsulated in PEG hydrogels,” *Osteoarthritis Cartilage*, vol. 18, no. 1, pp. 126–137, 2010.

8. Appendix

Supplementary Material

This chapter contains supplementary data of the experimental work.

Viability and remodeling of subchondral bone

The remodeling activity of subchondral bone was investigated by means of deposition of mineralized matrix. Therefore, the culture media was supplemented at day 28 or day 42 with calcein-AM (4 μ M) for three days in bone media and cultured further (till day 42 or day 56 respectively) before harvested and tissue processed for plastic embedding. Tissue slices (OCE without defect) were desplastified as described and fluorescence images (excitation at 488 nm) were taken. Fluorescence images at two different magnifications are shown in figure 35 A-D and overlay with bright-field image in figure 35 A'-D'.

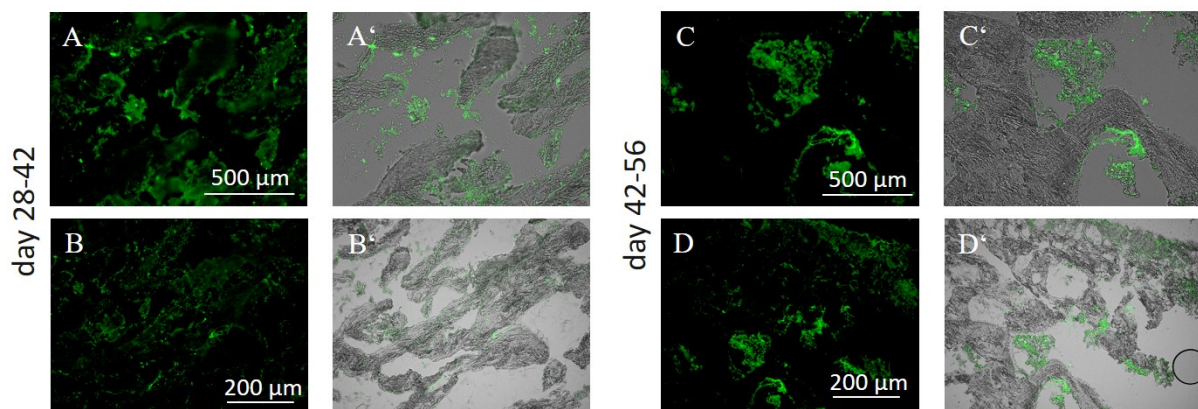


Figure 35 Calcein labeling of subchondral bone of osteochondral explant (diameter 8 mm) cultured for 56 days *ex vivo* with tissue specific media. (A-D) Fluorescent images of osteochondral explant visualizing calcium binding fluorochrome (calcein-AM) deposited at site of active mineralization within two weeks of *ex vivo* culture (day 28-42 and day 42-56) at two different magnifications. (A'-D') Overlay of brightfield images and fluorescent images. Incorporation of calcein-AM at site of active mineralization indicates active bone remodeling. (Scale bar (A, A', C, C') 500 μ m, (B, B', D, D') 200 μ m)

Isotype controls for immuno-histological stainings

Isotype controls for immuno-histological stainings are shown in figure 36. All controls, neither isotypes nor second antibody only, do not show positive staining. Following, primary antibody binds specifically to antigen in immuno-histological stainings.

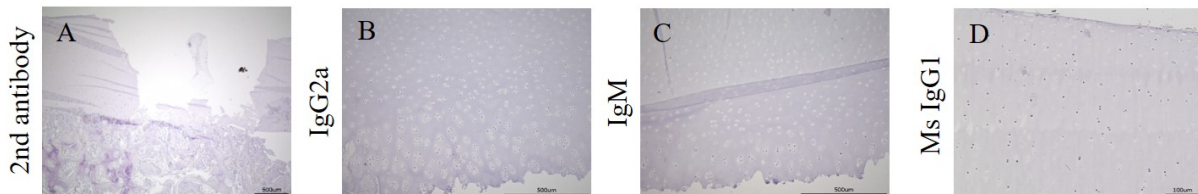


Figure 36 Isotype controls for histological staining on porcine articular cartilage. (A) second antibody only, (B) IgG2a, (C) IgM and (D) MsIgG1. (Scale bar (A-C) 500 µm, (D) 100 µm)

Phenotypic characterization of pChondrocytes and porcine articular cartilage

Immuno-fluorescent and -histological stainings for matrix proteins (aggrecan, collagen II, collagen X, proCollagen I) and transcription factors (SOX9, RunX2) are shown in figure 37. Chondrogenic markers collagen VI and SOX9 were preserved in both groups after *in vitro* culture without supplementation of TGF- β in culture media. pChondrocytes synthesized cartilagenous matrix after 28 days in pellet culture and under free swelling condition that was mainly present in periphery with tendency of hypertrophy (collagen X). pChondrocytes embedded in collagen I hydrogel implanted in osteochondral model (no TGF- β was added in culture media) shows homogenous cartilage matrix synthesis (collagen II and aggrecan) with weak collagen X and proCollagen I synthesis on bottom.

Influence of defect depth on cartilage regeneration

The influence of cartilage defect depth on cell infiltration and cartilage defect regeneration was analysed in OCE with 1 mm chondral defects cultured for 28 days with tissue specific media. A collection of safranin-O stainings to visualize proteoglycans is shown in figure 38.

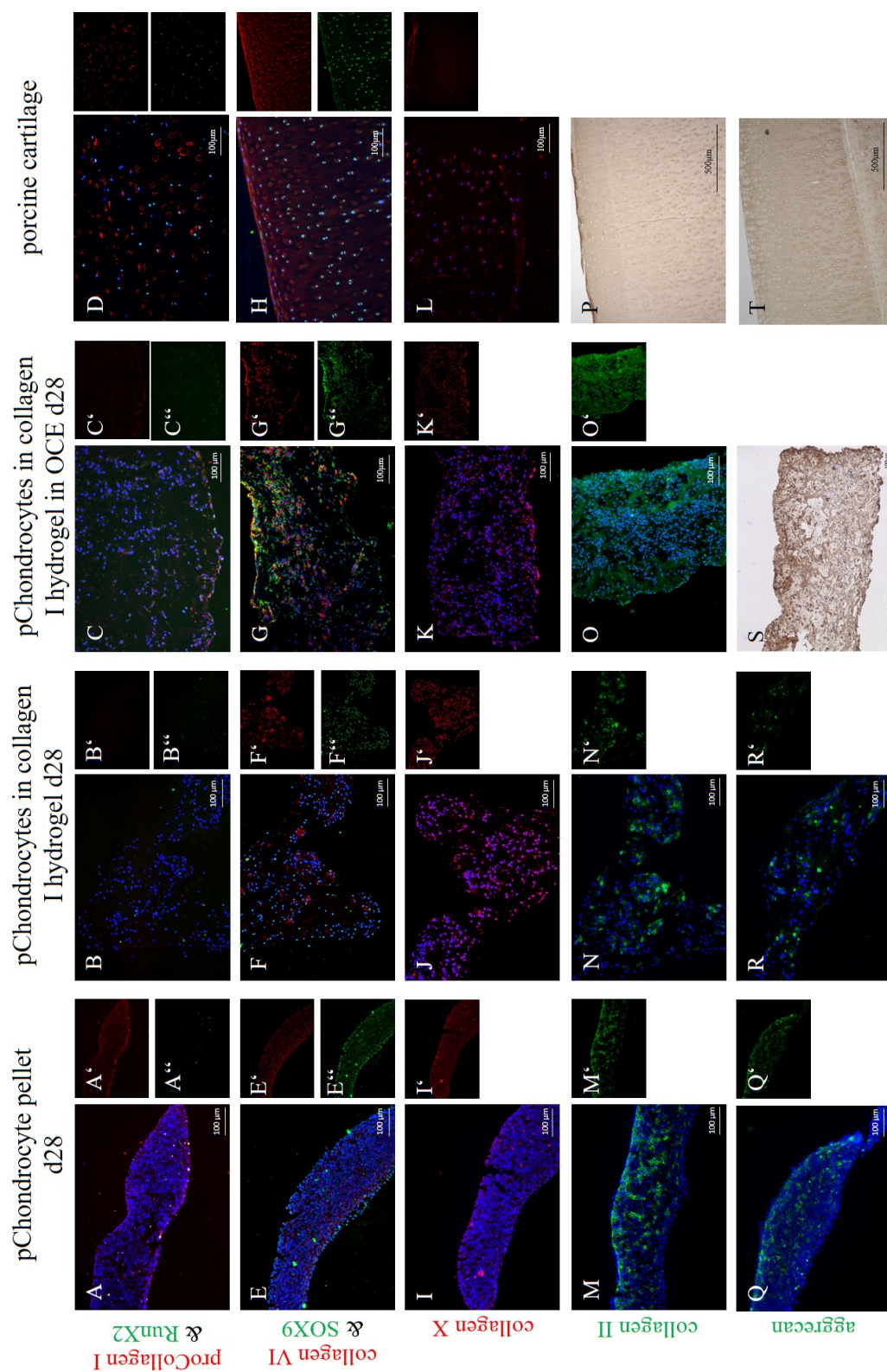


Figure 37 Immuno-fluorescent and -histological stainings of pChondrocyte pellet, embedded in collagen I hydrogel cultured for 28 days under free swelling conditions or in osteochondral defect model and native porcine cartilage. (A-T) Merged images of selected antibody (red and/or green) and DAPI (blue) nuclei staining with (A'-R') antibody only staining at respective wavelength. (Scale bar (A-O, Q, R) 100 μm, (P, T) 500 μm)

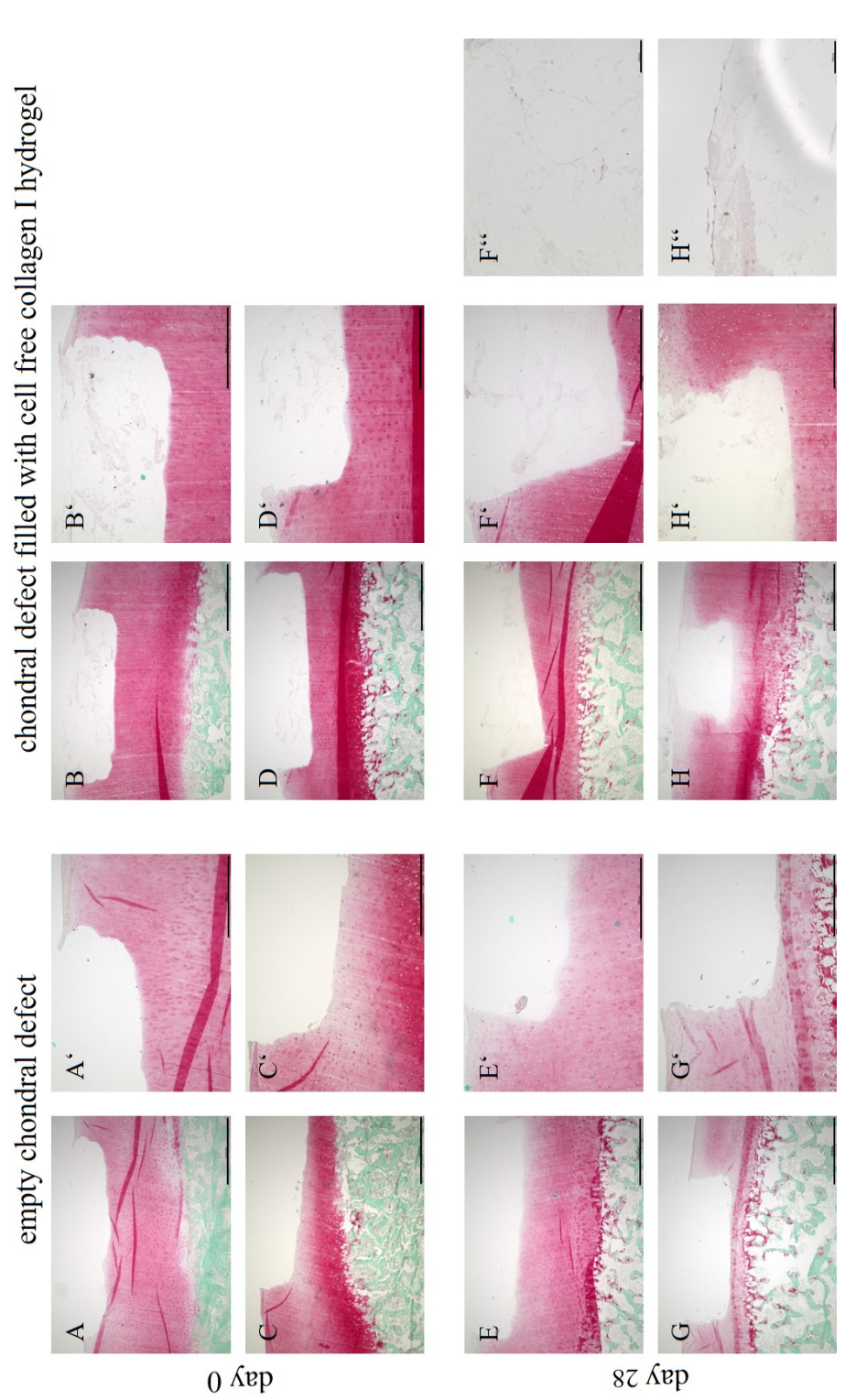


Figure 38 Safranin-O staining of chondral defects at day 0 and after 28 days *ex vivo* culture. (A-A') Empty chondral defect in osteochondral explant (OCE) and (B-B') filled with cell free collagen I hydrogel. After 28 days *ex vivo* culture there was no cartilage tissue formation in (E-E') untreated and (F-F') collagen I treated group. (F'') Minor single cells invaded the collagen I hydrogel are visible at higher magnification. (Scale bar (A-D) 1000 μm, (A'-D') 500 μm, (D'') 100 μm)

Curriculum vitae

Personal data

Andrea Schwab

Professional experience

- 11/2013–present Doctoral researcher
Department Tissue Engineering and Regenerative Medicine
University Hospital Würzburg, Germany
- 09/2013–10/2013 Student employee
Fraunhofer Project Group 'Regenerative Therapies for Oncology and
Musculoskeletal' Disease Würzburg, Germany
- 10/2012–09/2013 Student assistant
Fraunhofer Project Group 'Regenerative Therapies for Oncology and
Musculoskeletal' Disease Würzburg, Germany
- 08/2012–09/2012 Internship
Fraunhofer Institute for silicate research (ISC), Particle Technology
Group, Würzburg, Germany
- 03/2012–03/2012 Internship
Research group Mesenchymal Stem Cell Biology, Orthopedic Center for
Musculoskeletal Research, König-Ludwig-Haus, Würzburg, Germany

Education

- 11/2013-06/2017 PhD thesis
'Development of an osteochondral cartilage defect model', Graduate
School of Life Sciences, Julius-Maximilians-University Würzburg (su-
pervised by Prof. Heike Walles)
- 10/2008–09/2013 Studies in Technology of Functional Materials

- Julius-Maximilians-University Würzburg, Germany
- 09/2013 Master of Science
'Influence of structured biomaterials to the differentiation of stem cells in co-culture with endothelial cells', Julius-Maximilians-University Würzburg, Germany (supervised by Prof. Heike Walles)
- 09/2011 Bachelor of Science
'Novel injectable and moldable PLGA-CaP scaffolds for bone regeneration', Julius-Maximilians-University Würzburg, Germany (supervised by Prof. John E. Davies)
- 09/2005–07/2008 German Gymnasium (A-level)
Commercial High School, Bad Mergentheim, Germany

Advanced trainings and experiences abroad

- 2015 Research stay abroad (3 months)
Life Tec Group BV, Eindhoven, The Netherlands
- 2015 Basic course for animal welfare and experimental animal science (1 week) Julius-Maximilians-University Würzburg, Germany
- 2014 Workshop on 'Biomaterialien in der chirurgischen Anwendung' (1 day)
Deutsche Gesellschaft fr Biomaterialien e.V., Dresden, Germany
- 2013 Intensive practical course on paraffin and polymer embedding (1 week)
MORPHISTO Evolutionsforschung und Anwendung GmbH, Frankfurt am Main, Germany
- 2013 Summer School (2 weeks)
'Regenerative Medicine', Utrecht University, The Netherlands
- 2011 Exchange student (3 months)
Institute of Biomaterials and Biomedical Engineering, University of Toronto, Canada

Place, Date

Signature

List of publication and congress participation

Data presented in this thesis are partially published in peer-reviewed publications, preprinted and presented at national and international conferences:

Peer-reviewed articles

- **Andrea Schwab***, Annick Meeuwssen, Franziska Ehlicke, Jan Hansmann, Lars Mulder, Anthal Smits, Heike Walles and Linda Kock; 'Ex vivo culture platform for assessment of cartilage repair treatment strategies', ALTEX, 2017, vol. 34, no. 2, p. 267-277, doi.org/10.14573/altex.1607111. Epub 2016 Oct 21.
- Michael J. Chen*, Jonathan P. Whiteley, Collin P. Please, **Andrea Schwab**, Franziska Ehlicke, Sarah L. Waters, Helen M. Byrne; 'Inducing chondrogenesis in MSC/chondrocyte Co-Cultures Using Exogenous TGF- β : A Mathematical Model', preprint, bioRxiv 141119; doi: <https://doi.org/10.1101/141119> .
- Laura S. Kimpton*, **Andrea Schwab**, Franziska Ehlicke, Sarah L. Waters, Collin P. Please, Jonathan P. Whiteley, Helen M. Byrne; 'A mathematical model for cell infiltration and proliferation in a chondral defect', Journal of theoretical biology, 2017 (in revision).
- Davide Confalonieri*, **Andrea Schwab***, Heike Walles, Franziska Ehlicke; Advanced Therapy Medicinal Products: A Guide for Human Bone Marrow-derived Mesenchymal Stromal Cells Applications in Bone and Cartilage Tissue Engineering, Tissue Engineering part B, 2017 (submitted).

Further publications

- **Andrea Schwab***, Sebastian Naczenski, Andreas Diegeler, Szymon Kurdyn, Franziska Ehlicke, Florian Gröber, Heike Walles; Artificial Tissue Cutter (ARTcut): an automated device to create standardized and reproducible wounds in soft and hard tissues (in preparation)

International conferences and symposia

- Schwab *et al.*, Poster 'Artificial Tissue Cutter: Creation of standardized chondral defects in an osteochondral model' (European Chapter Meeting of the Tissue Engineering and Regenerative Medicine International Society European (TERMIS-EU), Davos, Switzerland, 26–30 June, 2017)
- Schwab *et al.*, Talk 'Ex vivo cartilage defect model: Screening of innovative hydrogel systems revealed material dependent regeneration' (ICRS), Sorrent, Italy, 24–27 September, 2016)
- Schwab *et al.*, Talk 'Screening novel hydrogels in an ex vivo cartilage defect model' (TERMIS-EU, 2016 Uppsala, Sweden, June 28–July 01, 2016)
- Schwab *et al.*, Poster 'Ex vivo osteo–chondral organ culture' (4th TERMIS world congress, Boston, USA, September 08–11, 2015)
- Schwab *et al.*, Poster 'In vitro osteochondral test system in cartilage regeneration' (World Conference on Regenerative Medicine, Leipzig, October 21–23, 2015)
- Schwab *et al.*, Poster 'In vitro osteochondral test system in cartilage regeneration' (4th International Conference Strategies in Tissue Engineering, Würzburg, Germany, June 10–12 2015)

National conferences and symposia

- Schwab *et al.*, Talk: 'Ex vivo cartilage defect model: Evaluation of cartilage hydrogels' (Deutscher Kongress für Orthopädie und Unfallchirurgie (DKOU 2016). Berlin, October 25–28, 2016)
- Schwab *et al.*, Talk 'Ex vivo Knorpeldefektmodell zur Testung neuer Hydrogelmateriale und Behandlungsmethoden' (VI. Münchner Symposium für experimentelle Orthopädie und Unfallchirurgie. Munich, July 15–16, 2016)
- Schwab *et al.*, Talk 'In vitro osteochondral test system for biomaterial screening in cartilage regeneration' (Netherlands Society for Biomaterials and Tissue Engineering (NBTE). Lunteren, November 31–December 01, 2015)

Affidavit / Eidesstattliche Erklärung

Affidavit

I hereby confirm that my thesis entitled 'Development of an osteochondral cartilage defect model' is a result of my own work. I did not receive any help or support from commercial consultants. All sources and or materials applied are listed and specified in this thesis. Furthermore, I confirm that this thesis hat not yet been submitted as part of another examination process neither in identical nor in similar form.

Place, Date

Signature

Eidesstattliche Erklärung

Hiermit erkläre ich an Eides statt, die Dissertation 'Entwicklung eines osteochondralen Knorpeldefektmodells' eigenständig, d.h. insbesondere selbständig und ohne Hilfe eines kommerziellen Promotionsberaters, angefertigt und keine anderen als die von mir angegebenen Quellen und Hilfsmittel verwendet zu haben.

Ich erkläre außerdem, dass die Dissertation weder in gleicher noch in ähnlicher Form bereits in einem anderen Prüfungsverfahren vorgelegen hat.

Ort, Datum

Unterschrift

Danksagung

Mein besonderer Dank richtet sich an Prof. Heike Walles. Sie hat es mir ermöglicht unter ihrer Betreuung meine Promotion am Lehrstuhl Tissue Engineering und Regenerative Medizin durchzuführen. Vielen Dank für dein Vertrauen und die Unterstützung über die letzten Jahre hinweg.

Weiterhin vielen Dank an Herrn Prof. Jürgen Groll und Prof. Gerjo van Osch für die Betreuung meiner Doktorarbeit als Zweit- bzw. Drittgutachter.

Ein besonderer Dank gilt Franziska Ehlicke für die wissenschaftliche Betreuung im Labor und dem Korrekturlesen meiner Doktorarbeit und den Abstracts. Bei der Isolation der vielen „plugs“ konnte ich mich immer auf deine tatkräftige Unterstützung verlassen und deine fachlichen Ratschläge und Anregungen haben meine Promotion in vielerlei Hinsicht bereichert. Vielen Dank für deine Unterstützung.

Danke an alle Kollegen des Lehrstuhls Tissue Engineering und Regenerative Medizin für die offene und kollegiale Arbeitsatmosphäre und die Hilfsbereitschaft im Laboralltag.

Mein besonderer Dank geht an Antje Kremer für die abenteuerlichen (Fern-) Reisen und kleinen Ausflüge nach Feierabend, die mir immer wieder Kraft und neue Energie gegeben haben. Danke, dass du immer ein offenes Ohr für mich hast und wir weiterhin viele Abenteuer erleben werden.

Ebenfalls danke an Sebastian Naczenski und Alexa Buß für die gemeinsame Zeit im Labor, insbesondere eure Ausdauer an den langen Labortagen, an denen wir die Kulturen für eure Abschlussarbeiten angesetzt haben.

Vielen Dank an alle Kooperationspartner:

Ein großes Dankeschön möchte ich an unsere Projektpartner von LifeTec für eure offene, zuverlässige und erfolgreiche Kooperation aussprechen. Mein spezieller Dank geht an Linda Kock für deine enge und unterstützende Zusammenarbeit und der Entwicklung der osteochondralen Kulturplattform. Vielen Dank, dass du mir einen dreimonatigen Gastaufenthalts zur Durchführung der großen experimentellen Studie im Rahmen des EU Projekts HydroZONES bei LifeTec ermöglicht hast.

Weiterhin möchte ich meinen Dank an Prof. Dr. Georg Krohne am Biozentrum Würzburg für die Durchführung von REM-Aufnahmen, Dr. Daniel Haddad vom Forschungszentrum Magnet-Resonanz-Bayern (MRB) e.V. für die MRT und CT Aufnahmen und der Metzgerei

Kirchner für die Bereitstellung der porcinen Kniegelenken aussprechen.

Innerhalb des HydroZONES Konsortiums möchte ich mich besonders bei Simone Stichler, Felix Schrön und Anna Abbadessa für die Bereitstellung der Hydrogele, die sie entwickelten, bedanken. Vivian Mouser und Felix Schrön nochmals herzlichen Dank, dass ihr mir beim Herstellen der Hydrogele tatkräftig unterstützt habt.

Allen übrigen HydroZONES Projektpartnern möchte ich ebenfalls meinen danken für eure Unterstützung und die gute Zusammenarbeit, aber auch eure Gastfreundschaft bei den jährlichen Projekttreffen in Pamplona, Utrecht und Würzburg. Danke auch an die EU für die Finanzierung ('HydroZONES - The work leading to these results has received funding from the European Union Seventh Framework Programme (FP7/2007-2013) under grant agreement n° 309962').

Meiner Familie möchte ich ebenfalls danken für den Rückhalt und die Unterstützung während der letzten Jahre. Ich bin euch sehr dankbar, dass ihr immer für mich da seid und hinter mir steht.